

BWR Anticipated Transients Without Scram in the MELLLA+ Expanded Operating Domain

Part 4:
Sensitivity Studies for Events
Leading to Emergency Depressurization

AVAILABILITY OF REFERENCE MATERIALS IN NRC PUBLICATIONS

NRC Reference Material

As of November 1999, you may electronically access NUREG-series publications and other NRC records at NRC's Library at www.nrc.gov/reading-rm.html. Publicly released records include, to name a few, NUREG-series publications; *Federal Register* notices; applicant, licensee, and vendor documents and correspondence; NRC correspondence and internal memoranda; bulletins and information notices; inspection and investigative reports; licensee event reports; and Commission papers and their attachments.

NRC publications in the NUREG series, NRC regulations, and Title 10, "Energy," in the *Code of Federal Regulations* may also be purchased from one of these two sources.

1. The Superintendent of Documents

U.S. Government Publishing Office
Mail Stop IDCC
Washington, DC 20402-0001
Internet: bookstore.gpo.gov
Telephone: (202) 512-1800
Fax: (202) 512-2104

2. The National Technical Information Service

5301 Shawnee Rd., Alexandria, VA 22312-0002
www.ntis.gov
1-800-553-6847 or, locally, (703) 605-6000

A single copy of each NRC draft report for comment is available free, to the extent of supply, upon written request as follows:

Address: U.S. Nuclear Regulatory Commission

Office of Administration
Publications Branch
Washington, DC 20555-0001
E-mail: distribution.resource@nrc.gov
Facsimile: (301) 415-2289

Some publications in the NUREG series that are posted at NRC's Web site address www.nrc.gov/reading-rm/doc-collections/nuregs are updated periodically and may differ from the last printed version. Although references to material found on a Web site bear the date the material was accessed, the material available on the date cited may subsequently be removed from the site.

Non-NRC Reference Material

Documents available from public and special technical libraries include all open literature items, such as books, journal articles, transactions, *Federal Register* notices, Federal and State legislation, and congressional reports. Such documents as theses, dissertations, foreign reports and translations, and non-NRC conference proceedings may be purchased from their sponsoring organization.

Copies of industry codes and standards used in a substantive manner in the NRC regulatory process are maintained at—

The NRC Technical Library

Two White Flint North
11545 Rockville Pike
Rockville, MD 20852-2738

These standards are available in the library for reference use by the public. Codes and standards are usually copyrighted and may be purchased from the originating organization or, if they are American National Standards, from—

American National Standards Institute

11 West 42nd Street
New York, NY 10036-8002
www.ansi.org
(212) 642-4900

Legally binding regulatory requirements are stated only in laws; NRC regulations; licenses, including technical specifications; or orders, not in NUREG-series publications. The views expressed in contractor-prepared publications in this series are not necessarily those of the NRC.

The NUREG series comprises (1) technical and administrative reports and books prepared by the staff (NUREG-XXXX) or agency contractors (NUREG/CR-XXXX), (2) proceedings of conferences (NUREG/CP-XXXX), (3) reports resulting from international agreements (NUREG/IA-XXXX), (4) brochures (NUREG/BR-XXXX), and (5) compilations of legal decisions and orders of the Commission and Atomic and Safety Licensing Boards and of Directors' decisions under Section 2.206 of NRC's regulations (NUREG-0750).

DISCLAIMER: This report was prepared as an account of work sponsored by an agency of the U.S. Government. Neither the U.S. Government nor any agency thereof, nor any employee, makes any warranty, expressed or implied, or assumes any legal liability or responsibility for any third party's use, or the results of such use, of any information, apparatus, product, or process disclosed in this publication, or represents that its use by such third party would not infringe privately owned rights.

BWR Anticipated Transients Without Scram in the MELLLA+ Expanded Operating Domain

Part 4: Sensitivity Studies for Events Leading to Emergency Depressurization

Manuscript Completed: April 2014
Date Published: June 2015

Prepared by:
Lap-Yan Cheng, Joo Seok Baek, Arantxa Cuadra, Arnold Aronson,
David Diamond, and Peter Yarsky*

Nuclear Science and Technology Department
Brookhaven National Laboratory

*U.S. Nuclear Regulatory Commission

Tarek Zaki, NRC Project Manager

NRC Job Codes V6150 and F6018

Office of Nuclear Regulatory Research

ABSTRACT

This is the fourth in a series of reports on the response of a boiling water reactor (BWR) to anticipated transients without reactor scram (ATWS) when operating in the expanded operating domain “MELLLA+.” In this report, we analyze the ATWS events initiated by the closure of main steam isolation valves and requiring emergency depressurization (ED). The analysis is done at the beginning-of-cycle and end-of-full-power-life. Our objective is to understand the sensitivity of ATWS-ED events to the initial operating core flow and to the spectrally corrected moderator density history (void history). We also consider different strategies for controlling the water level.

We simulate the ATWS events for 2500 seconds, a sufficiently long time for us to identify and understand the response of key components and the potential for damaging the fuel or causing the containment to fail. These events lead to the automatic trip of recirculation pumps, and to the operator actions to manually activate the automatic depressurization system when the wetwell (suppression pool) has reached the heat capacity temperature limit, and to regulate power by controlling the water level and injecting soluble boron.

The simulations were carried out using the TRACE/PARCS code system and the models we developed for a previous study with all relevant BWR systems.

TABLE OF CONTENTS

| | |
|---|------|
| ABSTRACT | iii |
| TABLE OF CONTENTS | v |
| LIST OF FIGURES | vii |
| LIST OF TABLES | ix |
| ACKNOWLEDGMENTS | xi |
| ACRONYMS | xiii |
| 1 INTRODUCTION | 1-1 |
| 1.1 Background | 1-1 |
| 1.2 Objectives | 1-1 |
| 1.3 Methodology | 1-2 |
| 1.4 Organization of Report | 1-3 |
| 2 SENSITIVITY STUDIES FOR MSIV CLOSURE EVENTS | 2-1 |
| 2.1 Introduction | 2-1 |
| 2.2 Effect of Reduced Core Flow at BOC | 2-4 |
| 2.3 Effect of Void History Modeling at EOFPL | 2-13 |
| 2.4 Effect of Reduced Core Flow at EOFPL | 2-19 |
| 2.5 Effect of Level Control at EOFPL with Reduced Core Flow | 2-33 |
| 3 SUMMARY AND CONCLUSIONS | 3-1 |
| 3.1 ATWS Events Initiated by MSIV Closure – Sensitivity Cases | 3-1 |
| 3.2 Applying TRACE/PARCS to ATWS-ED Events | 3-3 |
| 4 REFERENCES | 4-1 |
| APPENDIX A - Comparison of TRACE Executables | A-1 |
| APPENDIX B - Selection of Time-Step Size and Numerical Method | B-1 |

LIST OF FIGURES

| | | |
|-------------|---|------|
| Figure 2.1 | Radially Averaged Axial Power Distribution at BOC - Effect of Reduced Flow.... | 2-5 |
| Figure 2.2 | Radially Averaged Axial Moderator Density at BOC - Effect of Reduced Flow.... | 2-5 |
| Figure 2.3 | Reactor Power - BOC, TAF+5, 85% & 75% Flow | 2-7 |
| Figure 2.4 | Reactor Power - Early Phase of Transient..... | 2-7 |
| Figure 2.5 | Total Reactivity - BOC, TAF+5, 85% & 75% Flow | 2-8 |
| Figure 2.6 | Core Reactivity - BOC, TAF+5, 75% Flow..... | 2-8 |
| Figure 2.7 | Reactor Pressure - BOC, TAF+5, 85% & 75% Flow | 2-9 |
| Figure 2.8 | Core Flow - BOC, TAF+5, 85% & 75% Flow | 2-10 |
| Figure 2.9 | Downcomer Water Level - BOC, TAF+5, 85% & 75% Flow | 2-10 |
| Figure 2.10 | Boron Inventory in the Core Region - BOC, TAF+5, 85% & 75% Flow | 2-11 |
| Figure 2.11 | Peak Clad Temperature - BOC, TAF+5, 85% & 75% Flow | 2-12 |
| Figure 2.12 | Suppression Pool Temperature - BOC, TAF+5, 85% & 75% Flow..... | 2-12 |
| Figure 2.13 | Drywell Pressure - BOC, TAF+5, 85% & 75% Flow..... | 2-13 |
| Figure 2.14 | Radially Averaged Axial Power Distribution at EOFPL, Effect of Spectrally Corrected Void History | 2-14 |
| Figure 2.15 | Reactor Power - EOFPL, TAF+5, UH & UHSPH | 2-15 |
| Figure 2.16 | Reactor Pressure - EOFPL, TAF+5, UH & UHSPH | 2-16 |
| Figure 2.17 | Core Flow - EOFPL, TAF+5, UH & UHSPH..... | 2-16 |
| Figure 2.18 | Downcomer Water Level - EOFPL, TAF+5, UH & UHSPH | 2-17 |
| Figure 2.19 | Boron Inventory in the Core Region - EOFPL, TAF+5, UH & UHSPH | 2-17 |
| Figure 2.20 | Core Reactivity - EOFPL, TAF+5, UHSPH | 2-18 |
| Figure 2.21 | Suppression Pool Temperature - EOFPL, TAF+5, UH & UHSPH..... | 2-18 |
| Figure 2.22 | Drywell Pressure - EOFPL, TAF+5, UH & UHSPH..... | 2-19 |
| Figure 2.23 | Radially Averaged Axial Power Distribution at EOFPL - Effect of Reduced Core Flow..... | 2-20 |
| Figure 2.24 | Radially Averaged Axial Moderator Density Distribution at EOFPL - Effect of Reduced Core Flow..... | 2-20 |
| Figure 2.25 | Reactor Power - EOFPL, TAF-2 Cases | 2-22 |
| Figure 2.26 | Reactor Power (0 to 600 s) - EOFPL, TAF-2 Cases | 2-22 |
| Figure 2.27 | Reactor Pressure - EOFPL, TAF-2 Cases..... | 2-23 |
| Figure 2.28 | Core Flow - EOFPL, TAF-2 Cases | 2-24 |
| Figure 2.29 | Downcomer Water Level - EOFPL, TAF-2 Cases..... | 2-24 |
| Figure 2.30 | Feedwater Flowrate - EOFPL, TAF-2, 75% Flow..... | 2-25 |
| Figure 2.31 | Feedwater Flowrate - EOFPL, TAF-2, 85% Flow..... | 2-25 |
| Figure 2.32 | Steamline Flow - EOFPL, TAF-2, 75% Flow..... | 2-26 |
| Figure 2.33 | Void Fraction in Core Bypass (Ring 1) - EOFPL, TAF-2, 75% Flow..... | 2-27 |
| Figure 2.34 | Boron Inventory in the Core - EOFPL, TAF-2 Cases | 2-28 |
| Figure 2.35 | Effective Injection Boron Concentration - EOFPL, TAF-2, 75% Flow | 2-29 |
| Figure 2.36 | Core Reactivity - EOFPL, TAF-2, 75% Flow | 2-29 |
| Figure 2.37 | Core Reactivity - EOFPL, TAF-2, 85% Flow | 2-30 |
| Figure 2.38 | Peak Clad Temperature - EOFPL, TAF-2 Case..... | 2-31 |
| Figure 2.39 | Suppression Pool Temperature - EOFPL, TAF-2 Cases | 2-32 |
| Figure 2.40 | Drywell Pressure - EOFPL, TAF-2 Cases..... | 2-32 |
| Figure 2.41 | Reactor Power - EOFPL, 85% Flow Cases | 2-35 |
| Figure 2.42 | Reactor Power (0 to 600 s) - EOFPL, 85% Flow Cases | 2-35 |
| Figure 2.43 | Reactor Pressure - EOFPL, 85% Flow Cases | 2-36 |
| Figure 2.44 | Core Flow - EOFPL, 85% Flow Cases | 2-36 |
| Figure 2.45 | Downcomer Water Level - EOFPL, 85% Flow Cases | 2-37 |

| | | |
|-------------|--|------|
| Figure 2.46 | Void Fraction in Core Bypass (Ring-1) - EOFPL, TAF-2, 85% Flow | 2-37 |
| Figure 2.47 | Core Average Void Fraction - EOFPL, TAF-2, 85% Flow | 2-38 |
| Figure 2.48 | Boron Inventory in the Core - EOFPL, 85% Flow Cases | 2-39 |
| Figure 2.49 | Effective Injection Boron Concentration - EOFPL, TAF-2, 85% Flow..... | 2-39 |
| Figure 2.50 | Effective Injection Boron Concentration - EOFPL, TAF, 85% Flow | 2-40 |
| Figure 2.51 | Effective Injection Boron Concentration - EOFPL, TAF+5, 85% Flow | 2-40 |
| Figure 2.52 | Core Reactivity - EOFPL, TAF+5, 85% Flow | 2-41 |
| Figure 2.53 | Core Reactivity - EOFPL, TAF, 85% Flow | 2-42 |
| Figure 2.54 | Peak Clad Temperature - EOFPL, 85% Flow Cases | 2-43 |
| Figure 2.55 | Suppression Pool Temperature - EOFPL, 85% Flow Cases..... | 2-43 |
| Figure 2.56 | Drywell Pressure - EOFPL, 85% Flow Cases | 2-44 |

LIST OF TABLES

| | | |
|-----------|---|------|
| Table 1.1 | Simulation Conditions of the ATWS-ED Sensitivity Cases..... | 1-2 |
| Table 2.1 | Simulation Conditions of ATWS-ED Cases..... | 2-1 |
| Table 2.2 | Version of TRACE Executable Used | 2-2 |
| Table 2.3 | ATWS-ED Scenario..... | 2-3 |
| Table 2.4 | Reference for the Initial Steady-State | 2-4 |
| Table 2.5 | Comparison of Key Results for BOC, TAF+5 Cases..... | 2-6 |
| Table 2.6 | Comparison of Key Results for EOFPL, TAF+5 Cases..... | 2-15 |
| Table 2.7 | Comparison of Key Results for EOFPL, TAF-2 Cases..... | 2-21 |
| Table 2.8 | Comparison of Key Results for EOFPL, 85% Flow Cases | 2-33 |

ACKNOWLEDGMENTS

This project was a joint effort of Brookhaven National Laboratory (BNL) and U.S. Nuclear Regulatory Commission staff. The authors wish to thank the Project Manager, Tarek Zaki, and his predecessor, Istvan Frankl, for their support and technical feedback. We greatly appreciated the efforts of the staff in the Office of Nuclear Regulatory Research, Reactor Systems Code Development Branch, to quickly assess and implement improvements, as they were identified, in the computer codes used in the project. We also appreciate the work done by Lynda Fitz in finalizing this document and providing administrative support.

ACRONYMS

| | |
|---------|---|
| 3D | Three Dimensional |
| ADF | Assembly Discontinuity Factor |
| ADS | Automatic Depressurization System |
| ATWS | Anticipated Transient Without SCRAM |
| ATWS-ED | Anticipated Transient Without SCRAM with Emergency Depressurization |
| ATWS-I | Anticipated Transient Without SCRAM with Instability |
| BNL | Brookhaven National Laboratory |
| BOC | Beginning-of-Cycle |
| BWR | Boiling Water Reactor |
| CB | Control Block in TRACE Input |
| CONTAN | Containment Component in TRACE Input |
| CST | Condensate Storage Tank |
| CW | Core-Wide |
| DC | Downcomer |
| DW | Drywell |
| DWO | Density-Wave Oscillation |
| ED | Emergency Depressurization |
| EOFPL | End-of-Full-Power-Life |
| EPU | Extended Power Uprate |
| FCT | Fuel Centerline Temperature |
| FCW | Flow Control Window |
| FOM | Figure-of-Merit |
| FW | Feedwater |
| GE | General Electric |
| GEH | GE Hitachi |
| HCTL | Heat Capacity Temperature Limit |
| MELLLA+ | Maximum Extended Load Line Limit Analysis Plus |
| MSIV | Main Steam Isolation Valve |
| NEM | Nodal Expansion Method |
| NRC | U.S. Nuclear Regulatory Commission |
| OLTP | Original Licensed Thermal Power |
| PARCS | Purdue Advanced Reactor Core Simulator |
| PCT | Peak Clad Temperature |
| PHE | Peak-Hot-Excess-Reactivity |
| RPS | Reactor Protection System |
| RPT | Recirculation Pump Trip |
| RPV | Reactor Pressure Vessel |
| RWL | Reactor Water Level |
| SETS | Stability Enhancing Two-Step method |
| S-I | Semi-Implicit Numerics |
| SLCS | Standby Liquid Control System |
| SP | Suppression Pool |
| SRV | Safety Relief Valve |
| TAF | Top-of-Active Fuel |
| TRACE | TRAC-RELAP Advanced Computational Engine |
| UH | Void History |
| UHSPH | Void History Spectrally Corrected |
| WR | Water Rod |

1 INTRODUCTION

1.1 Background

The operating power of boiling water reactors (BWRs) has been increasing in recent years, sometimes to 120% of their original licensed thermal power (OLTP). This places them in an expanded operating domain, and changes how they maneuver in the power-flow operating map. One option being pursued, “maximum extended load line limit analysis plus” (MELLLA+) operation [1], raises questions about how the plant will respond to anticipated transients without scram (ATWS). This report is one of several from Brookhaven National Laboratory (BNL) that describes how these events were simulated with state-of-the-art codes, and details the results of that analysis.

In a previous report [2] we discussed how MELLLA+ operation affects the power-flow operating map, and the impact of this during an ATWS event. If the initiating event is a turbine trip, then after the recirculation pumps automatically trip, the reactor evolves to a relatively high power-to-flow condition and, specifically, to a region of the power-flow map where unstable power oscillations are likely to occur. Their occurrence, if unmitigated, may damage the fuel. Additionally, the severity of the power oscillations may hamper the effectiveness of mitigation strategies. For example, ATWS events typically are mitigated by injecting dissolved boron via the standby liquid control system (SLCS). The occurrence of oscillation-induced flow reversal in the core inlet may reduce the rate at which this soluble absorber is delivered to the reactor core’s active region. The results of our studies of these ATWS events with core instability (ATWS-I) are given in [2, 3].

If the initiating event is the closure of main steam isolation valves (MSIVs), the concern is the amount of energy placed into containment during the mitigation period. This thermal load may exhaust the available capacity for suppressing pressure of the containment wetwell, thereby prompting the operators to undertake manual emergency depressurization according to standard emergency operating procedures. The emergency depressurization raises several concerns: (1) the reactor may have undergone a beyond-design-basis event, and the fuel may have been damaged, (2) the pressure suppression capacity of the containment may have been exhausted, and, (3) the pressure boundary of the reactor coolant may have been bypassed by manually opening the valves of the automatic depressurization system. We discuss our study of some of these ATWS events with emergency depressurization (ATWS-ED) in a companion report [4].

1.2 Objectives

We discussed in a previous report [4] our findings on the ATWS-ED events obtained with a TRACE BWR/5 model modified to become a BWR/4-like model with lower plenum SLCS injection. We gained significant insights on the reactor’s behavior and the ability to mitigate these events. In the present study, our objective was to understand the sensitivity of ATWS-ED events to the operating core flow and to the spectrally corrected moderator density history (void history). Such a correction involves taking into account the impact of factors, such as leakage or control state, on the neutron energy spectrum. Our study considers different strategies for controlling water level (top-of-active-fuel (TAF) \pm a given number of feet), and different times in the fuel cycle (beginning-of-cycle (BOC) and end-of-full-power-life (EOFPL)). Table 1.1 summarizes the specific cases considered. In the context of this study, the nominal core flows for the BOC and the EOFPL conditions are assumed, respectively, to be 85% and 105% of the

rated flow. Results of the sensitivity cases listed in Table 1.1 are compared with results of the corresponding reference cases we presented in a previous report [4].

Table 1.1 Simulation Conditions of the ATWS-ED Sensitivity Cases

| Case ID | Exposure | Core Flowrate, % | Reactor Water Level Strategy | SLCS Injection |
|---------|-----------------------------|------------------|------------------------------|----------------|
| 4B | BOC | 75 ¹ | TAF+5 | Lower Plenum |
| 10D | EOFPL | 75 ¹ | TAF-2 | Lower Plenum |
| 10A | EOFPL | 85 ² | TAF+5 | Lower Plenum |
| 11A | EOFPL | 85 ² | TAF | Lower Plenum |
| 12A | EOFPL | 85 ² | TAF-2 | Lower Plenum |
| 10C | EOFPL UHSPH ³ | 105 | TAF+5 | Lower Plenum |

¹ No adjustment made to the control rod bank to achieve criticality (requested by the NRC)

² Upper-peaked power shape in the allowable operating domain

³ Void history spectrally corrected (UHSPH)

1.3 **Methodology**

The methodology used in the present study is the same as that used in our previous ones [2, 4] where it was explained in detail. Our basic tool is TRACE/PARCS that couples the modeling of thermal-hydraulics throughout all relevant reactor components (TRACE) with modeling the neutronics in the core (PARCS). The applicability of the code package to ATWS was assessed and confirmed [5]; previous studies [2, 3, 4] offered additional insights into its capability. Indeed, one of the objectives of those studies was to further assess the capabilities of TRACE/PARCS to calculate the phenomena associated with BWR ATWS events under MELLLA+ conditions.

The reactor systems/components that we model are the following: the steam line, including the turbine bypass and stop valves, the safety/relief valves, and the main steam isolation valves; the recirculation loop, including the recirculation pumps; the feedwater and reactor water level control; the reactor core isolation cooling with an option to draw from the condensate storage tank or the suppression pool; the standby liquid control system; the primary containment (drywell and wetwell) with pool cooling; and, the vessel, including its core, steam separator/dryer, and jet pumps.

The core requires detailed attention and, in the neutronics model, each fuel bundle is individually represented. In the thermal-hydraulic model, we lump the bundles into 27 thermal-hydraulic channel groups. Nuclear data for each bundle are a function of thermal-hydraulic variables, and the presence of control blades and soluble boron. The models for three different times in the fuel cycle are available: BOC, peak-hot-excess-reactivity (PHE), and EOFPL. Within each bundle, four different types of fuel rods are modeled.

We assessed the validity of these models partly by comparing the steady-state results for power distributions with those obtained by the vendor, GE-Hitachi (GEH). They also are compared with those obtained using 382 thermal-hydraulic channel groups, as we used for the ATWS-I studies. The results are documented in [4].

1.4 Organization of Report

Chapter 2 contains our analysis of the sensitivity calculations, including our consideration of the effect of reduced core-operating flow and the effect of the spectrally corrected moderator density history (void history). We give our conclusions in Chapter 3 and references in Chapter 4. Appendix A compares the results from two versions of the TRACE executable that we used in this study. Appendix B explores the sensitivity of the ATWS-ED results to two aspects of the TRACE numerical computation, the numerical scheme employed and the size of the time-step.

2 SENSITIVITY STUDIES FOR MSIV CLOSURE EVENTS

2.1 Introduction

We conducted sensitivity studies to evaluate the effects of reduced core flow and of spectrally corrected moderator density history (void history). Table 2.1 lists all the ATWS-ED transients that we analyzed. The findings from the first eleven cases therein were presented in a previous report [4] and are considered the base reference cases. The remaining six are the sensitivity cases (as listed in Table 1.1) and are the subject of this report.

Table 2.1 Simulation Conditions of ATWS-ED Cases

| Case ID | Exposure | Core Flowrate, % | Reactor Water Level Strategy | SLCS Injection |
|--|-----------------------------|------------------|------------------------------|----------------|
| 6 | BOC | 85 | TAF-2 | Lower Plenum |
| 7 | PHE | 85 | TAF+5 | Lower Plenum |
| 4 | BOC | 85 | TAF+5 | Lower Plenum |
| 7C | PHE | 85 | TAF+5 | Upper Plenum |
| 5 | BOC | 85 | TAF | Lower Plenum |
| 10 | EOFPL | 105 | TAF+5 | Lower Plenum |
| 12 | EOFPL | 105 | TAF-2 | Lower Plenum |
| EDSI ¹ | BOC | 85 | TAF | Lower Plenum |
| 9 | PHE | 85 | TAF-2 | Lower Plenum |
| 8 | PHE | 85 | TAF | Lower Plenum |
| 11 | EOFPL | 105 | TAF | Lower Plenum |
| Listed Below are the Current Sensitivity Cases | | | | |
| 4B | BOC | 75 ³ | TAF+5 | Lower Plenum |
| 10D | EOFPL | 75 ³ | TAF-2 | Lower Plenum |
| 10A | EOFPL | 85 ⁴ | TAF+5 | Lower Plenum |
| 11A | EOFPL | 85 ⁴ | TAF | Lower Plenum |
| 12A | EOFPL | 85 ⁴ | TAF-2 | Lower Plenum |
| 10C | EOFPL UHSPH ² | 105 | TAF+5 | Lower Plenum |

¹ Simulation with semi-implicit (S-I) numerics

² Void history spectrally corrected (UHSPH)

³ No adjustment made to the control rod bank to achieve criticality (requested by the NRC)

⁴ Upper-peaked power shape in the allowable operating domain

The analysis of the sensitivity cases utilized the same TRACE/PARCS models as those we previously employed in our ATWS-ED studies [4] the models, summarized in Section 1.3, are explained in detail in [4]. The same input model was used in all six sensitivity cases; however, they were analyzed using three different executable versions of TRACE, as denoted for each case in Table 2.2.

Table 2.2 Version of TRACE Executable Used

| Case ID | Exposure | Core Flowrate, % | Reactor Water Level Strategy | TRACE Executable |
|----------------|-----------------|-------------------------|-------------------------------------|-------------------------|
| 4B | BOC | 75 | TAF+5 | V5.540_fxValveChoke.x |
| 10D | EOFPL | 75 | TAF-2 | V5.0p3P32m07co_x64.exe |
| 10A | EOFPL | 85 | TAF+5 | V5.540_fxValveChoke.x |
| 11A | EOFPL | 85 | TAF | V5.540_fxValveChoke.x |
| 12A | EOFPL | 85 | TAF-2 | V5.0p3P32m07co.x |
| 10C | EOFPL UHSPH | 105 | TAF+5 | V5.540_fxValveChoke.x |

The Linux and Windows executables are identified by their filename extensions “.x” and “.exe” respectively. All eleven of the base reference cases were analyzed via V5.540_fxValveChoke.x, a version that is very similar to the latest released version of TRACE (V5.541 is V5 Patch 3). However, this version of the executable failed to complete two of the EOFPL cases at reduced flow (75% and 85%) with water-level reduction to TAF-2. The difficulty appears to be related to failure of PARCS to converge when the reactor power is at decay heat levels. We subsequently utilized a revised version of TRACE, V5.0p3P32m07co, to complete the two TAF-2 sensitivity cases. The following are two of the relevant changes made in the PARCS module of TRACE that enabled us to complete the TAF-2 simulations:

1. A limiter was added to the assembly discontinuity factor (ADF) adjustment factor, on the left and right faces of the considered node.
2. For the nodal expansion method (NEM) kernel, we also placed a limit on the lowest value for surface flux.

Appendix A has further discussions on using different TRACE executables in the simulation of ATWS-ED transients.

In addition to using a modified version of TRACE, the simulation of the two TAF-2 sensitivity cases required the following changes in executing the transient:

1. For the EOFPL 85% flow TAF-2 case, the Linux executable, V5.0p3P32m07co.x, terminated due to a failure in the thermal-hydraulic calculation for the CONTAN component. We changed the CSTEP input for the CONTAN from 1.0 to 0.5 to successfully eliminating the execution error. We note that no error was experienced in the Windows executable, even without the input change.
2. A power spike was observed at about 700 s in the EOFPL 75% flow TAF-2 case using the Linux executable, V5.0p3P32m07co.x. We are no longer investigating the cause of the anomaly; the transient was simulated successfully to completion by using the equivalent executable for the Windows platform, namely V5.0p3P32m07co_x64.exe.
3. We analyzed all three EOFPL TAF-2 cases, the 105% flow (base reference case), the 85% flow, and the 75% flow, using the semi-implicit (S-I) numerical scheme with a maximum time-step size of 0.02 s. Our attempts failed to run the cases using the stability enhancing two-step method (SETS) with a maximum time-step size of 0.01 s.

Appendix B examines the sensitivity of the results to the numerical scheme and to the maximum time-step size. It includes the findings from a sensitivity study, cited in footnote b in [4], examining the impact of the size of the time-step and the numerics on the natural circulation flow through the core and the downcomer.

The ATWS with emergency depressurization (ATWS-ED) of interest is initiated by a spurious closure of the main steam isolation valves (MSIVs) with subsequent failure of the reactor protection system (RPS) to SCRAM the reactor. The same ATWS-ED scenario, as used in the previous report [4] and summarized in Table 2.3, was applied to the sensitivity cases.

Table 2.3 ATWS-ED Scenario

| Event | Timing/Setpoint |
|--------------------------------|--|
| Begin transient simulation | 0.0 s |
| MSIV closure | 10.0 s (0.5 s delay + 4 s closure time) |
| Recirculation pump trip (2RPT) | Reactor pressure vessel (RPV) pressure exceeds 7.651 MPa |
| SRVs cycling | See Table 2.4 in [4] |
| Reactor water level reduction | 130.0 s |
| Begin boron injection | 211.0 s |
| Emergency depressurization | Suppression pool temperature exceeds 344.26 K |
| Reactor water level recovery | 2180.0 s |
| End of simulation | 2500.0 s |

We note that the scenario includes four actions by the operator [4].

1. Water level control to top-of-active-fuel (TAF), to TAF plus five feet (TAF+5), or TAF minus two feet (TAF-2). This is accomplished at 130 s by artificially raising the calculated water level by a fixed amount (over a 0.1 s interval), and feeding it into the water-level control system.
2. Boron injection. This is initiated at 211 s and linearly ramped to full flow within 60 s.
3. Emergency depressurization (ED). Operator actuation of the automatic depressurization system (ADS) is triggered when the heat capacity temperature limit (HCTL) of the suppression pool reaches a simulated setpoint at 344.26 K.
4. Water level recovery to normal water level. This is accomplished at 2180 s by reducing the artificial water level adjustment to zero over 100 seconds.

All transient cases were run as a restart case from a TRACE/PARCS-coupled steady-state. We give details for executing the code in Section 2.1 of [4]. The initial steady-state conditions for the sensitivity cases were established earlier and are reported in [4]. Table 2.4 identifies the corresponding sections in [4] that provide the initial steady-state results for the sensitivity cases.

Table 2.4 Reference for the Initial Steady-State

| Case ID | Exposure | Core Flowrate, % | Reactor Water Level Strategy | Sections in [Error! Reference source not found.] that Describe the Initial Steady-State Conditions |
|----------------|-----------------|-------------------------|-------------------------------------|---|
| 4B | BOC | 75 | TAF+5 | Section 3.1.4 |
| 10D | EOFPL | 75 | TAF-2 | Section 3.3.5 |
| 10A | EOFPL | 85 | TAF+5 | Section 3.3.5 |
| 11A | EOFPL | 85 | TAF | Section 3.3.5 |
| 12A | EOFPL | 85 | TAF-2 | Section 3.3.5 |
| 10C | EOFPL UHSPH | 105 | TAF+5 | Section 3.3.4 |

The general progression of all cases is similar and a synopsis of the ATWS-ED transient is provided in Section 4.1 of [4]. Descriptions of the representative base cases for the BOC and EOFPL cycle conditions, respectively, are set out in Sections 4.2 and 4.4 of [4].

The results of the six sensitivity cases are compared with their corresponding base reference cases and with each other. In the context of the sensitivity study, these base reference cases have the following initial core flows as defined in [4].

BOC: 85% of rated flow

EOFPL: 105% of rated flow

Section 2.2 compares Case 4B to Case 4 [BOC TAF+5: 75% and 85% (the reference case) flow]. Section 2.3 discusses the effect of the spectrally corrected void history, comparing Cases 10C and 10 [EOFPL TAF+5: UHSPH and UH (the reference case)]. Section 2.4 examines the effects of reduced core flow at EOFPL, comparing Cases 10D, 12A and 12 [EOFPL TAF-2: 75%, 85% and 105% (the reference case) flow]. Finally, Section 2.5 compares the three EOFPL cases at 85% flow, Cases 10A, 11A and 12A (EOFPL 85% flow: TAF+5, TAF and TAF-2).

2.2 Effect of Reduced Core Flow at BOC

We examined the effect of reduced core flow at BOC in a case (Case 4B) with initial core flow at 75% rated (which is lower than, and thus bounding of, the lowest core flow allowable along the MELLLA+ upper boundary in the power-flow operating map at the highest allowable power level), along with a water level strategy of TAF+5. This sensitivity case is compared with the results of the reference case, Case 4, which was detailed in [4]. Our implementation of the reduced core flow at BOC in the TRACE BWR model was discussed in Section 3.1.4 in [4]. Figure 2.1 and Figure 2.2, reproduced from [4], show the distribution of steady-state axial power and axial moderator density as calculated by PARCS for different initial core flows at BOC. The results demonstrate that reducing the core flow shifts the boiling boundary downward axially in the core. This shift also slightly shifts the power generation downward.

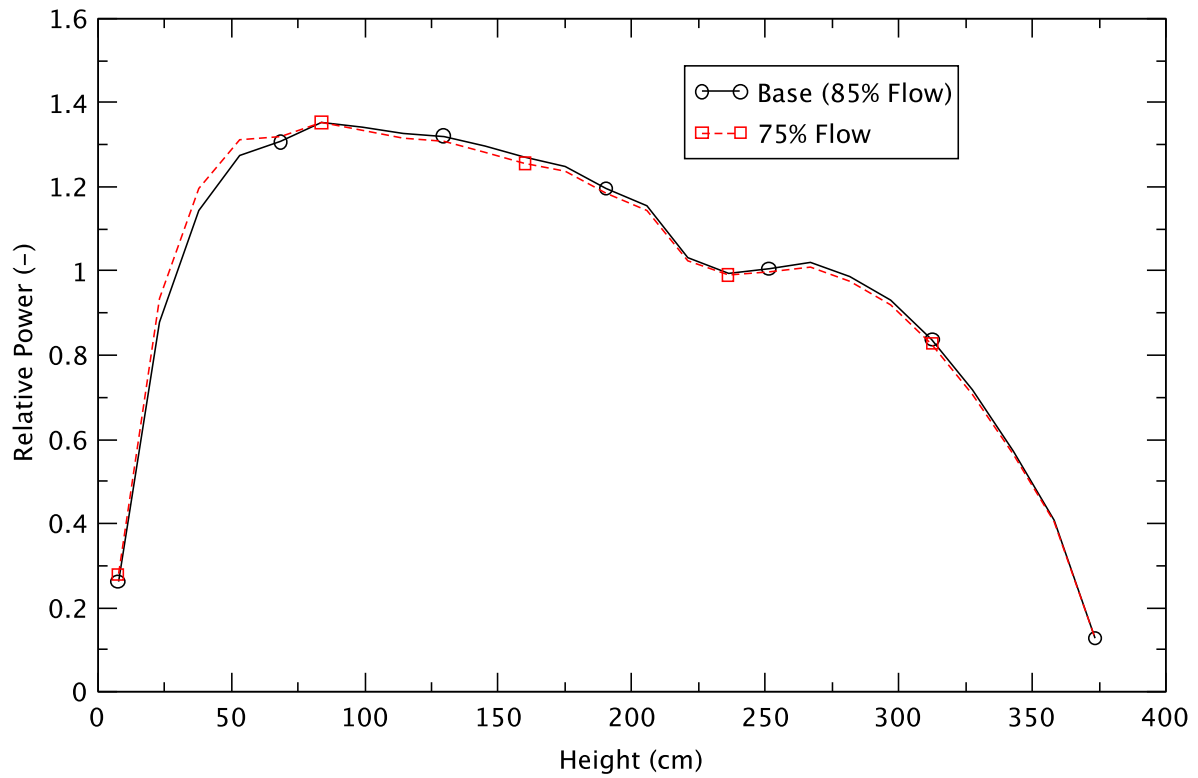


Figure 2.1 Radially Averaged Axial Power Distribution at BOC - Effect of Reduced Flow

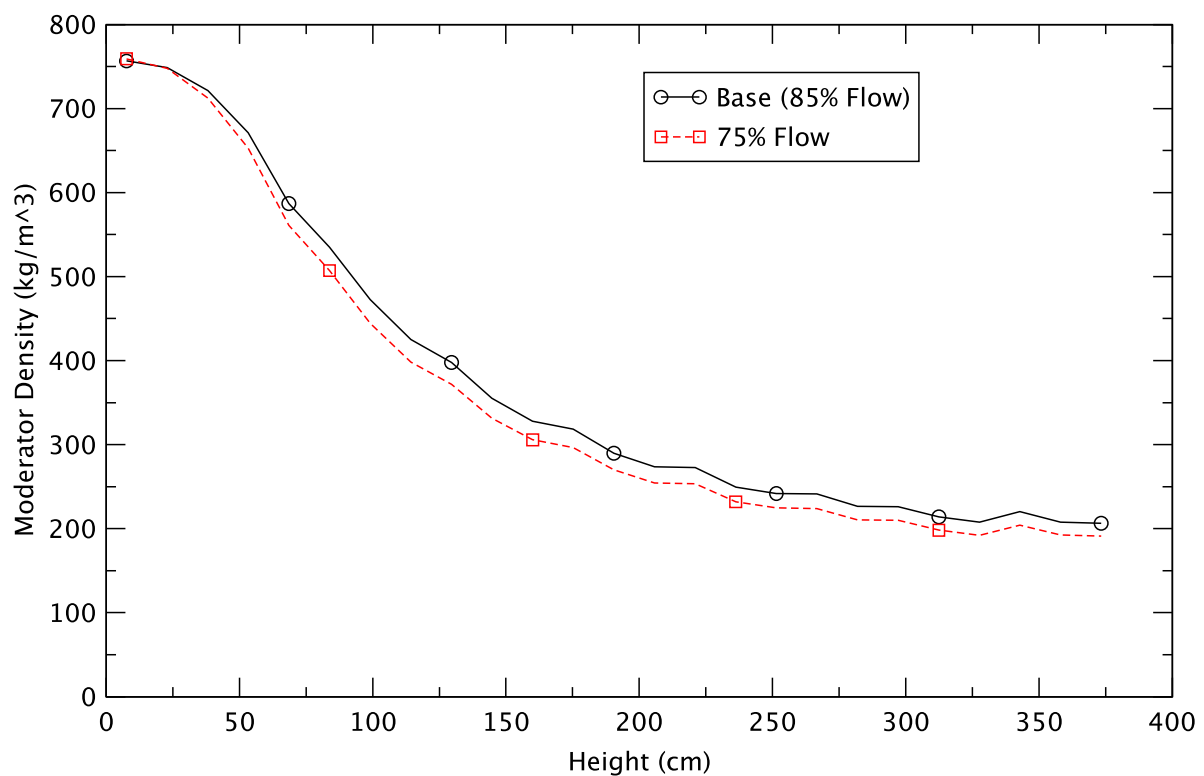


Figure 2.2 Radially Averaged Axial Moderator Density at BOC - Effect of Reduced Flow

The progression of the ATWS-ED transient exhibited by the sensitivity case is, in general, similar to the reference case; Table 2.5 compares some of their key results. The most significant difference between the two cases is in the maximum peak clad temperature (PCT, TRACE output parameter trhmax); the sensitivity case reaches a PCT of 1389 K, compared to 639 K for the reference case. A select set of plots (Figure 2.3 to Figure 2.13) compares and contrasts the transient responses of the two cases.

Table 2.5 Comparison of Key Results for BOC, TAF+5 Cases

| Key Event | 75% Flow | 85% Flow |
|---|-------------------|-------------------|
| Maximum PCT (trhmax-100) | 1389 K (158 s) | 639 K (147 s) |
| Core boron inventory (CB-359 (user defined TRACE control block output) > 0.01 kg) | 245 s | 245 s |
| Emergency depressurization | 266 s | 297 s |
| Maximum drywell pressure | 0.174 MPa (793 s) | 0.170 MPa (772 s) |
| Reactor shutdown (power remains <3.25% of initial power) | 1046 s | 975 s |
| Maximum suppression pool temperature | 372 K (1902 s) | 368 K (2156 s) |

The reactor power, shown in Figure 2.3 and in Figure 2.4 on an expanded time-scale, generally exhibits similar responses for the two cases. However, in the early phase of the transient, the sensitivity case (75% core flow) exhibits a slightly higher power than the reference case (85% flow). The higher core power after the recirculation pump trip (2RPT) for the reduced flow case reflects its higher total reactivity (compare Figure 2.5 to the reference case). The higher core power for the sensitivity case also is reflected in the earlier depressurization time and higher maximum drywell pressure and higher maximum suppression pool temperature (Table 2.5).

There is a break point in the power response for the reference case at about 500 s, while the sensitivity case shows a smoother decay after depressurization. A review of the total reactivity for the two cases (Figure 2.5) reveals slightly different behavior after the emergency depressurization. For the reference case, the total reactivity fluctuates very close to zero (null reactivity) between about 450 s to 500 s and then stays negative (on average) throughout the rest of the transient. For the sensitivity case, the total reactivity stays negative for the entire period after emergency depressurization. These different power transients most likely are due to the differences in the response of void reactivity to void formation as a result of the depressurization. Other components of the reactivity, including void reactivity (dm, moderator density), fuel reactivity (Tf, Doppler) and boron reactivity, are shown in Figure 2.6 for the sensitivity case. All the reactivity components in the two cases exhibit similar time dependence.

Figure 2.7 shows the reactor pressure. An earlier depressurization time for the sensitivity case is consistent with its higher reactor power relative to that of the reference case.

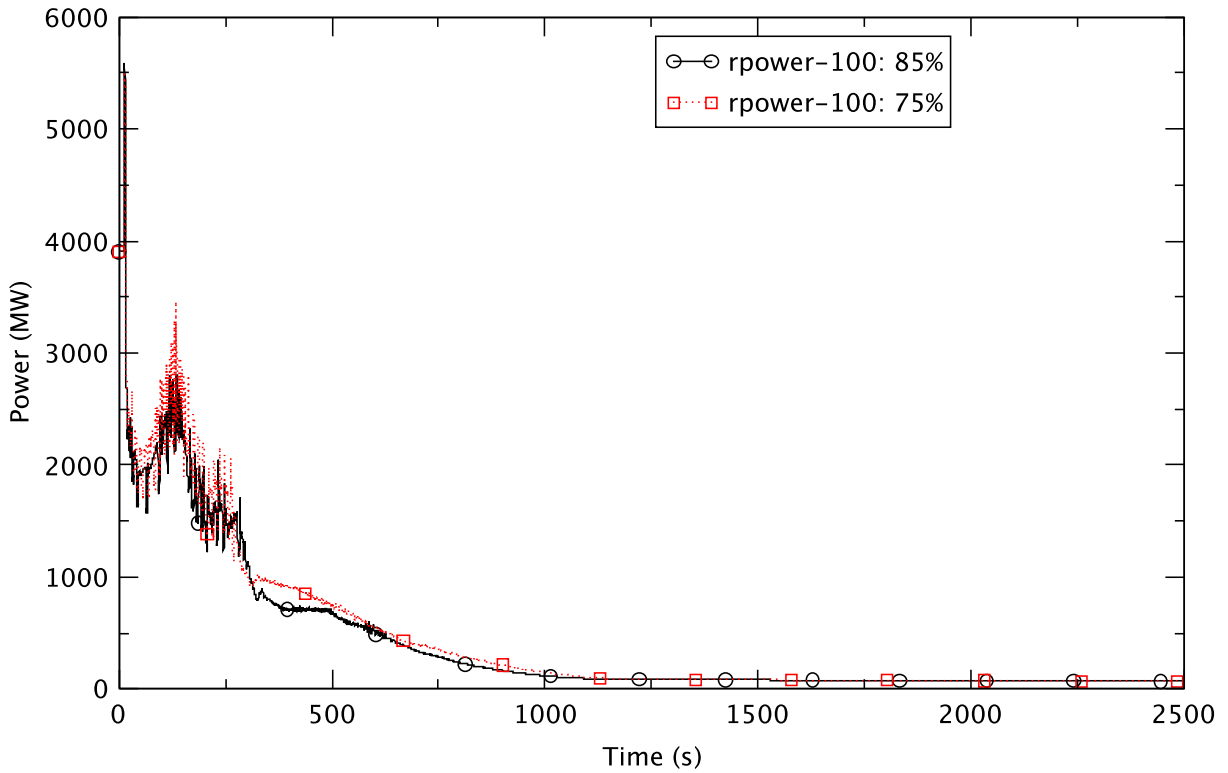


Figure 2.3 Reactor Power - BOC, TAF+5, 85% & 75% Flow

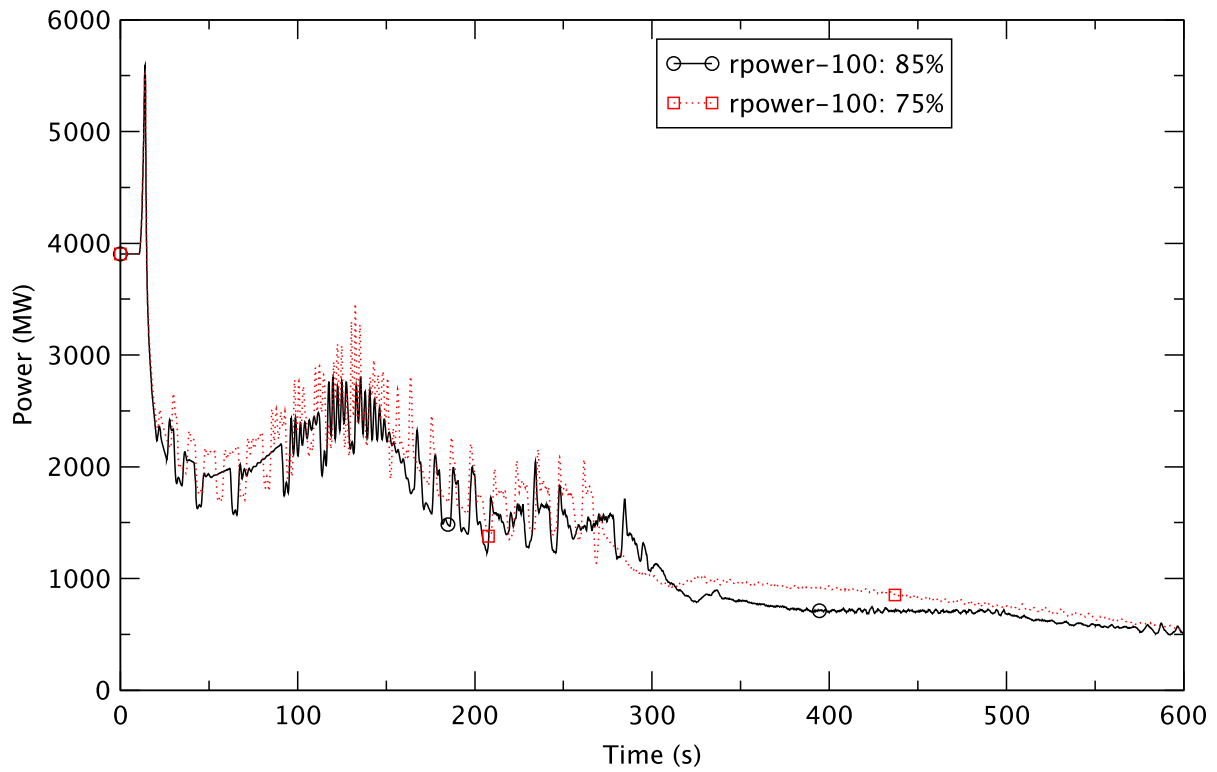


Figure 2.4 Reactor Power - Early Phase of Transient

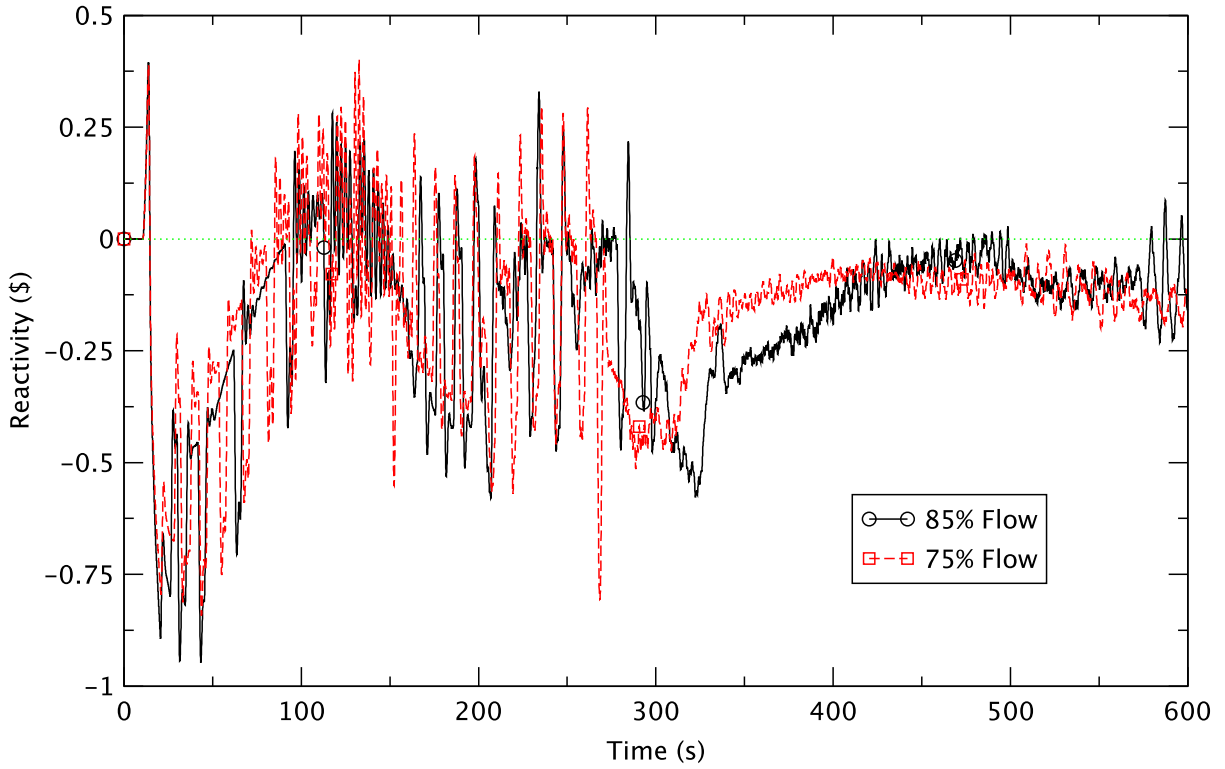


Figure 2.5 Total Reactivity - BOC, TAF+5, 85% & 75% Flow

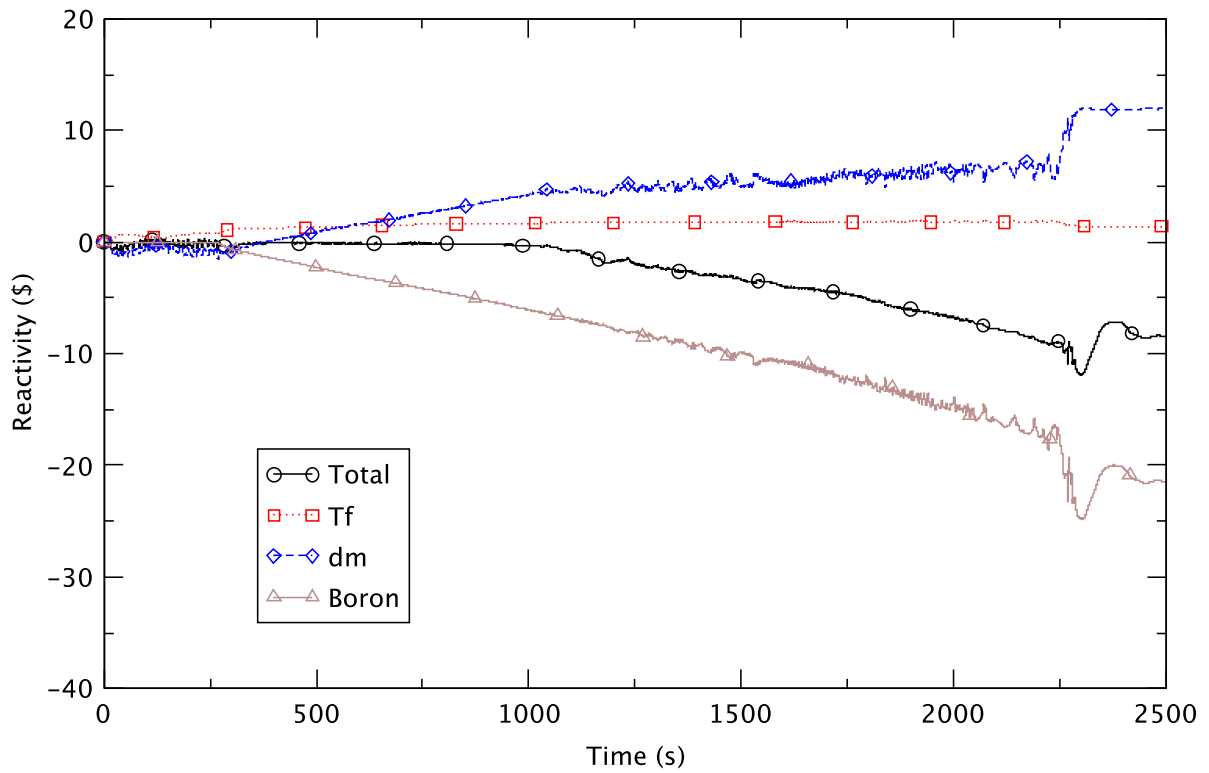


Figure 2.6 Core Reactivity - BOC, TAF+5, 75% Flow

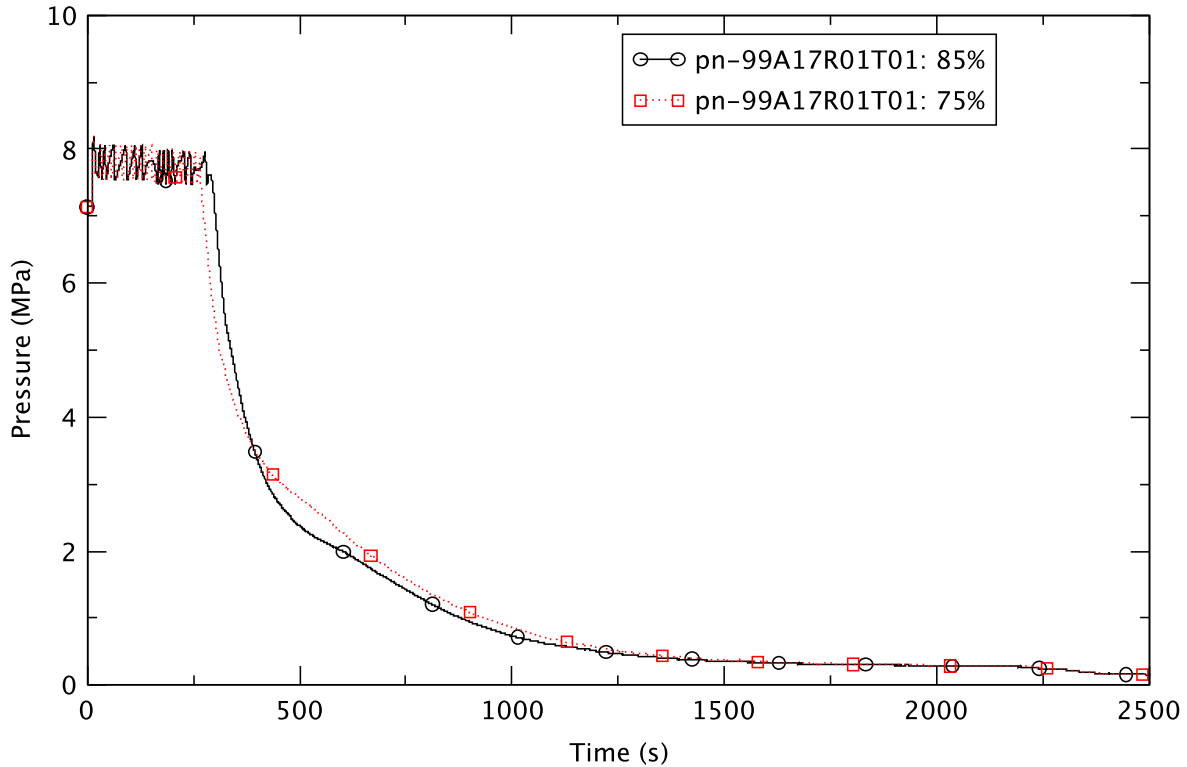


Figure 2.7 Reactor Pressure - BOC, TAF+5, 85% & 75% Flow

We compare the results of the core flow and the downcomer water level for the two cases, respectively, in Figure 2.8 and Figure 2.9. The sudden decrease in flow at 10s, shortly after the closure of the MSIVs, is due to the 2RPT. A further drop in core flow is noticed after the initiation of water level control to TAF+5 at 130 s. Natural circulation flow appears to be preserved for both cases after emergency depressurization at 266.4 s and 296.7 s, respectively, for the sensitivity case and the reference case. After about 1000 s, the core power in both cases has fallen sufficiently for the core to be refilled with water. This sets up a manometer-type oscillation (driven by the difference in the density head between the downcomer and the core) in the downcomer water level. The oscillation is evident in the fluctuations in the water level (Figure 2.9) between about 1000 s and 1500 s. During that period, the oscillating core flow (Figure 2.8) also trends to a decrease.

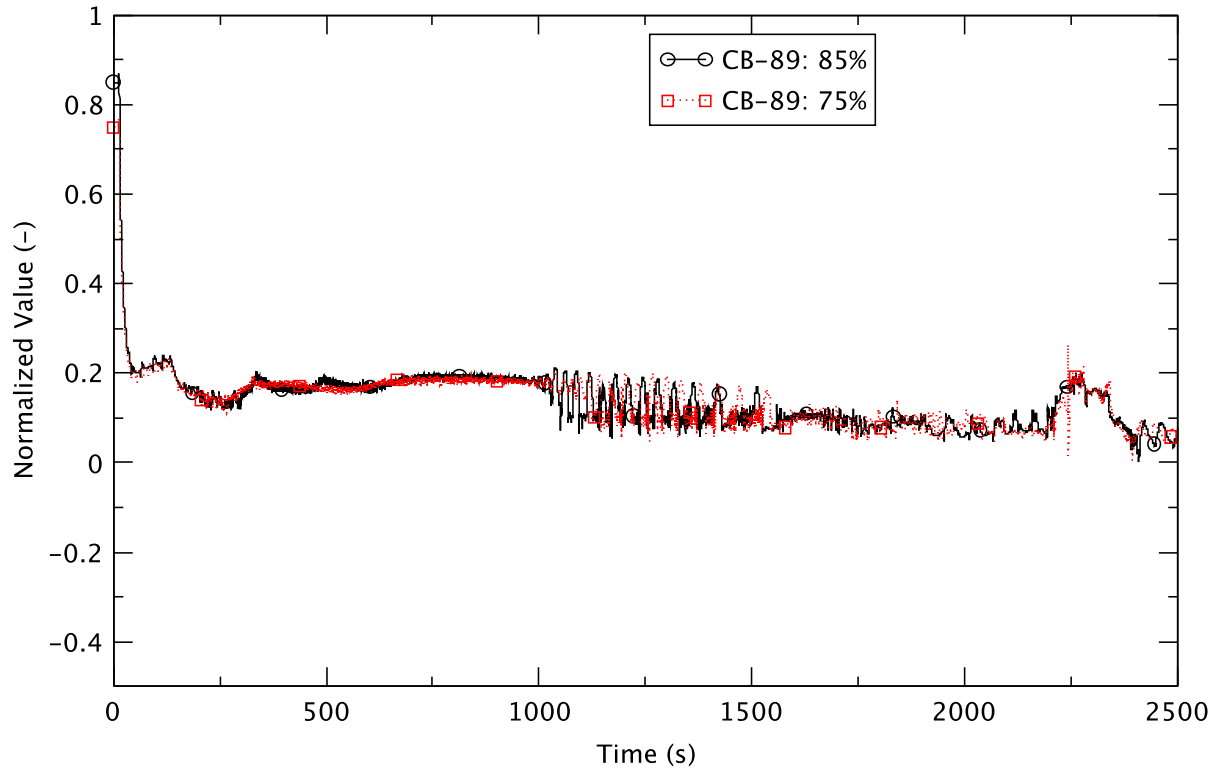


Figure 2.8 Core Flow - BOC, TAF+5, 85% & 75% Flow

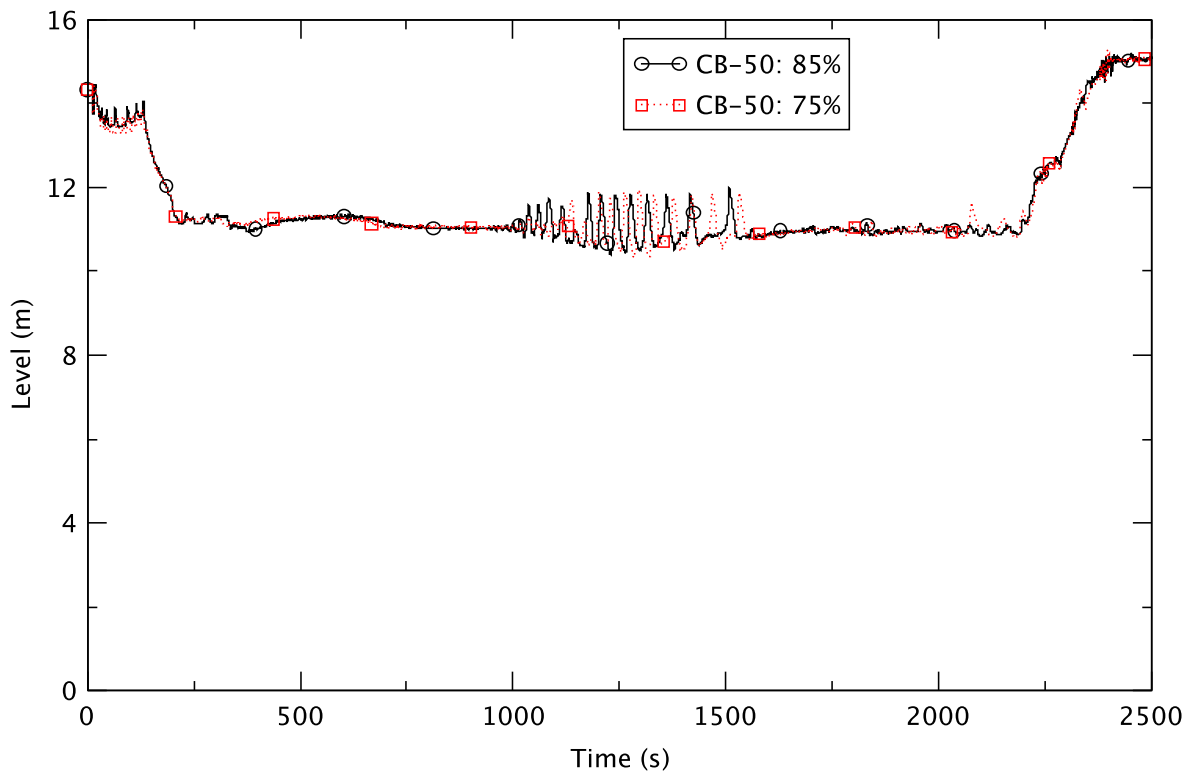


Figure 2.9 Downcomer Water Level - BOC, TAF+5, 85% & 75% Flow

Boron inventory in the core for both cases is shown in Figure 2.10. For both, the boron inventory increases with time. During mitigation, we assume that the operators maintain the downcomer water at a level sufficiently high to maintain natural circulation flow through the lower plenum. This flow will suffice to entrain all of the borated solution injected into the lower plenum through the SLCS, so resulting in the steady increase of boron inventory in the core.

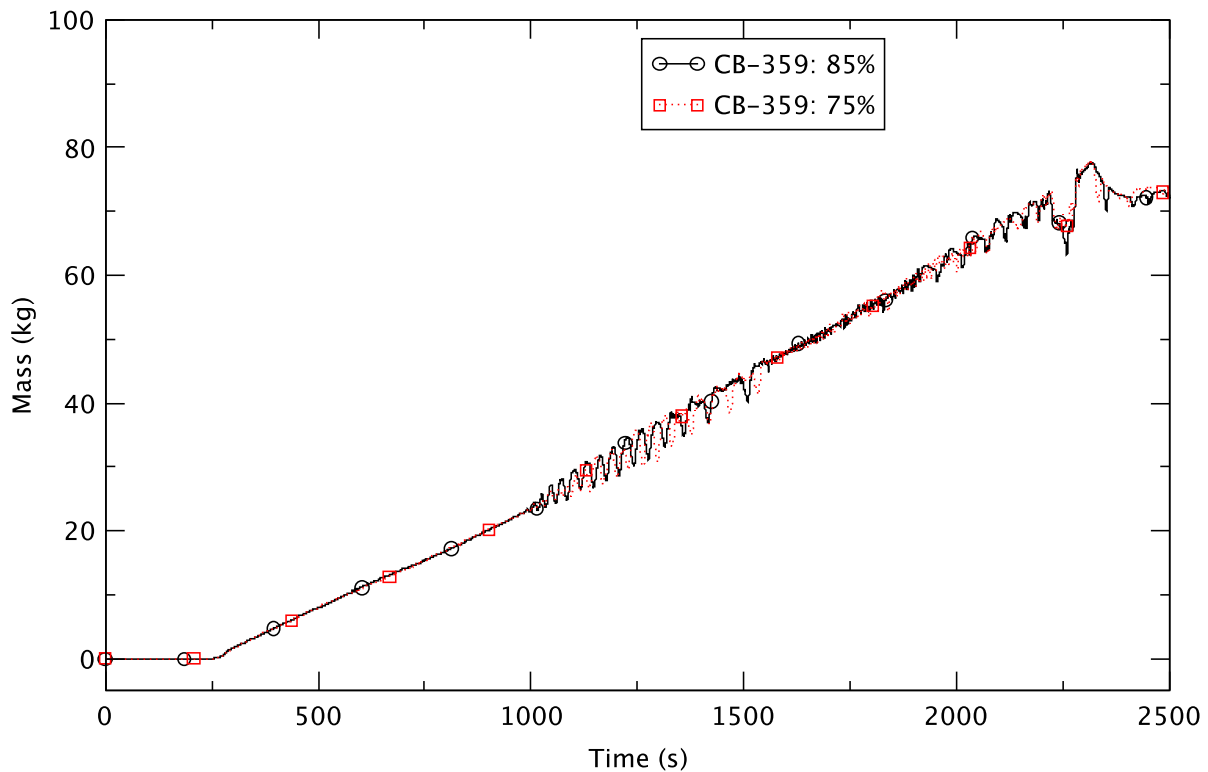


Figure 2.10 Boron Inventory in the Core Region - BOC, TAF+5, 85% & 75% Flow

As discussed earlier, the maximum PCT for the sensitivity case is more limiting than for the reference case. Figure 2.11 shows the maximum PCT for both, revealing that the incidence of dryout occurs at similar times, right after level control is initiated when core flow is decreasing. In the lower flow case, the cladding surface fails to rewet for several hundred seconds whereas in the higher flow case, there is periodic heat-up and rewet. The behavior of the PCT is consistent with the higher power for the lower flow case compared to that for the higher flow case. The maximum PCT for the core remains almost identical for the two cases after rewet is complete for all fuel rods.

The suppression pool water temperature (Figure 2.12) is a gauge for quantifying the cumulative energy relieved into the pool via the SRVs. The higher pool temperature exhibited by the sensitivity case is indicative of higher power relative to the reference case.

The transient response of the drywell pressure (Figure 2.13), with a higher maximum pressure for the sensitivity case, again is consistent with the observation that at reduced core flow (75%), the transient core power is higher than that in the reference case (85% flow).

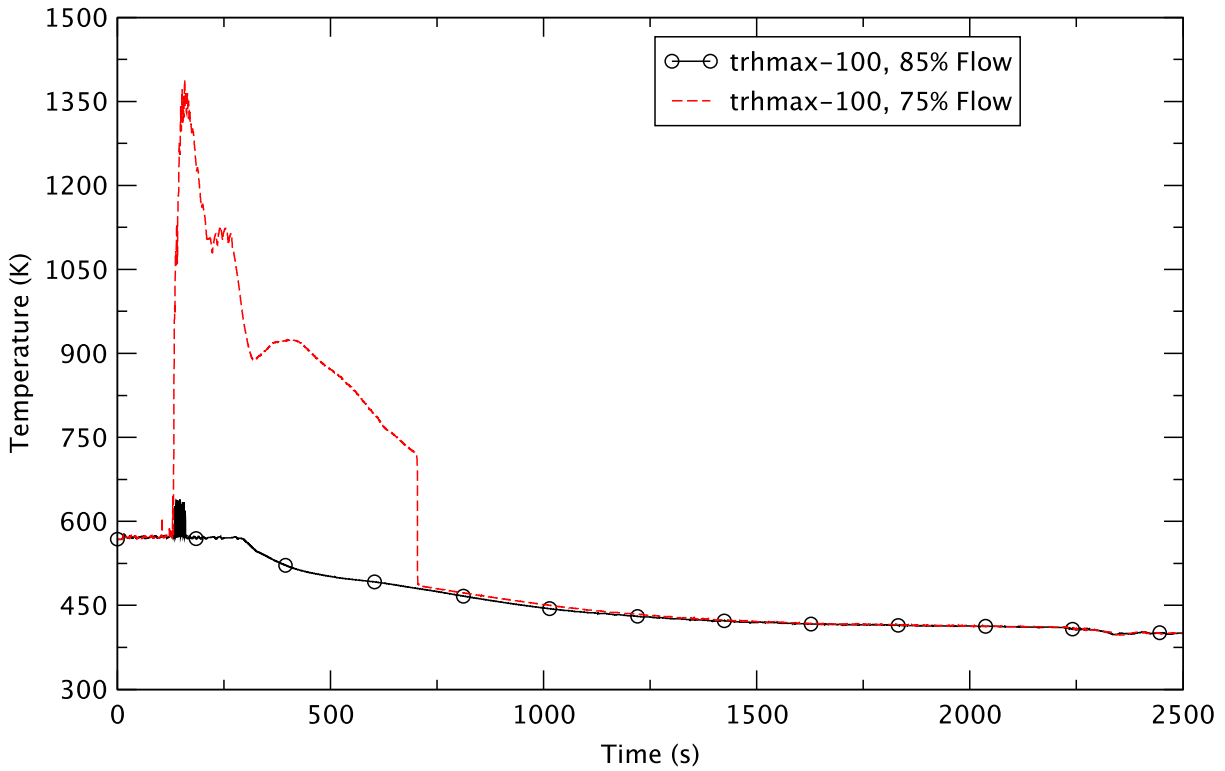


Figure 2.11 Peak Clad Temperature - BOC, TAF+5, 85% & 75% Flow

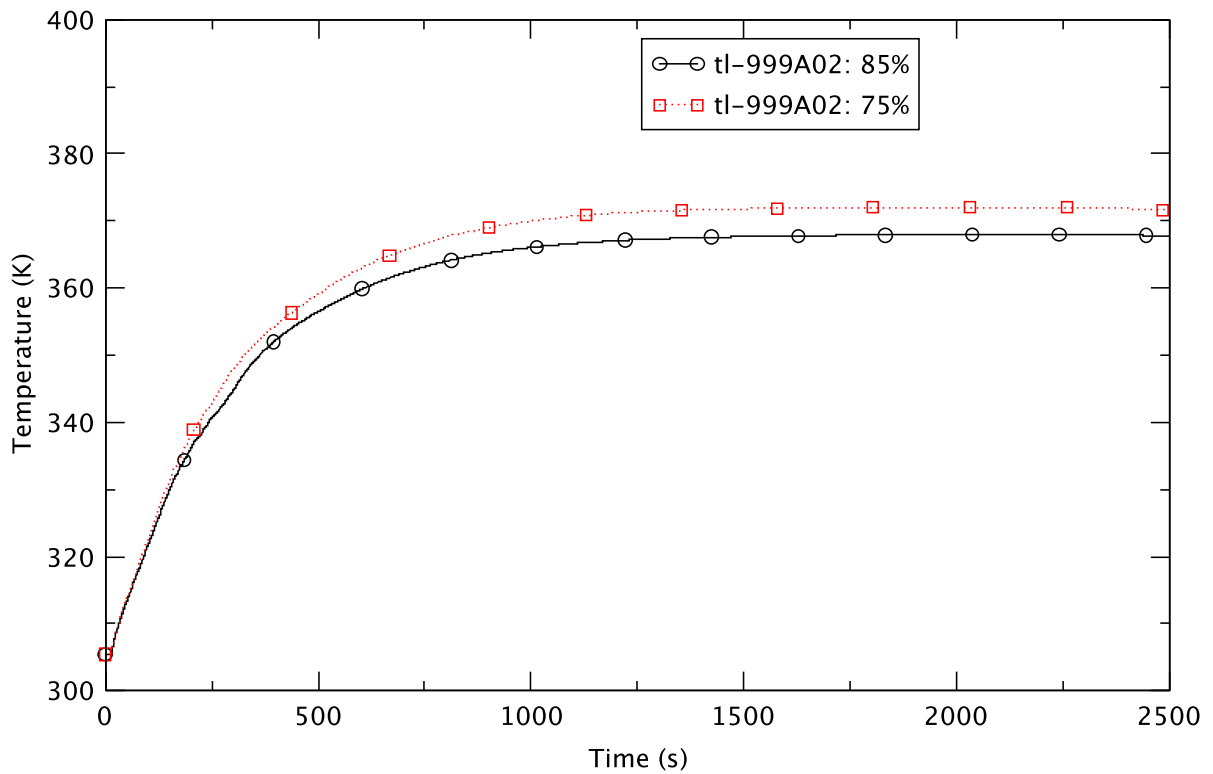


Figure 2.12 Suppression Pool Temperature - BOC, TAF+5, 85% & 75% Flow

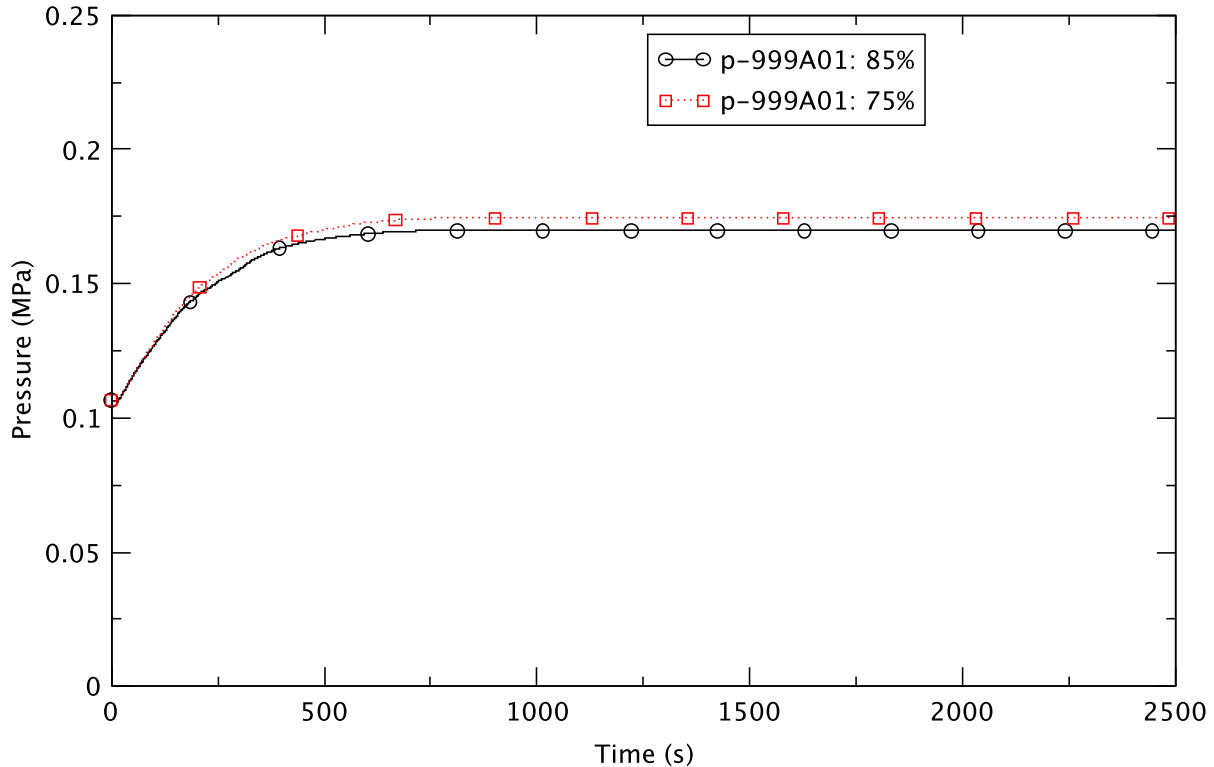


Figure 2.13 Drywell Pressure - BOC, TAF+5, 85% & 75% Flow

Our findings from the TRACE analysis indicate that even at reduced core flow the reactor remains shutdown due to the injected boron. There is no re-establishment of criticality, due to either the repressurization of the reactor vessel or dilution of the boron. Though the maximum PCT shows a significant increase at reduced core flow relative to the reference case, its magnitude still is 89 K below the 1478 K (2200°F) limit¹. Both the temperature of the suppression pool and the drywell's pressure stay below their limits.

2.3 Effect of Void History Modeling at EOFPL

The cross sections used by PARCS depend on several instantaneous variables, namely, control rod insertion, moderator density, fuel temperature, and boron concentration. They also depend on exposure (MWd/t) to account for burnup, and one or more other “history” parameters, so to correct for the effect of the neutron energy spectrum during burnup on the instantaneous cross-sections. The history parameter used to generate the cross sections for PARCS is the moderator density history (equivalent to the void history, UH). Another parameter that might be important to correct for energy spectrum changes during burnup, is the history of control rod position. GEH developed an approach accounting for the spectral history of the node by artificially changing the void history to provide an equivalent spectral effect.

In order to assess the effect of this correction, an EOFPL sensitivity case is run, replacing the UH distribution used with the cross section set in PARCS by a “void history spectrally corrected” (UHSPH) distribution provided by GEH. The implementation of the spectrally-corrected

¹ For beyond- design-basis ATWS events, there are no regulations explicitly limiting temperature. The acceptance criteria for ATWS evaluations are discussed in the NRC staff's standard review plan (NUREG-0800) [6]. The 1478 K temperature acceptance criterion therein for ATWS applies only to new plants; we use it herein as a reasonable informal limit.

moderator density history in the TRACE BWR model has been discussed in Section 3.3.4 in [4] Figure 2.14, reproduced from [4], compares the steady-state distribution of axial power calculated by PARCS for the EOFPL condition using the UH and the UHSPH moderator density histories. The results are essentially the same for the two void histories.

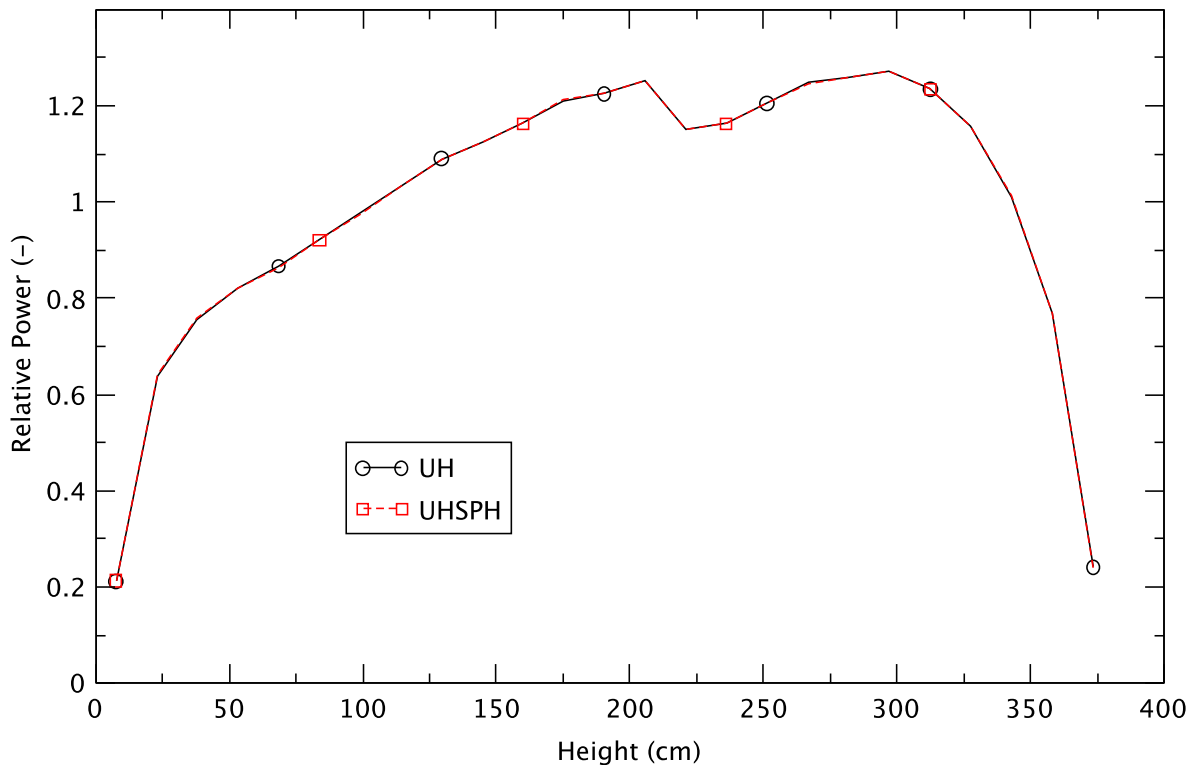


Figure 2.14 Radially Averaged Axial Power Distribution at EOFPL, Effect of Spectrally Corrected Void History

The EOFPL sensitivity case that utilized the UHSPH moderator density history is Case 10C with a TAF+5 water level control strategy. The corresponding reference case is Case 10, one of the base cases presented in [4].

Table 2.6 compares some of the key results for the two cases. A select set of plots (Figure 2.15 to Figure 2.22) compares and contrasts the transient responses of the two cases. The progression of the ATWS-ED transient exhibited by the sensitivity case essentially corresponds to the reference case. Discussions of the EOFPL ATWS-ED cases in Section 4.4 in [4] thus are applicable to the sensitivity case and are not repeated here.

Based on the simulation results, the two cases (UH and UHSPH) essentially are the same, and thus, the EOFPL ATWS-ED TAF+5 case is not sensitive to the GEH spectral correction to the void history (moderator density history). The assessment of the correctness of the GEH approach to this correction is outside the scope of the current analysis.

Table 2.6 Comparison of Key Results for EOFPL, TAF+5 Cases

| Key Event | UHSPH | UH |
|---|-------------------|-------------------|
| Maximum PCT (trhmax-100) | 577 K (14.3 s) | 577 K (14.3 s) |
| Core boron inventory (CB-359 (user defined TRACE control block output) > 0.01 kg) | 246 s | 246 s |
| Emergency depressurization | 404 s | 403 s |
| Maximum drywell pressure | 0.162 MPa (588 s) | 0.162 MPa (588 s) |
| Reactor shutdown (power remains < 3.25% of initial power) | 950 s | 937 s |
| Maximum suppression pool temperature | 359 K (2298 s) | 359 K (2288 s) |

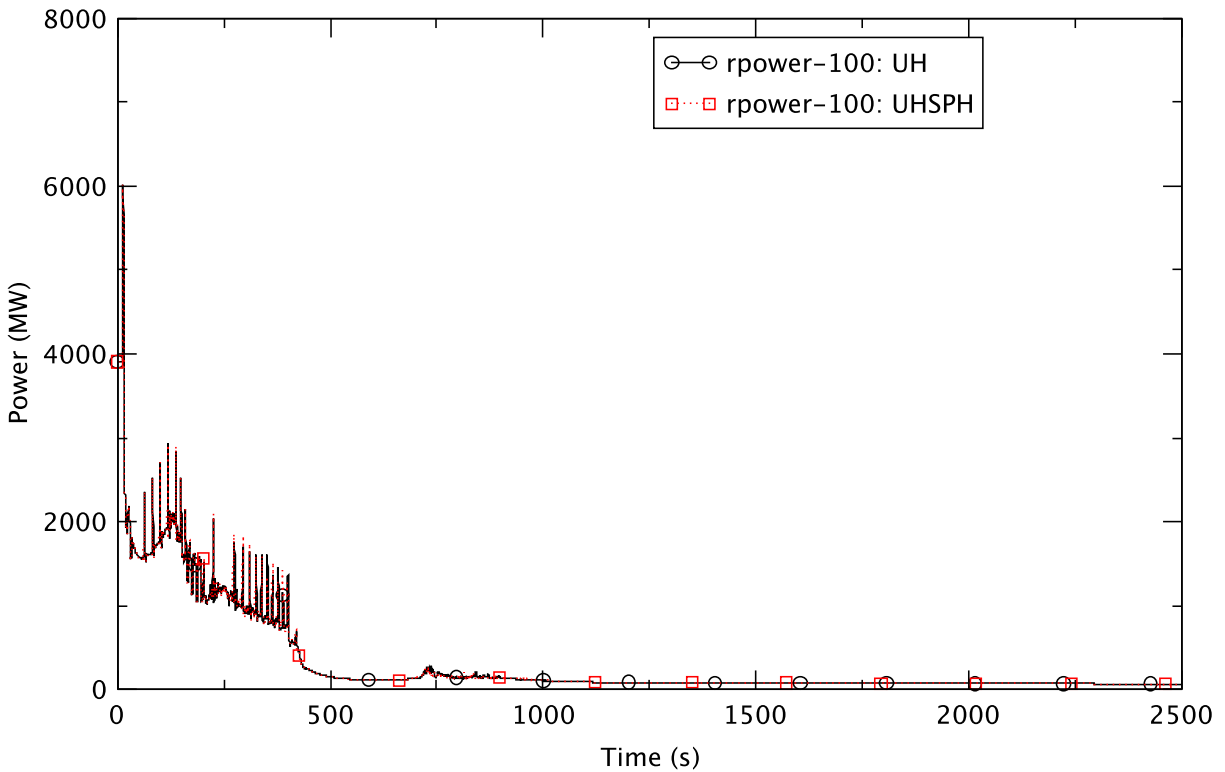


Figure 2.15 Reactor Power - EOFPL, TAF+5, UH & UHSPH

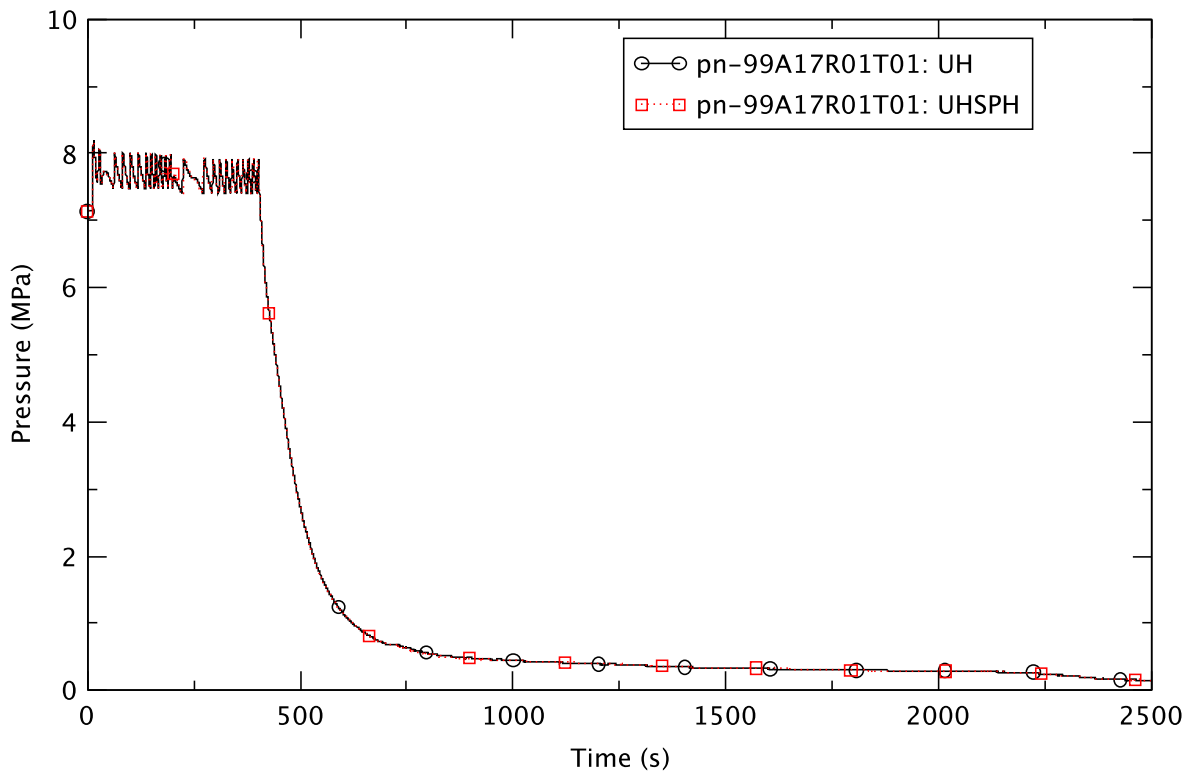


Figure 2.16 Reactor Pressure - EOFPL, TAF+5, UH & UHSPH

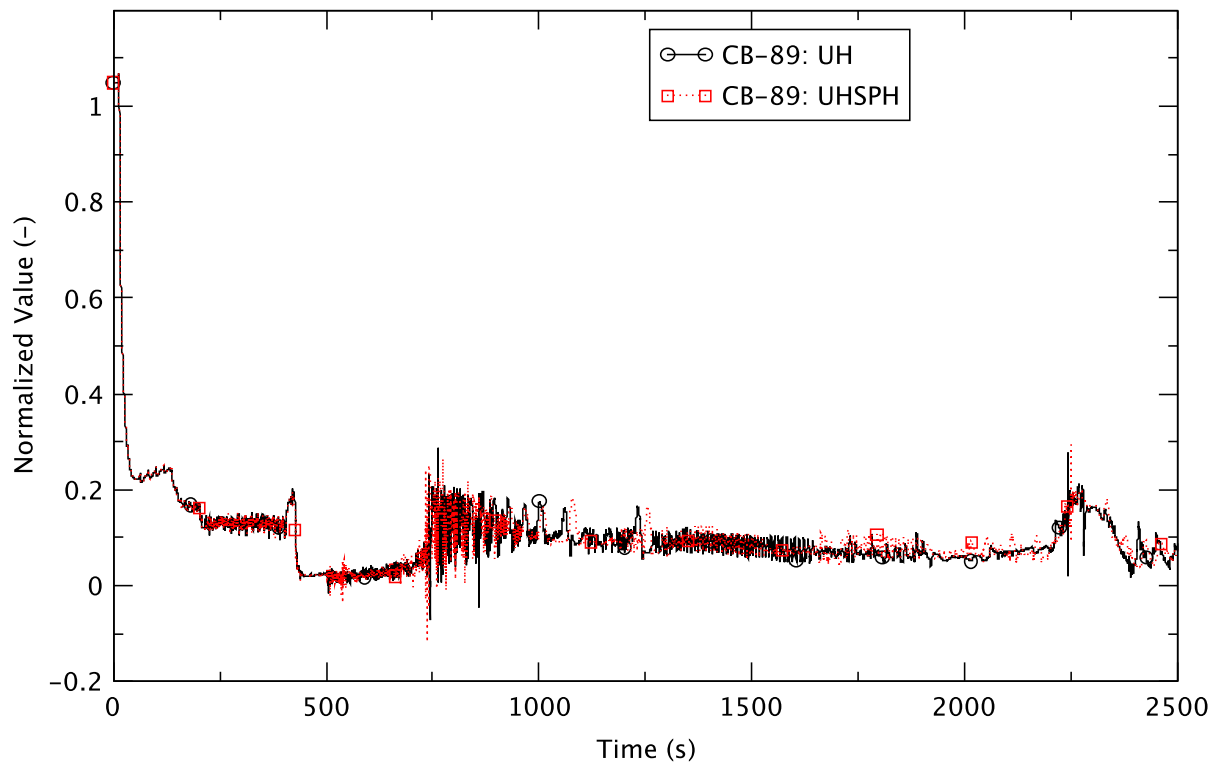


Figure 2.17 Core Flow - EOFPL, TAF+5, UH & UHSPH

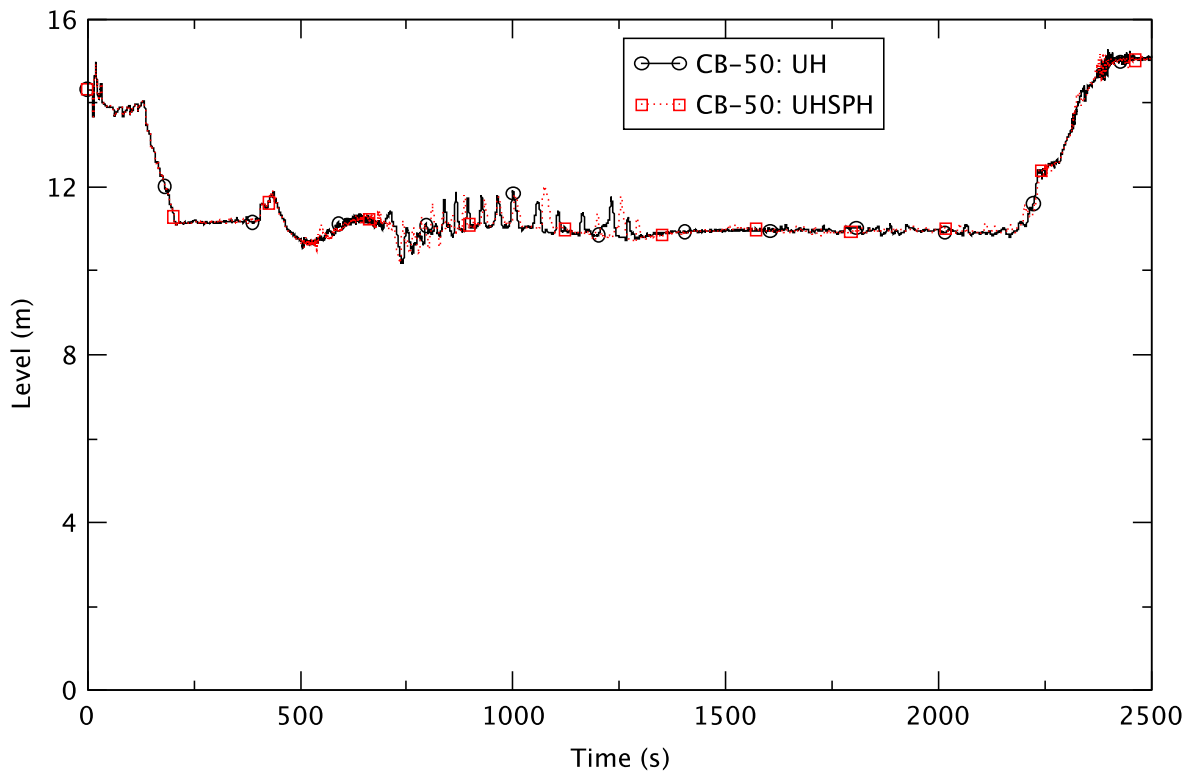


Figure 2.18 Downcomer Water Level - EOFPL, TAF+5, UH & UHSPH

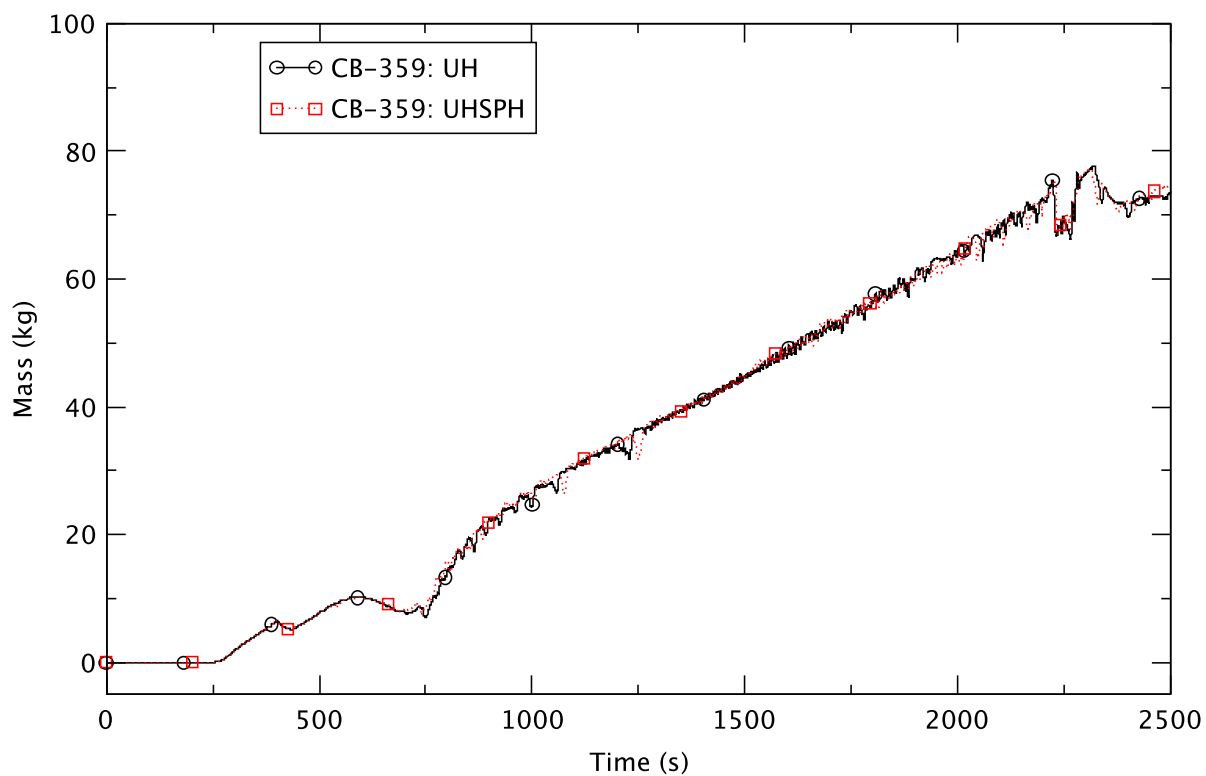


Figure 2.19 Boron Inventory in the Core Region - EOFPL, TAF+5, UH & UHSPH

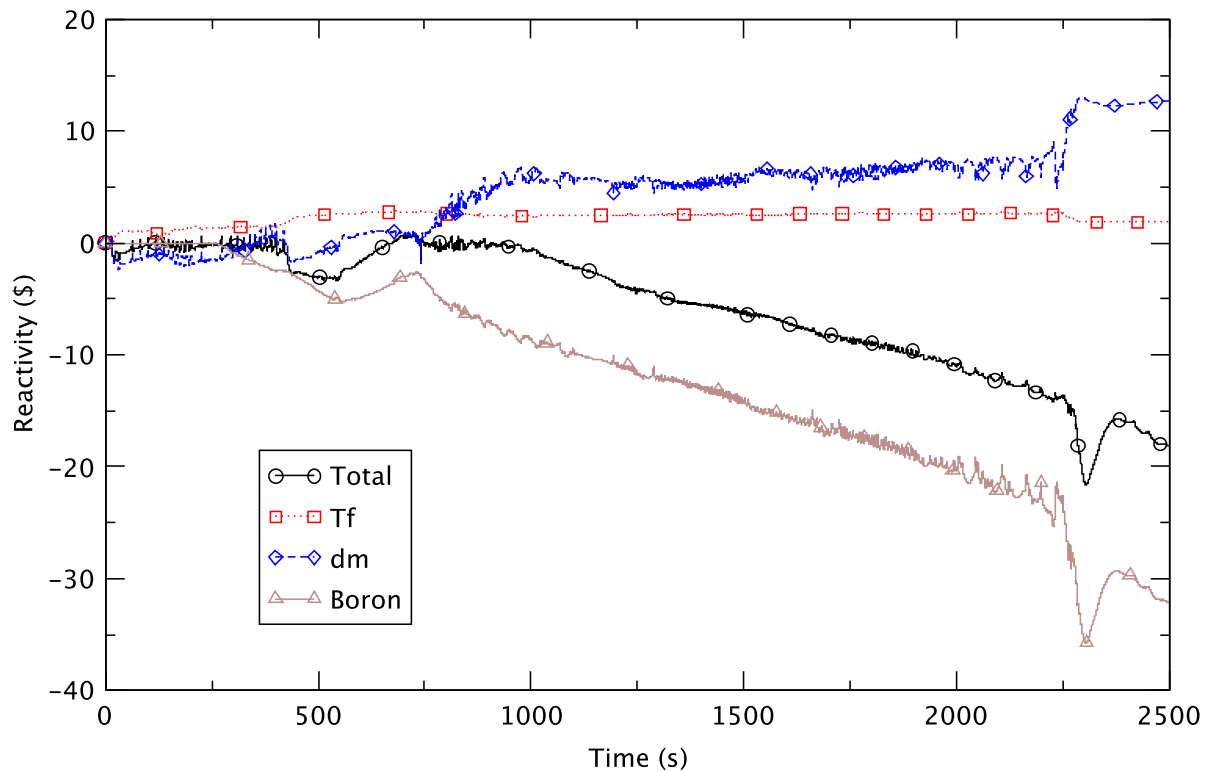


Figure 2.20 Core Reactivity - EOFPL, TAF+5, UHSPH

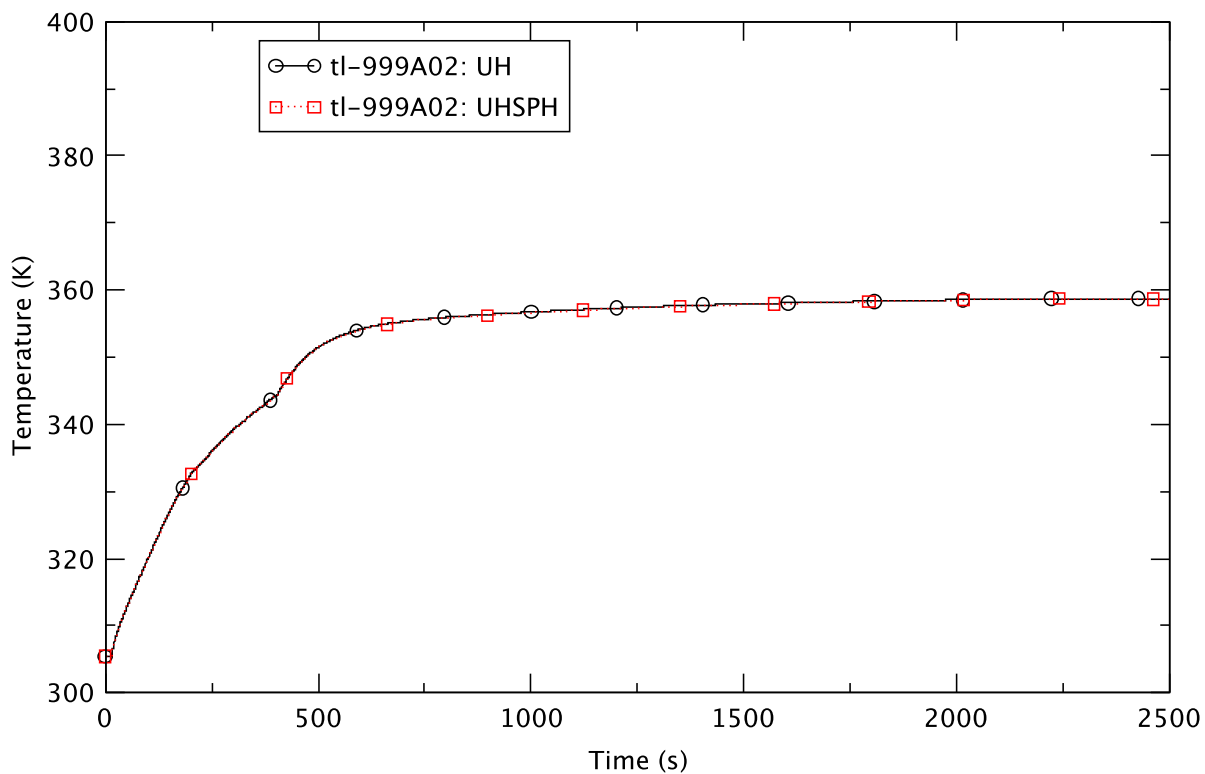


Figure 2.21 Suppression Pool Temperature - EOFPL, TAF+5, UH & UHSPH

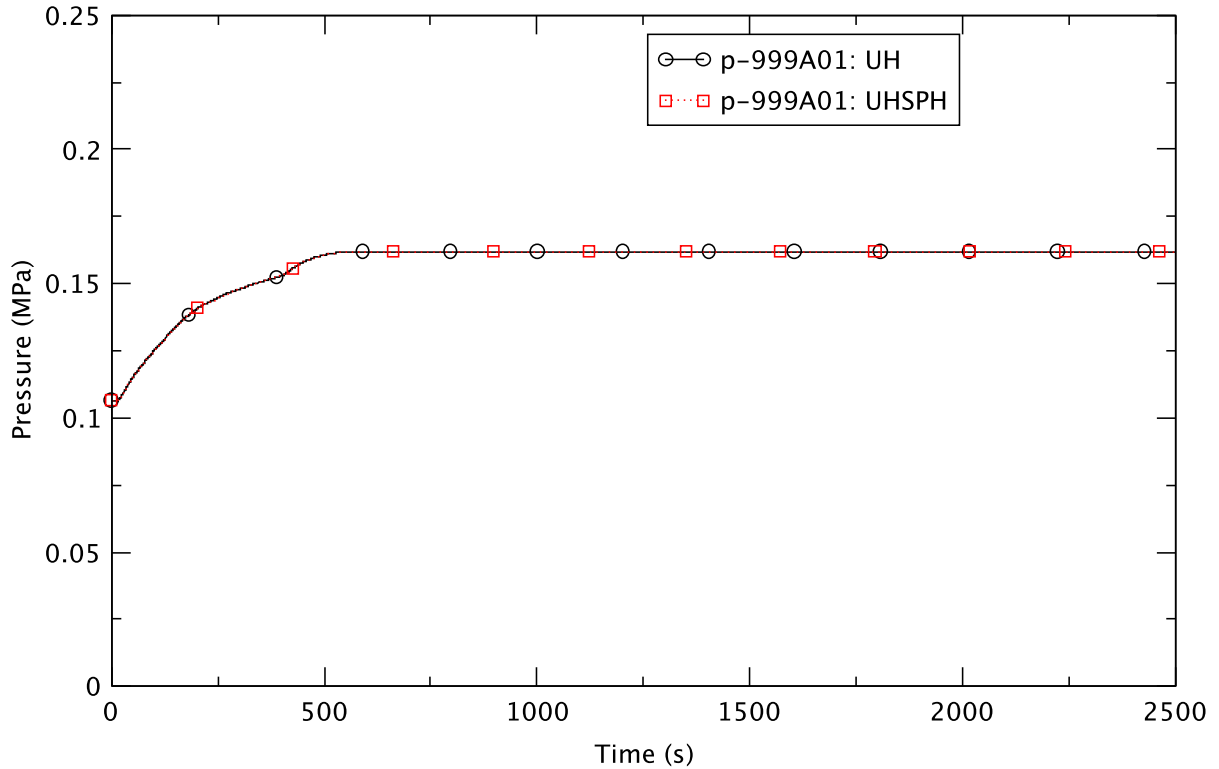


Figure 2.22 Drywell Pressure - EOFPL, TAF+5, UH & UHSPH

2.4 Effect of Reduced Core Flow at EOFPL

We present two sensitivity cases in this section to illustrate the effect of reduced core flow on the ATWS-ED transient at EOFPL with the water-level control to TAF-2. The initial core flows assumed for the two cases are 75% (Case 10D) and 85% (Case 12A) of the rated value. The reference case, Case 12, is at 105% flow and results for it were described [4]. The 85% flow corresponds to the lowest core flow allowable along the upper boundary of the MELLLA+ operating domain on the power-flow map. The 75% flow case represents a low-low flow condition that bounds the MELLLA+ domain. Simulating the latter requires an “eigenvalue offset” by PARCS (i.e., the predicted multiplication factor is less than unity and PARCS resets it to unity initially) so to achieve criticality. In effect, the analysis treats the low-low flow condition as being artificially critical.

Implementing the reduced core flow at EOFPL in the TRACE BWR model was discussed in Section 3.3.5 in [4]. Figure 2.23 and Figure 2.24, reproduced from [4], show the steady-state distributions of axial power and axial moderator density, calculated by PARCS for different initial core flows at EOFPL. The results confirm that reducing the core flow shifts the boiling boundary downward (towards core inlet), and also affects the axial power peaking by shifting more power to the lower core.

The progression of the ATWS-ED transient exhibited by the sensitivity cases is, in general, comparable to the reference case. Table 2.7 compares some of the key results for the three cases.

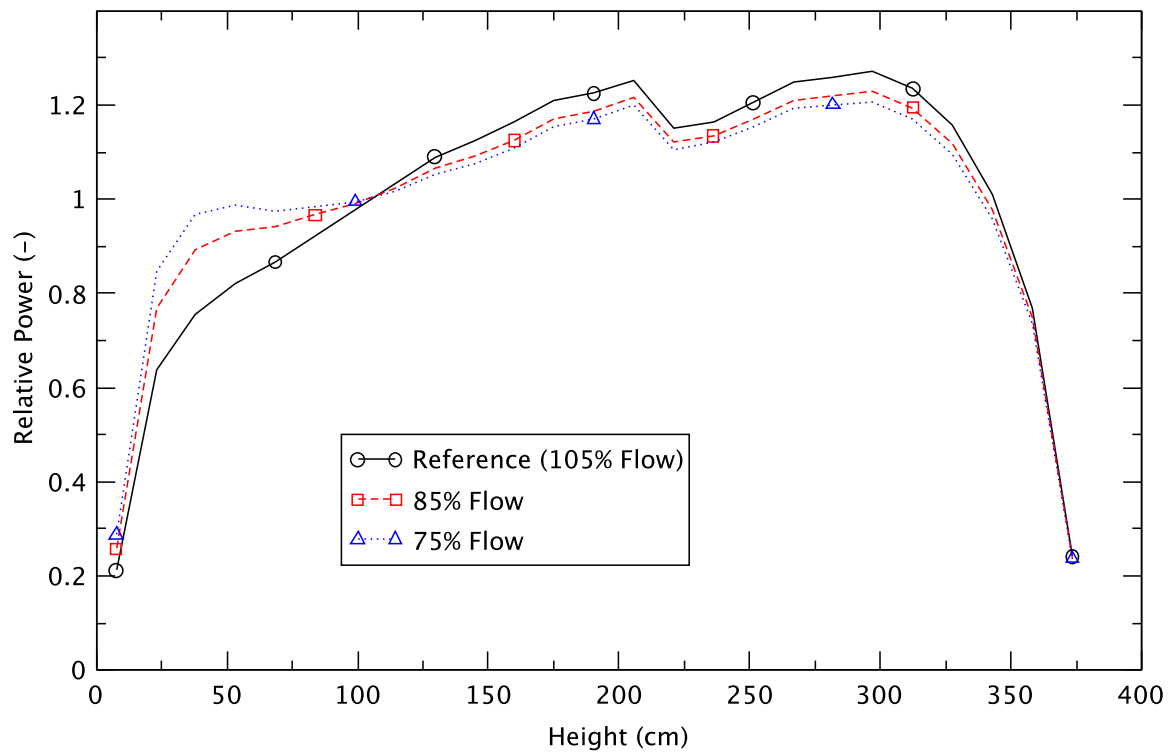


Figure 2.23 Radially Averaged Axial Power Distribution at EOFPL - Effect of Reduced Core Flow

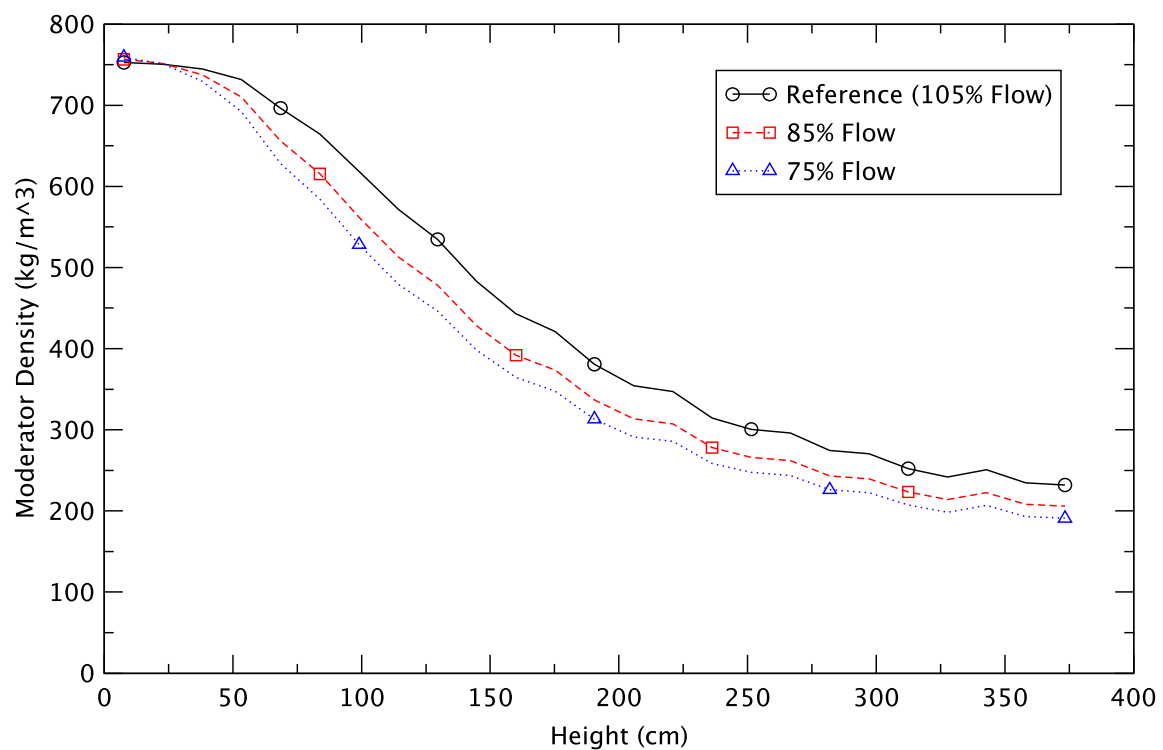


Figure 2.24 Radially Averaged Axial Moderator Density Distribution at EOFPL - Effect of Reduced Core Flow

Table 2.7 Comparison of Key Results for EOFPL, TAF-2 Cases

| Key Event | 75% Flow | 85% Flow | 105% Flow |
|---|----------------------|----------------------|----------------------|
| Maximum PCT (trhmax-100) | 1380 K (146 s) | 980 K (151 s) | 639 K (699 s) |
| Core boron inventory (CB-359 (user defined TRACE control block output) > 0.01 kg) | 251 s | 255 s | 264 s |
| Emergency depressurization | 309 s | 347 s | 450 s |
| Maximum drywell pressure | 0.163 MPa (501 s) | 0.162 MPa (541 s) | 0.160 MPa (648 s) |
| Reactor shutdown (power remains < 3.25% of initial power) | 1354 s | 1188 s | 887 s |
| Maximum suppression pool temperature | 362 K (2190 s) | 358 K (2205 s) | 357 K (2191 s) |

The most significant difference between the two sensitivity cases and the reference case is in the maximum peak clad temperature where the sensitivity cases reach temperatures of 1380 K and 980 K, compared to 639 K for the reference case. We also observe that the reactor power following the 2RPT trends inversely with the initial core flow because the 2RPT reduces the core flow (and hence reactivity) by a lesser amount when the initial core flow is lower. A higher reactor power generally entails a higher PCT. Thus, the trend of the PCT is consistent with the simulation results, viz., a higher PCT for a lower initial core flow. Furthermore, in this case, more energy is relieved to the containment, resulting in an earlier emergency depressurization, a higher temperature in the suppression pool, and a higher drywell pressure. The timing of the maximum PCT is very different between the sensitivity cases and the reference case. For the two sensitivity cases, the maximum PCT occurs much earlier, shortly after water level control is initiated at 130 s and before emergency depressurization while the core flow still is relatively high. During this stage, the fuel is predicted to enter dryout under relatively low-quality conditions, to fail to rewet, and to experience extended heatup. For the reference case, the fuel rewets during the early transient stage and the maximum PCT occurs after emergency depressurization (i.e., at a higher quality). By then, the core flow for the reference case is low because of water level control to TAF-2.

A select set of plots (Figure 2.25 to Figure 2.40) compares and contrasts the transient responses of the two sensitivity cases against the reference case.

Figure 2.25 plots the transient response of the reactor power for all three cases. All three power traces show a similar response; a power spike after the MSIV closure and power declines after 2RPT, lowering of water level, and depressurization. Figure 2.26 shows the reactor power for the first 600 s of the ATWS-ED transient. The simulation results demonstrate that a lower initial core flow leads to higher transient reactor power that also oscillates with higher amplitude (between roughly 110 s and 170 s) before the level reduction suppresses the reactor power. For a lower initial core flowrate, the reactor power level after 2RPT (i.e., under natural circulation conditions) is higher. The higher ratio of power-to-flow for the cases with a lower initial core flowrate evolve into more unstable conditions as subcooling of the core inlet increases during the event. The amplitude of power oscillations trends with the increasing power-to-flow ratio, as expected for density wave driven, unstable, power oscillations.

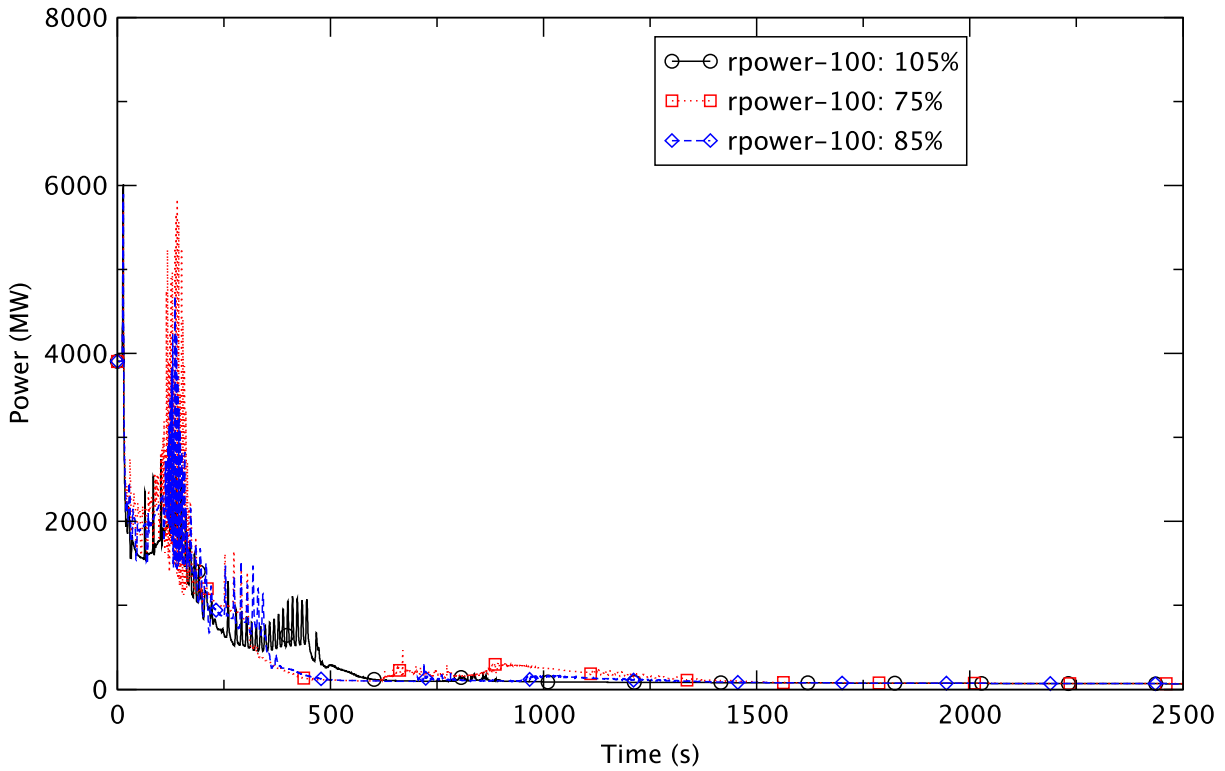


Figure 2.25 Reactor Power - EOFPL, TAF-2 Cases

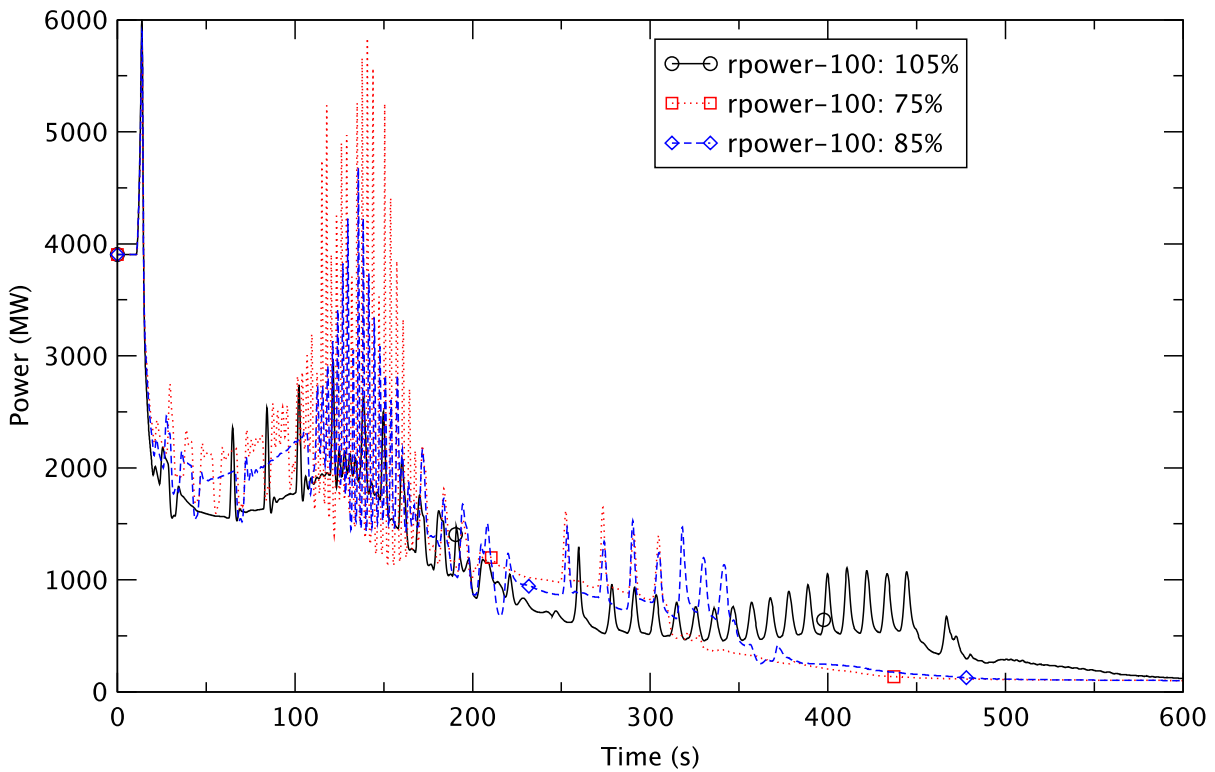


Figure 2.26 Reactor Power (0 to 600 s) - EOFPL, TAF-2 Cases

Between roughly 110 s and 170 s, the two sensitivity cases exhibit unstable density-wave oscillations (DWO) in the core. It is during this period when the reactor power-to-flow ratio is high that both reach the maximum PCT.

With a higher reactor power (due to higher total reactivity) after the 2RPT and the initiation of water-level control, the two sensitivity cases have an earlier emergency depressurization time than the reference case. The reactor pressure is shown in Figure 2.27. The rate of depressurization is similar for all three cases, and there is voiding in the lower plenum. The presence of void there and the core (due to flashing) disrupts the natural circulation flow from the downcomer to the core, so reducing the core flow (Figure 2.28). The core flow is higher for the two sensitivity cases after the level is controlled and before depressurization. The higher core flow is consistent with a higher core power for the sensitivity cases before the ED.

Downcomer level swell associated with the ED is evident in Figure 2.29 that depicts the water level for all three cases. Fluctuations in core flow and water level generally are related to refilling of the lower plenum and the core, and the injection of feedwater. Figure 2.30 and Figure 2.31 show the rate of feedwater flow for the two sensitivity cases; it correlates qualitatively with perturbations in core flow and the level of downcomer water, around 1500 s for the 75% flow case, and around 2000 s for the 85% flow case.

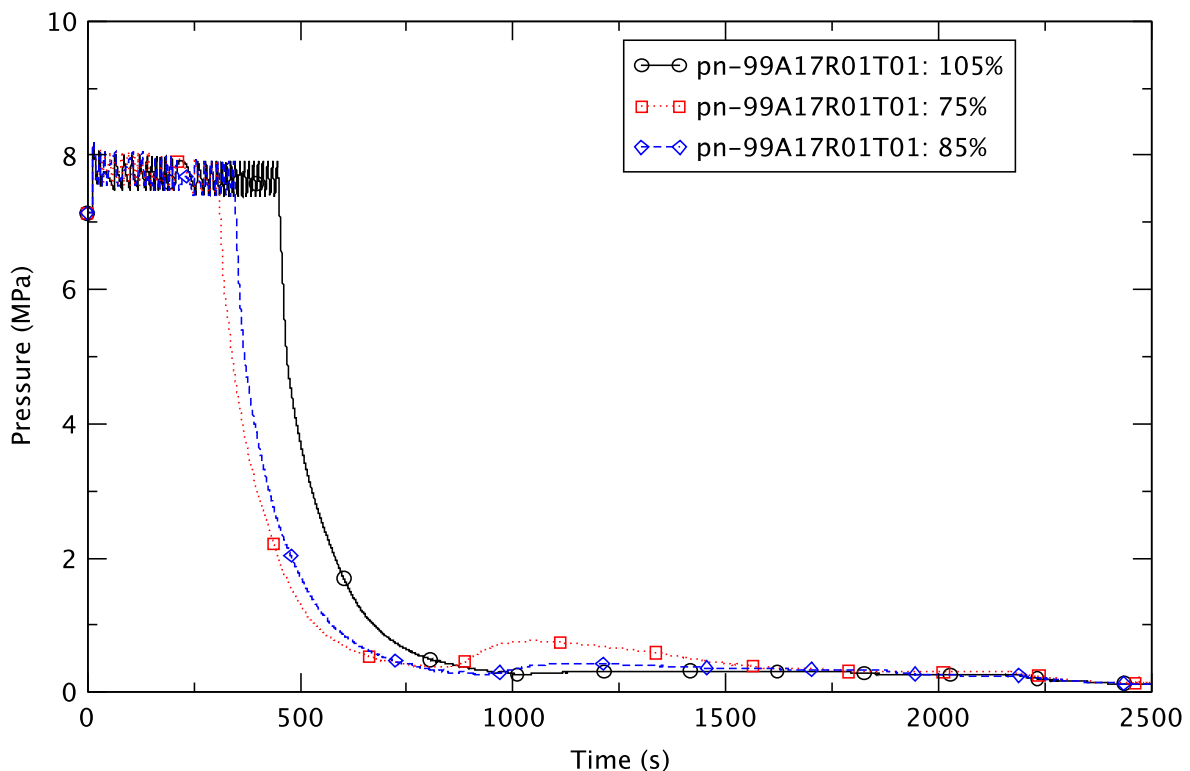


Figure 2.27 Reactor Pressure - EOFPL, TAF-2 Cases

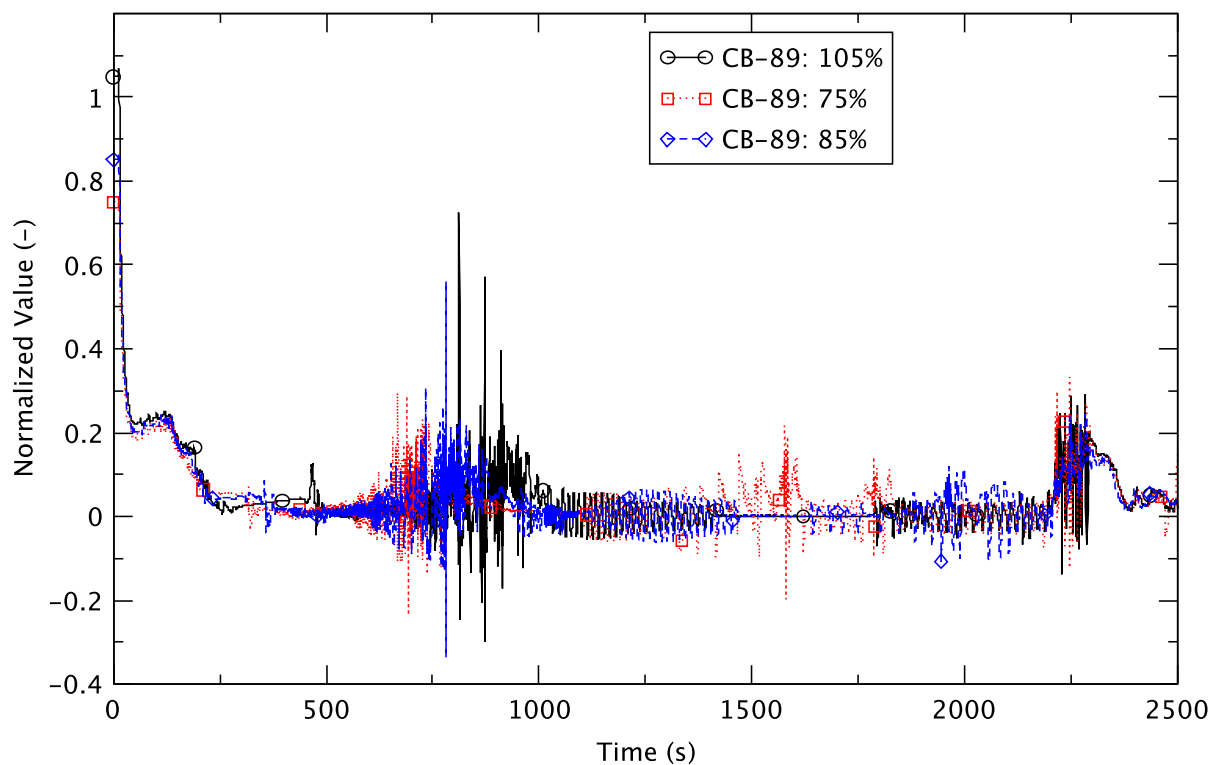


Figure 2.28 Core Flow - EOFPL, TAF-2 Cases

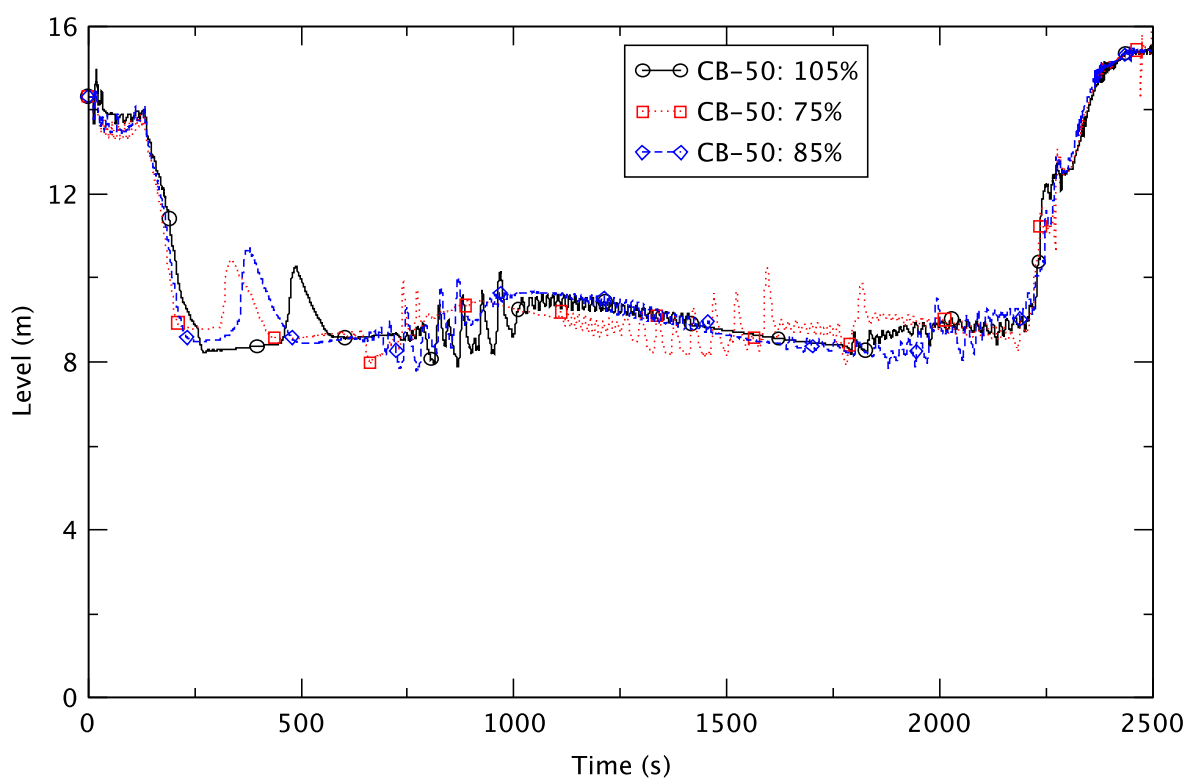


Figure 2.29 Downcomer Water Level - EOFPL, TAF-2 Cases

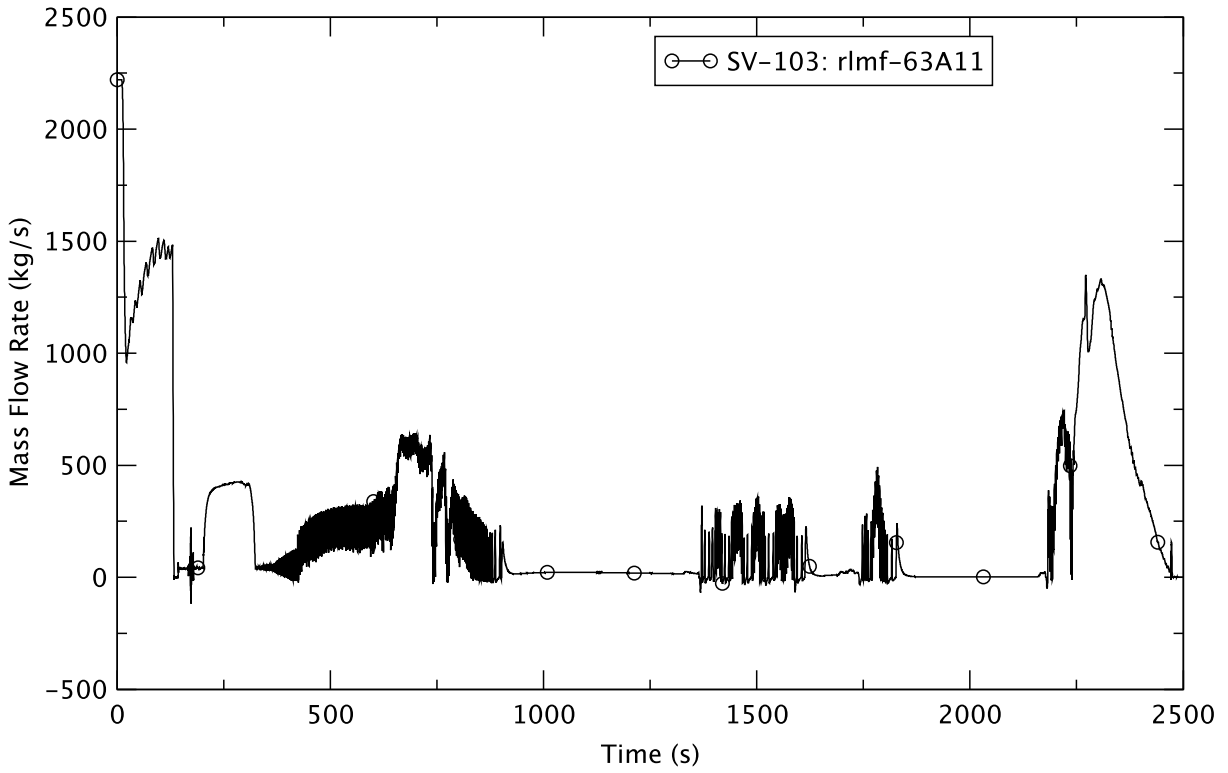


Figure 2.30 Feedwater Flowrate - EOFPL, TAF-2, 75% Flow

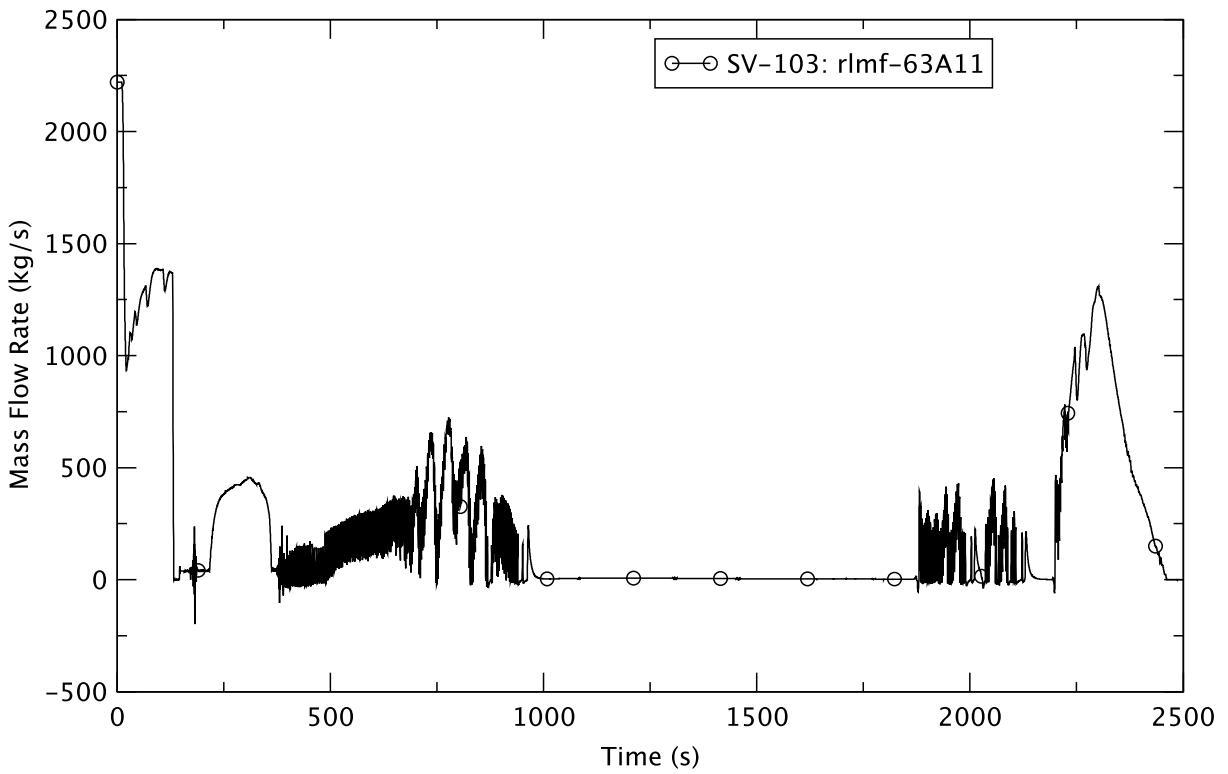


Figure 2.31 Feedwater Flowrate - EOFPL, TAF-2, 85% Flow

For the sensitivity case with 75% flow, it is observed from Figure 2.28 and Figure 2.29 that for a roughly 200-second period around 1000 s the water level and core flow are quite stable and there is a slight increase in reactor power. The increase in reactor power is confirmed by observing an increase in reactor pressure (Figure 2.27) and steamline flow (Figure 2.32) at about 1000 s. To a lesser extent, an increase in pressure is also observed in the case of 85% flow at about 1200 s.

For the 75% flow case, the core flow and downcomer water level begin to oscillate again after 1000 s. Further evidence of oscillatory conditions for the 75% flow case is in the core bypass void fraction, shown in Figure 2.33. Between 1000 s and 1700 s, the magnitude of oscillations in core flow and downcomer water level is lower for the 85% flow case and the reference case (105% flow) as is expected since power level is higher with 75% flow. Also, no voiding in the lower nodes of the core bypass region is observed in these two cases during that period.

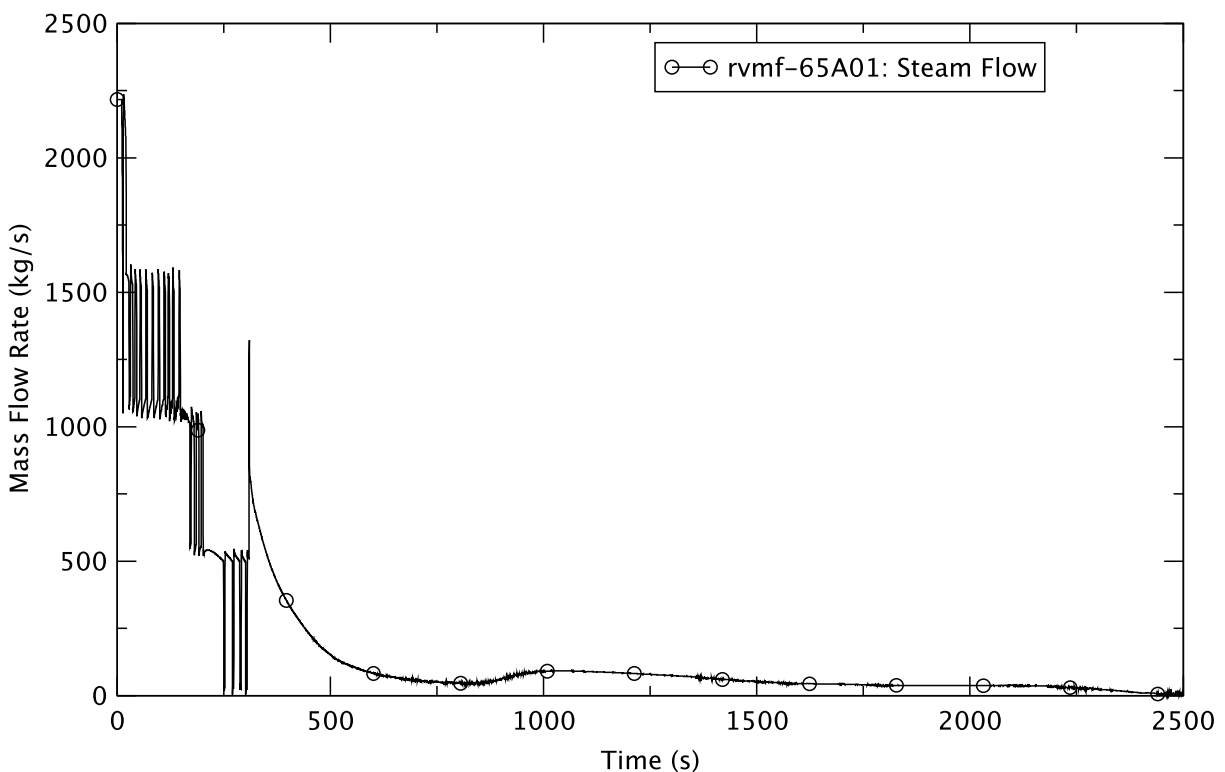


Figure 2.32 Steamline Flow - EOFPL, TAF-2, 75% Flow

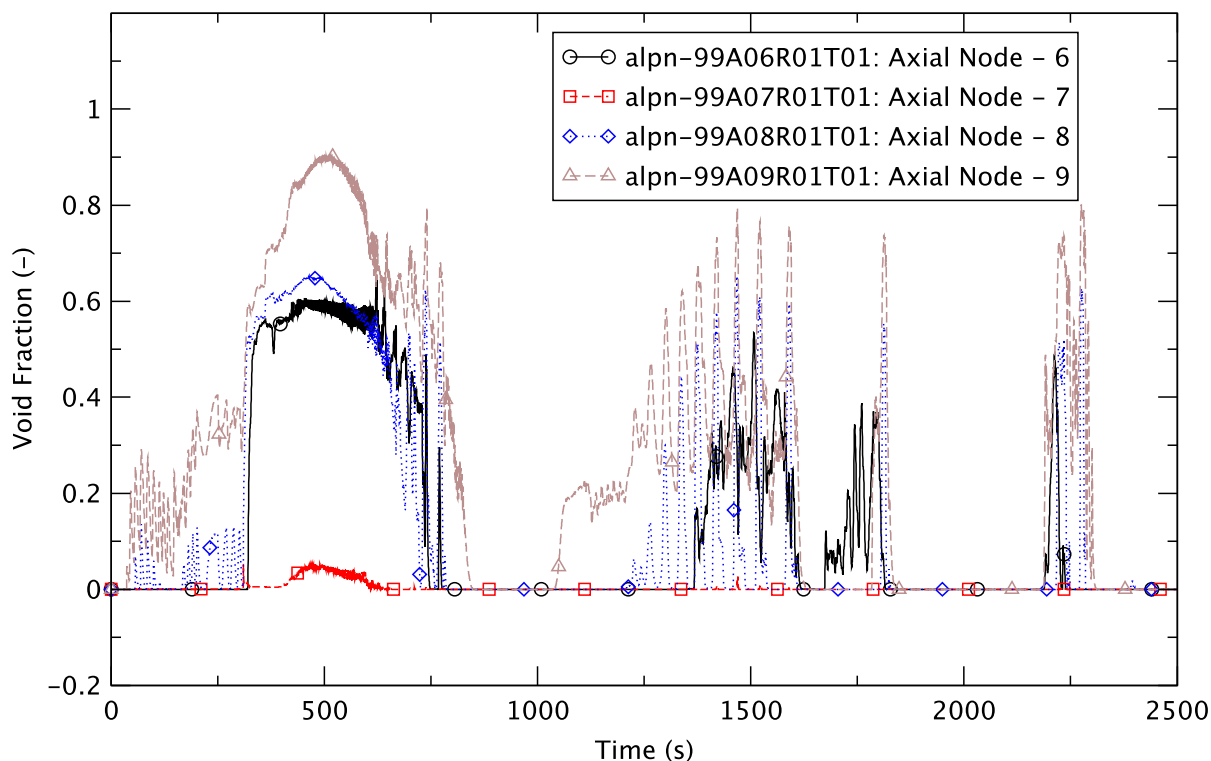


Figure 2.33 Void Fraction in Core Bypass (Ring 1) - EOFPL, TAF-2, 75% Flow

The boron inventory in the core is shown in Figure 2.34 for the three cases. The injection starts at 211 s and in all cases it takes about 40-50 s for the boron to reach the core. The rate of change in the boron inventory appears to be affected by the emergency depressurization due to its impact on core flow and voiding in the core. Thereafter, there is a period of slow growth in the boron inventory. At about 750 s, coincident with the refilling of the lower plenum, there is a marked increase in the boron inventory. The subsequent increase in boron at 1500 s and 2000 s for the 75% case and 85% case, respectively, is associated with effective re-mixing of stratified boron in the bottom of the lower plenum. This is taken into account in the TRACE simulation through an increase in the concentration of the injected boron, as calculated by the boron transport control scheme (Section 2.3.7 and Appendix A in [4] provide a discussion). The simulated, enhanced boron delivery reflects increased core flow due to feedwater flow and a higher level. For all three cases, the core boron inventory increases after level recovery, beginning at 2180 s. The effective injection boron concentration (an output of the boron transport model that accounts for re-mixing of boron in the lower plenum) for the 75% flow case is shown in Figure 2.35. The temporary increases in injected boron concentration above the nominal (0.02369 kg-B/kg-water) also account for the re-mixing of settled boron in the lower plenum of the reactor vessel. This is assumed to be a function of coolant flow in the lower plenum (Appendix A in [4] discusses the re-mixing model).

The reactivity components calculated by PARCS are shown in Figure 2.36 and Figure 2.37 for the 75% flow and 85% flow cases, respectively (Figure 4.113 in [4] gives the corresponding plot for 105% flow). In all three, the general trend of reactivities is similar. There is a decrease in the core's reactivity after depressurization due to voiding therein and a recovery of reactivity after refilling the core. As the transient progresses, only the injected boron contributes negative reactivity to the core. Both the fuel- (Doppler) and coolant (moderator density) reactivities are positive. Restoring water level at 2180 s positively increases the moderator density reactivity,

but that is more than compensated for by a corresponding rise in the negative contribution from the boron reactivity. Therefore, the reactor is maintained in a subcritical state during level recovery.

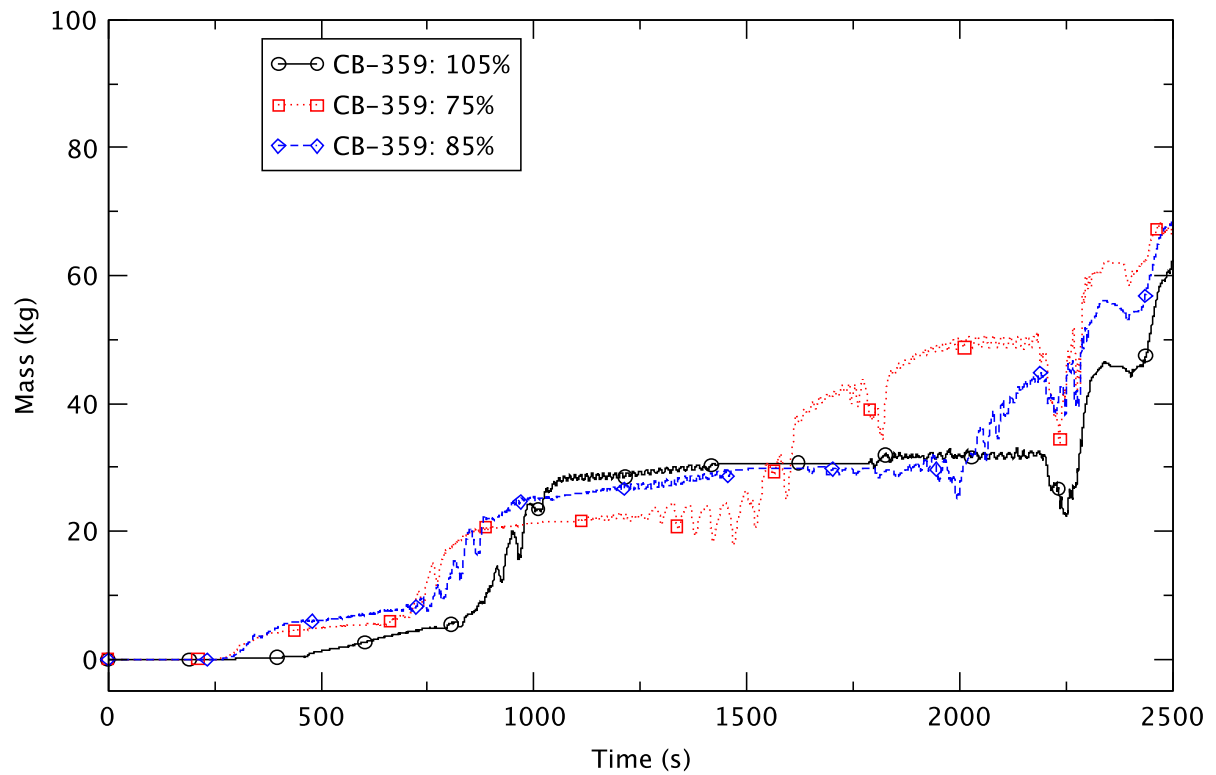


Figure 2.34 Boron Inventory in the Core - EOFPL, TAF-2 Cases

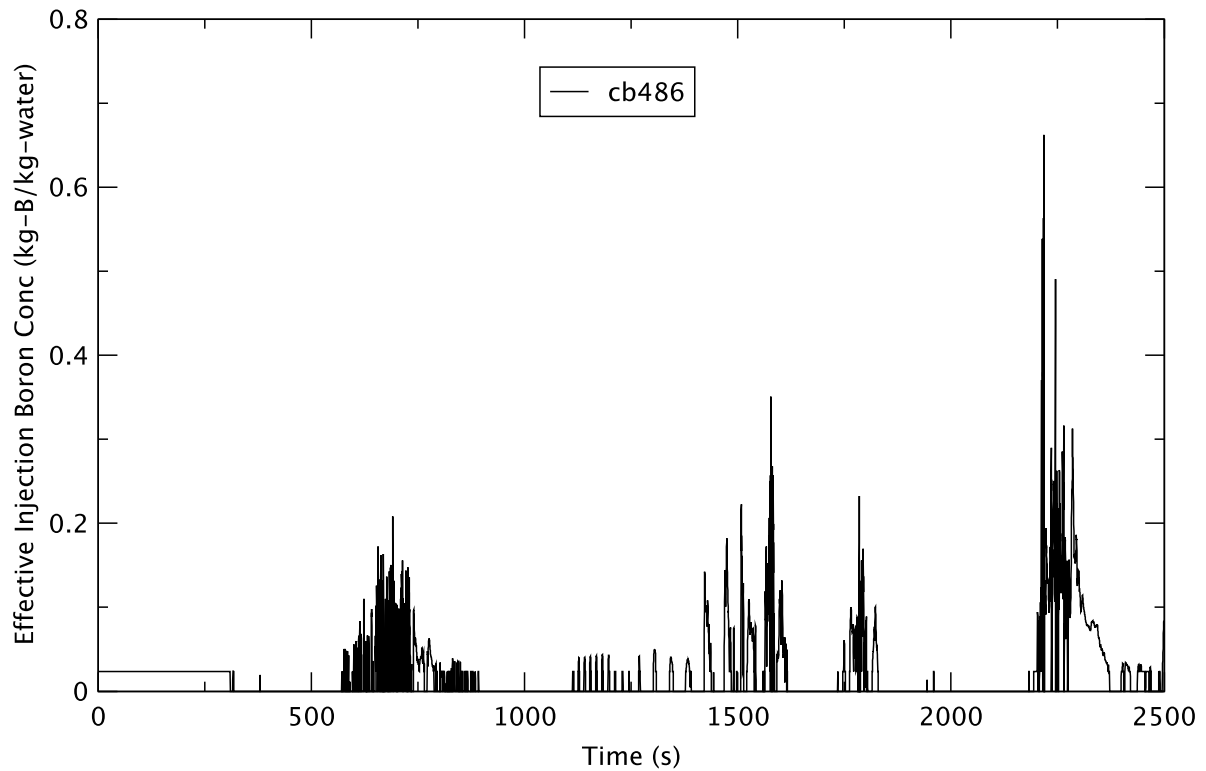


Figure 2.35 Effective Injection Boron Concentration - EOFPL, TAF-2, 75% Flow

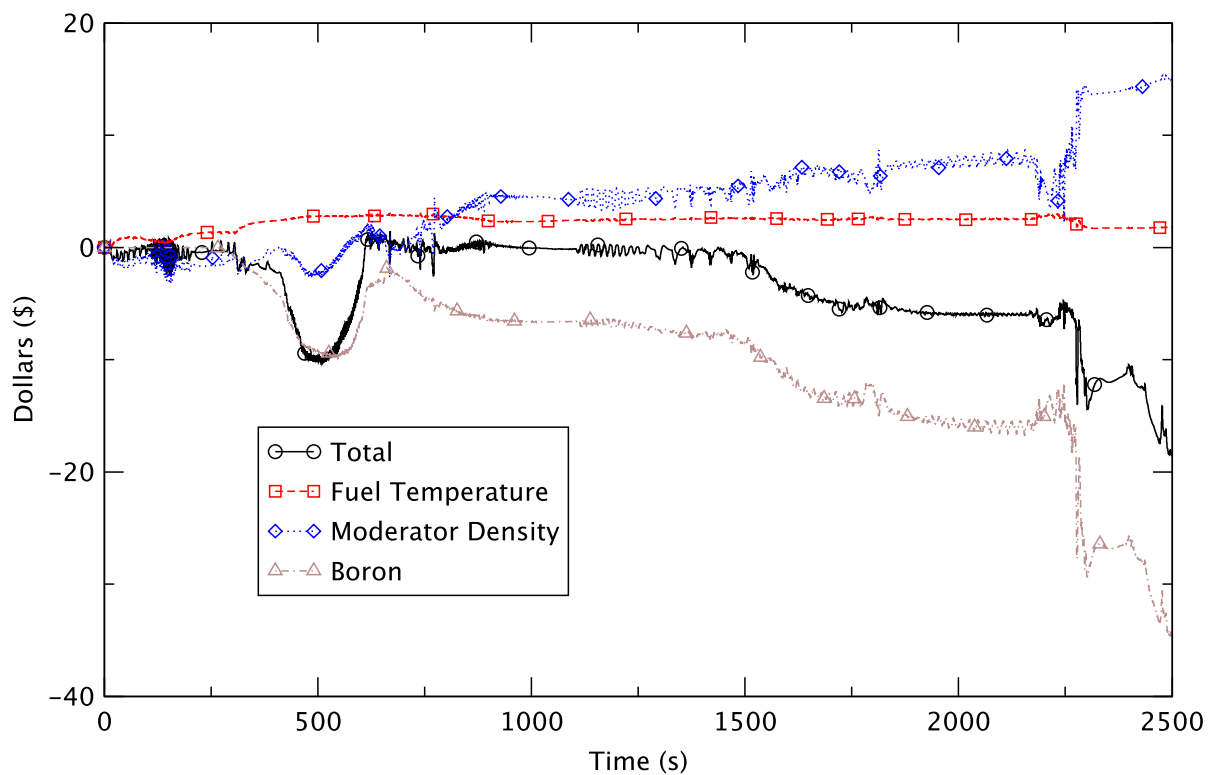


Figure 2.36 Core Reactivity - EOFPL, TAF-2, 75% Flow

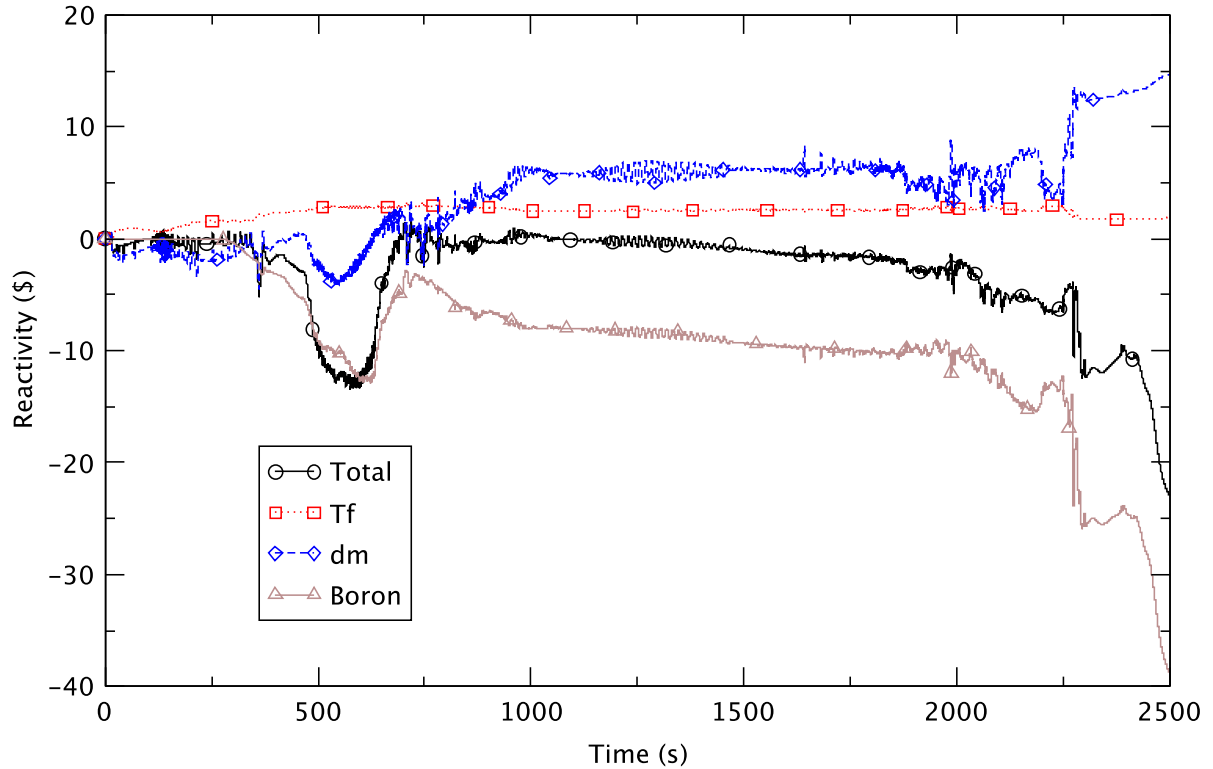


Figure 2.37 Core Reactivity - EOFPL, TAF-2, 85% Flow

One of the more distinguishing differences among the three cases is the maximum PCT, illustrated in Figure 2.38. The 75% and the 85% flow cases respectively reach a temperature of 1380 K and 980 K, compared to 639 K for the reference case. For the former two, the maximum PCT occurs early, right after level control is initiated when core flow is still relatively high. Also, for both cases the fuel experiences dryout with failure to rewet, leading to high PCT early in the transient. For the reference case (105% flow), the fuel does not experience extended heatup (because the power is lower) during the early transient, but there is a delayed heatup of the core when the reduction in core flow after depressurization has created substantial voiding in the core. Core voiding also transiently raises the maximum PCT for the two sensitivity cases, at around 600 s; furthermore, for both of them, a higher power after 2RPT entails an earlier dryout than in the reference case. For the two sensitivity cases, an unstable density wave oscillation (DWO) seemingly is the cause of PCT that occurs when the ratio of reactor power-to-flow is high.

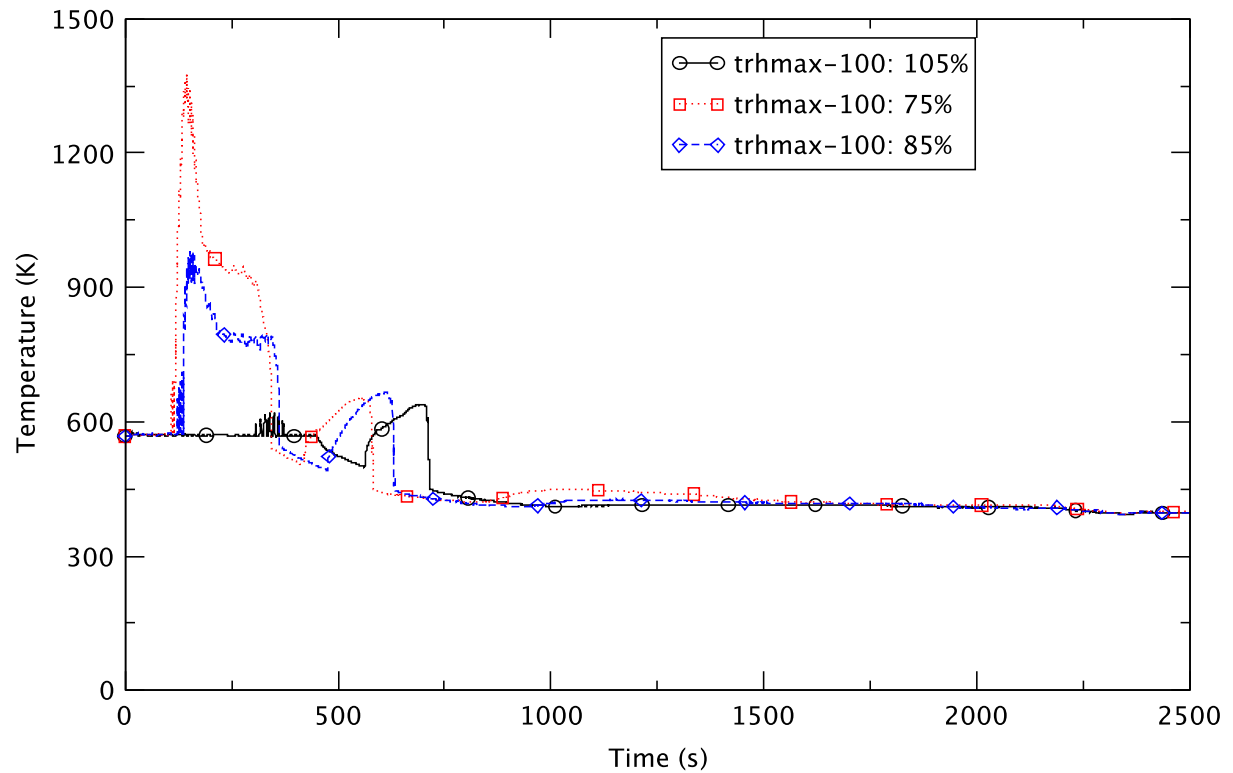


Figure 2.38 Peak Clad Temperature - EOFPL, TAF-2 Case

The water temperature in the suppression pool (Figure 2.39) indicates that energy is relieved to the pool via the SRVs. The 75% flow case has the highest pool temperature, followed by the 85% flow case and the reference case. In all three, the pool temperature stays below the limit (i.e., saturation temperature at one atmosphere of pressure).

The drywell pressure (Figure 2.40) exhibits a similar trend to the temperature in the suppression pool water. In all three cases, the maximum drywell pressure is low enough so as not to be of concern for containment integrity.

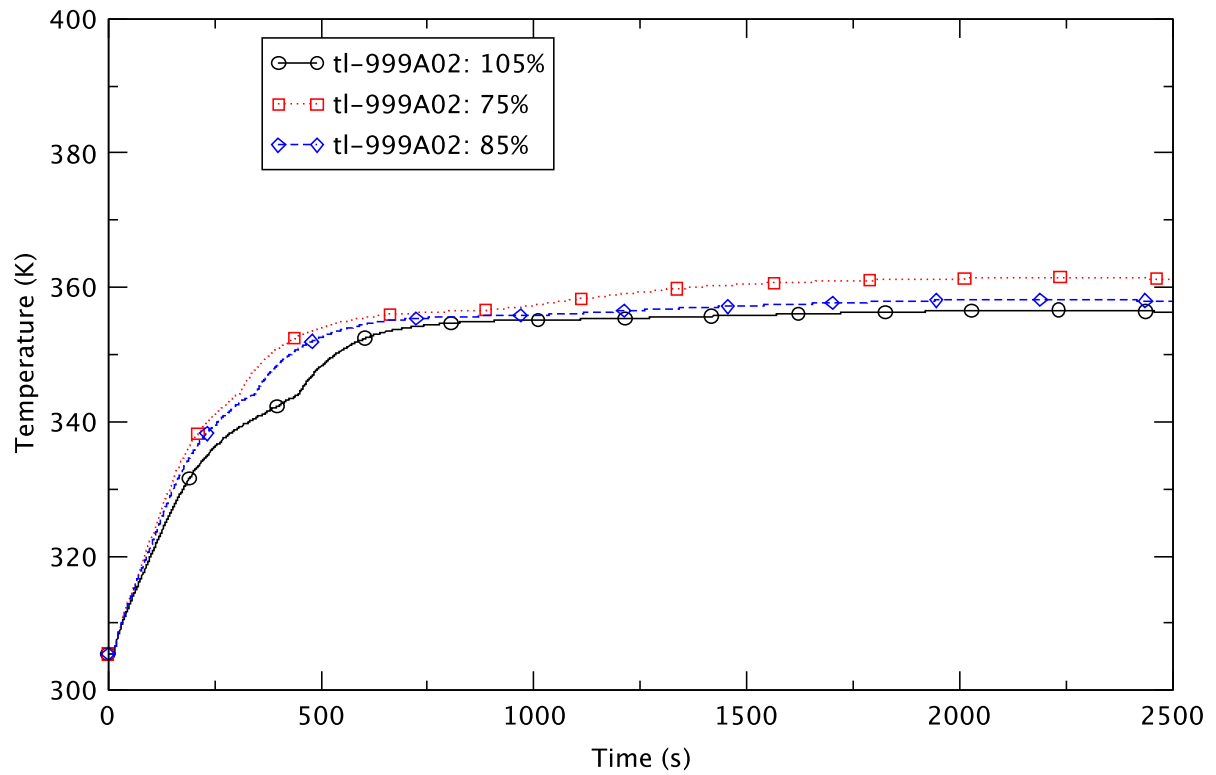


Figure 2.39 Suppression Pool Temperature - EOFPL, TAF-2 Cases

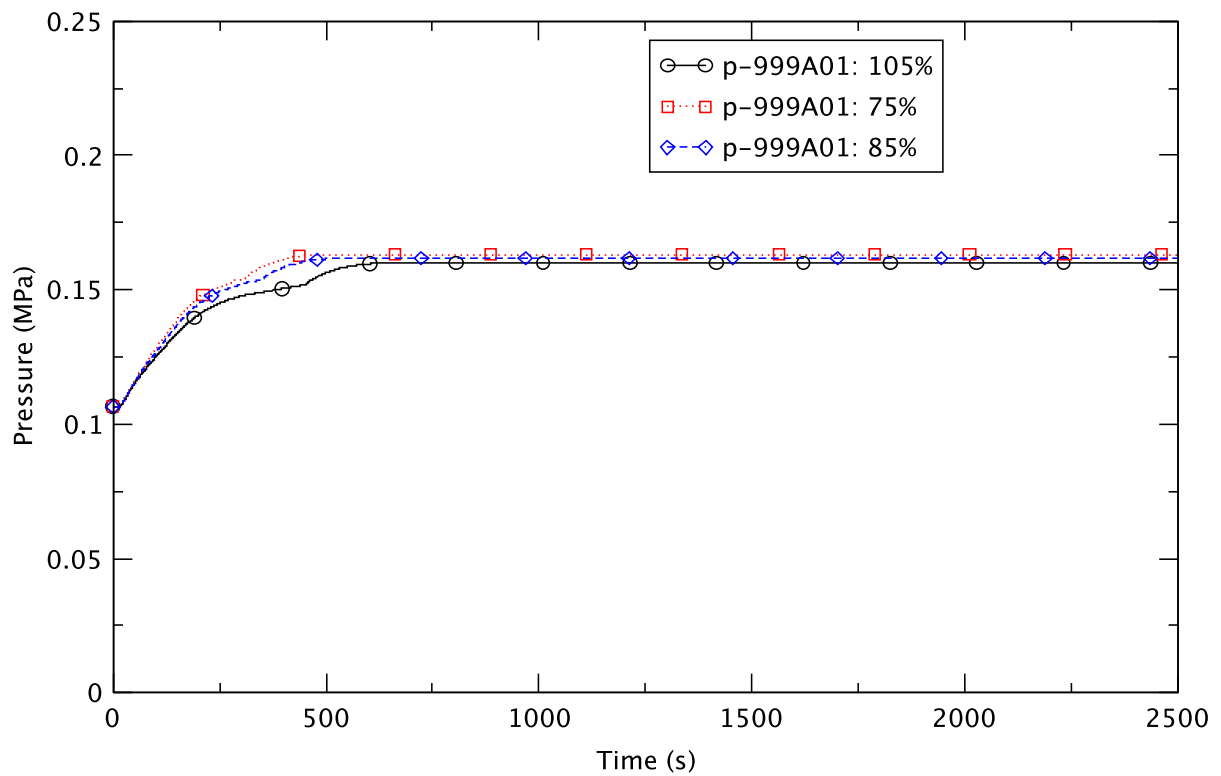


Figure 2.40 Drywell Pressure - EOFPL, TAF-2 Cases

2.5 Effect of Level Control at EOFPL with Reduced Core Flow

Three sensitivity cases at a reduced initial core flow of 85% of the rated value were done at EOFPL to evaluate the effect of level control to TAF+5, TAF, and TAF-2. An initial core flow at 85% of rated flow is near the lower range of the MELLLA+ operating domain. Compared to the base reference case at 105% flow, the reduced flow has an initial axial power distribution that peaks lower (nearer to the core inlet).

In general, the transient responses to water level control for the 85% flow sensitivity cases are very similar to the corresponding base cases (at EOFPL 105% flow; see Section 4.4.3 in [4]). Table 2.8 summarizes the key results for the three sensitivity cases.

Table 2.8 Comparison of Key Results for EOFPL, 85% Flow Cases

| Key Event | TAF | TAF-2 | TAF+5 |
|---|----------------------|----------------------|----------------------|
| Maximum PCT (trhmax-100) | 706 K (150 s) | 980 K (151 s) | 706 K (151 s) |
| Core boron inventory (CB-359 (user defined TRACE control block output) > 0.01 kg) | 249 s | 255 s | 245 s |
| Emergency depressurization | 355 s | 347 s | 310 s |
| Maximum drywell pressure | 0.162 MPa (546 s) | 0.162 MPa (541 s) | 0.169 MPa (789 s) |
| Reactor shutdown (power remains < 3.25% of initial power) | 1278 s | 1188 s | 983 s |
| Maximum suppression pool temperature | 360 K (2223 s) | 358 K (2205 s) | 367 K (2132 s) |

The most significant difference between the sensitivity cases and the base cases (with the three different water level strategies) is the higher transient reactor power in the former. This is reflected in their higher maximum PCT and earlier depressurization time (Table 4.10 in [4] shows the corresponding results for the EOFPL base-cases). Another difference is the early timing of the maximum PCT at TAF-2 for the sensitivity case (at 699 s for the corresponding base case).

Similar to the base cases, the sensitivity cases at TAF and TAF-2 exhibit several characteristics that differ from the TAF+5 sensitivity case:

- There is flashing in the lower plenum and the core after the emergency depressurization.
- Natural circulation is broken after ED and the reactor power decreases further.
- Boron is diluted when the lower plenum and the core are refilled.
- The boron inventory in the core does not increase monotonically.

We use a select set of plots (Figure 2.41 to Figure 2.56) to compare and contrast the transient responses of the three EOFPL sensitivity cases with the level control to TAF, TAF-2, and TAF+5.

The transient response of the reactor power for all three cases is shown in Figure 2.41. All three power traces display similar responses, viz., a power spike after MSIV closure and power decreases after the recirculation pump trip (2RPT), lowering the water level and depressurization. Figure 2.42 shows the reactor power for the first 600 s of the transient. Between roughly 110 s and 170 s, the reactor power oscillates with a frequency of ~ 0.4 Hz until the reduction in water level has suppressed reactor power. We attribute the transient increase in oscillatory reactor power before this reduction partly to a decline in the core inlet temperature (see discussion in Section 4.2.2 in [4]). Density-wave oscillations appear to cause the oscillatory reactor power between roughly 110 s and 170 s.

With a higher reactor power after the initiation of level control, the TAF+5 case displays the earliest ED time; the depressurization for the TAF-2 case is earlier than that of the TAF case. This difference was attributed to the lower boron reactivity in the former, thus, a slightly higher power up to the time of the depressurization (Section 4.2.3 in [4] gives a more detailed discussion). The reactor pressure for the three sensitivity cases is shown in Figure 2.43. The initial rate of depressurization for all is similar but the TAF+5 case takes longer to depressurize below 2 MPa. The TAF and TAF-2 cases show lower plenum voiding (flashing) after the ED, and the natural circulation flow in these two cases is “broken,” practically to zero core flow (Figure 2.44) along with a noticeable level swell in the downcomer (Figure 2.45). The lower core flow reflecting the break in natural circulation for TAF and TAF-2 explains their lower level of reactor power compared to TAF+5 (Figure 2.42).

For the TAF+5 case, natural circulation persists after the ED and the downcomer level swell is minor. Since the core flow remains higher for the TAF+5 case, the reactor power level likewise remains higher. During depressurization, the higher power in the TAF+5 case, and hence the higher steam generation rate in the RPV, slows down the rate of depressurization compared to the other cases (Figure 2.43).

For TAF and TAF-2, the fluctuations in core flow and water level between roughly 500 s and 800 s are caused by transient flow created by refilling of the lower plenum and the core. The void fraction in the core bypass region is shown in Figure 2.46 for TAF-2 to illustrate the refilling of the core. From about 1000 s onward, the core power in all three cases has dropped sufficiently so that water refills the core, setting a manometer-type oscillation in the downcomer water level. The oscillation is evident by the fluctuations in the water level (Figure 2.45) between about 1000 s and 1500 s. During that time, the oscillating core flow (Figure 2.44) also shows a decreasing trend in the TAF+5 case. The oscillatory condition in the core is observable from the average core void fraction as reported by the PARCS calculation (Figure 2.47).

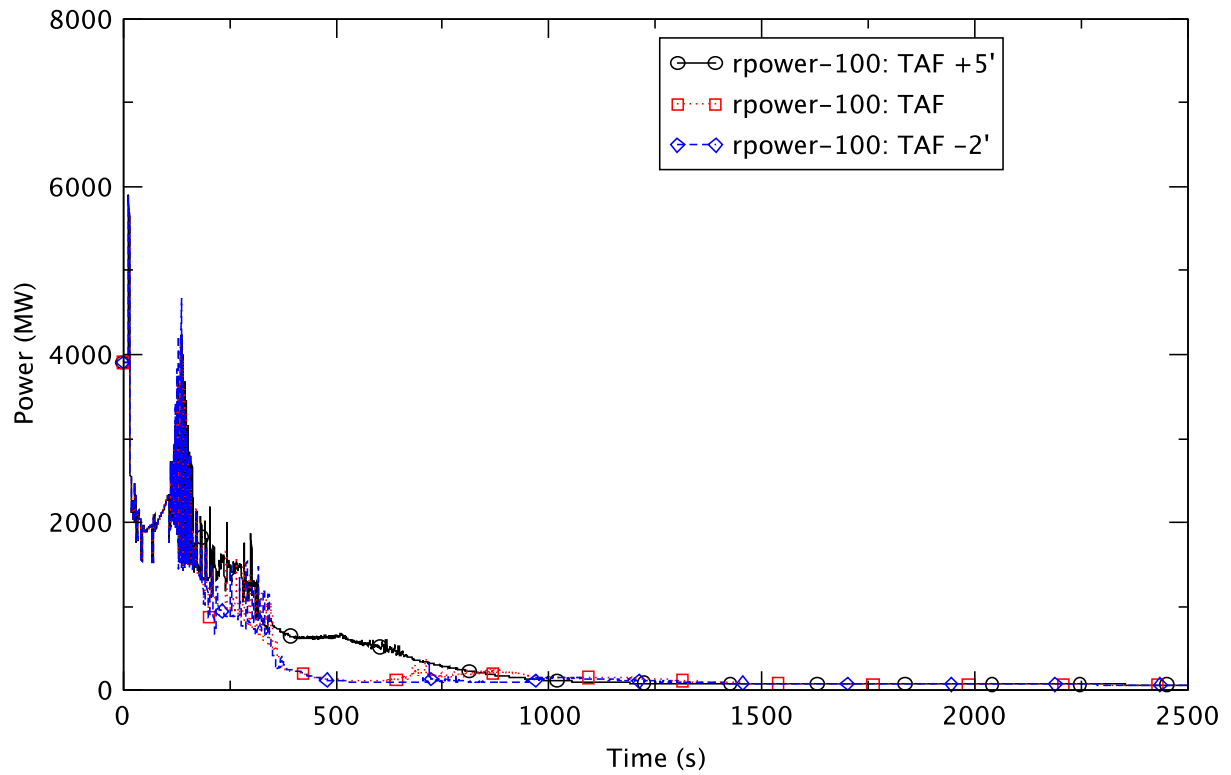


Figure 2.41 Reactor Power - EOFPL, 85% Flow Cases

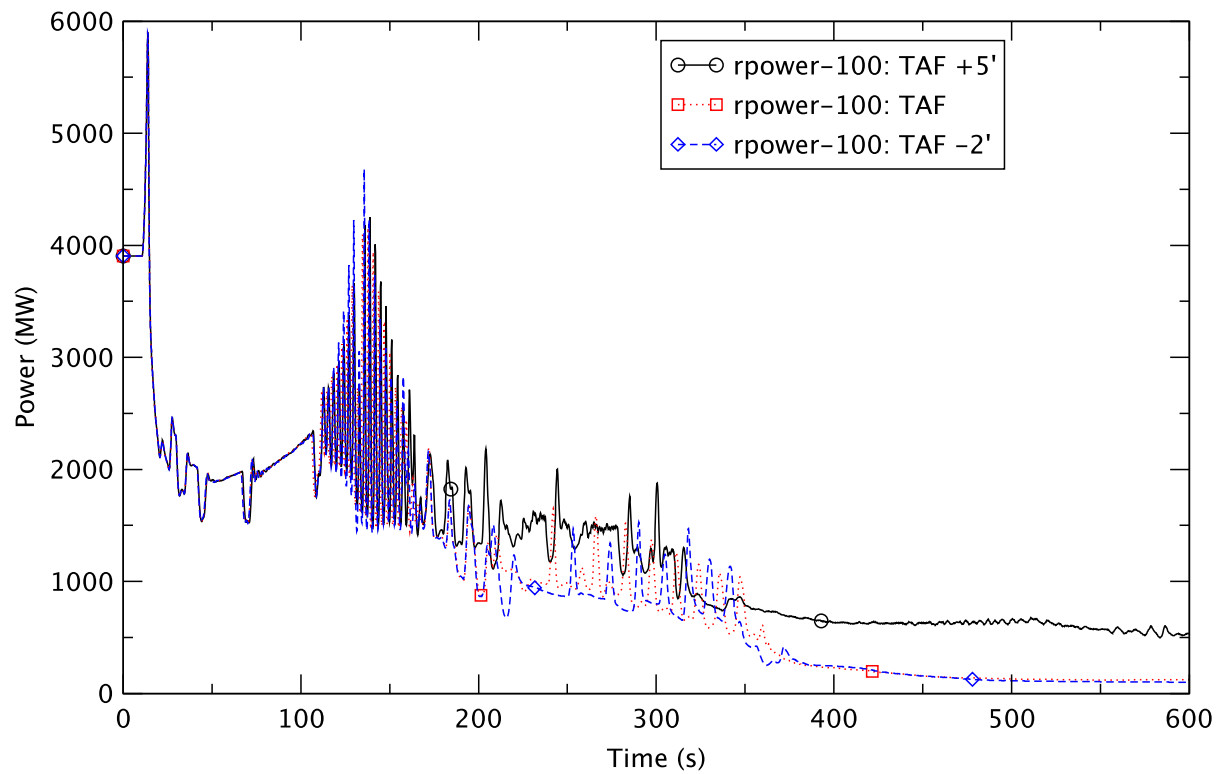


Figure 2.42 Reactor Power (0 to 600 s) - EOFPL, 85% Flow Cases

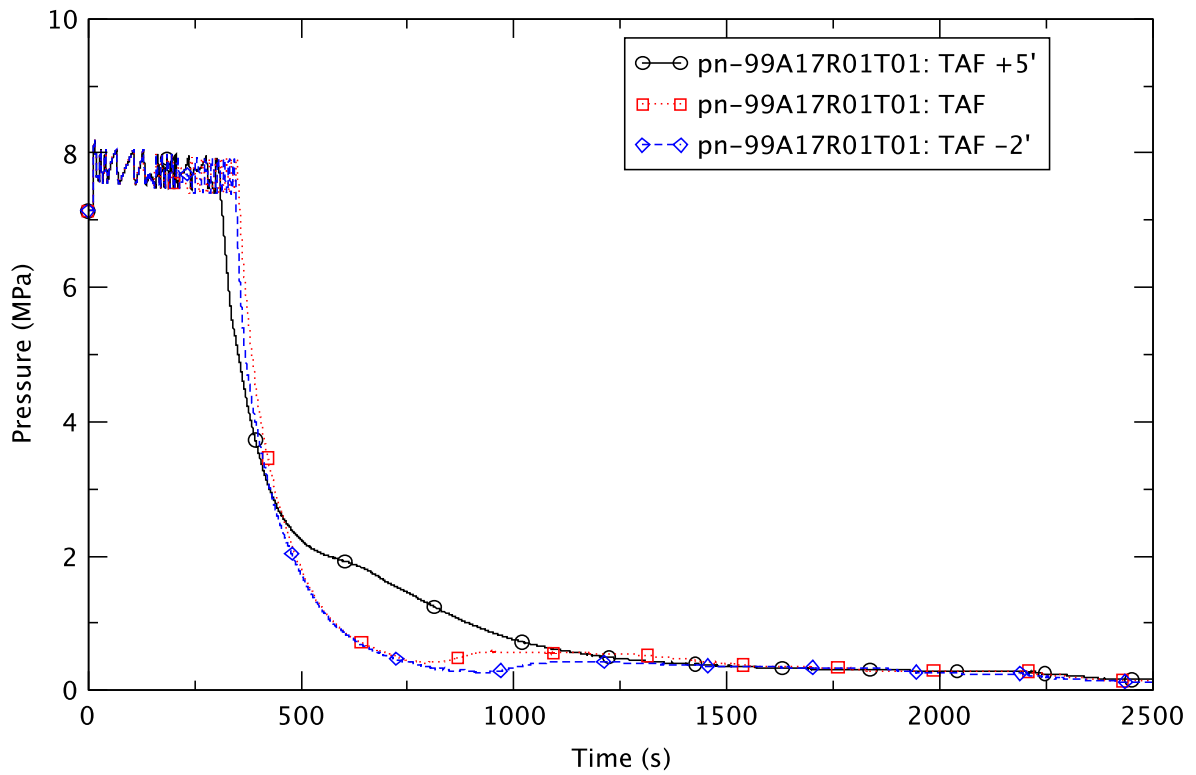


Figure 2.43 Reactor Pressure - EOFPL, 85% Flow Cases

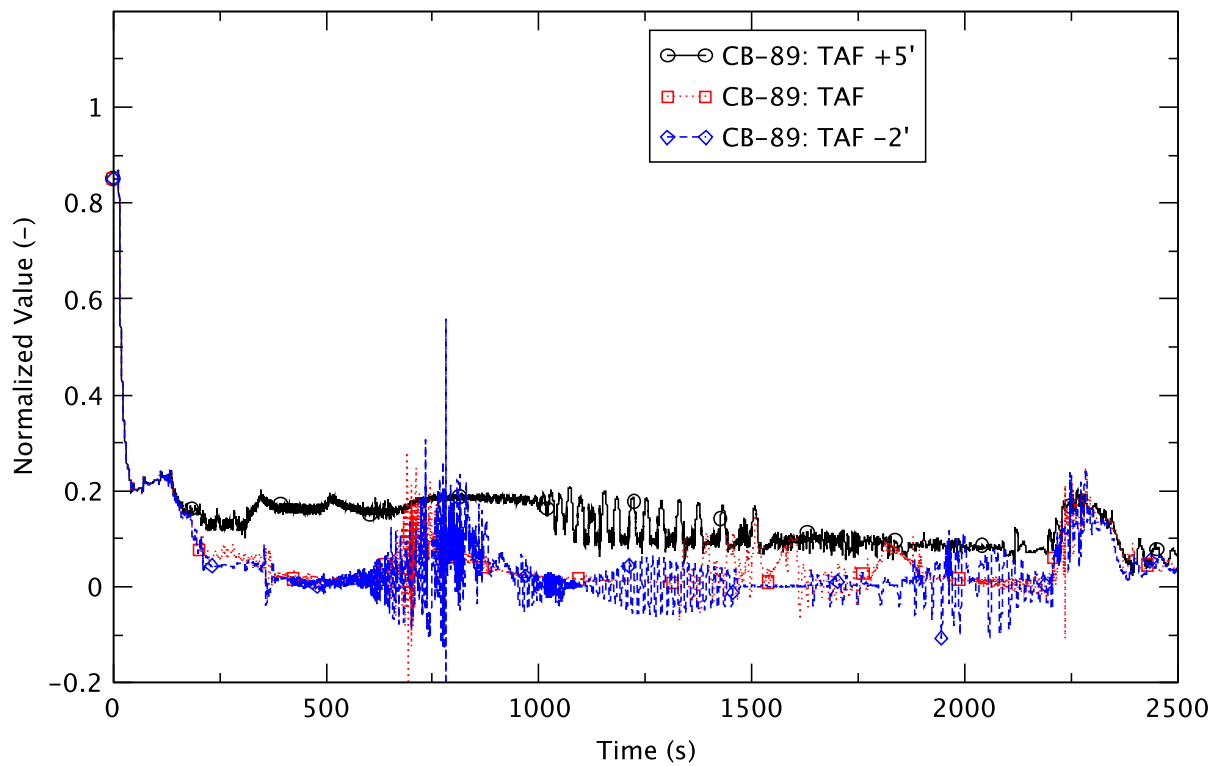


Figure 2.44 Core Flow - EOFPL, 85% Flow Cases

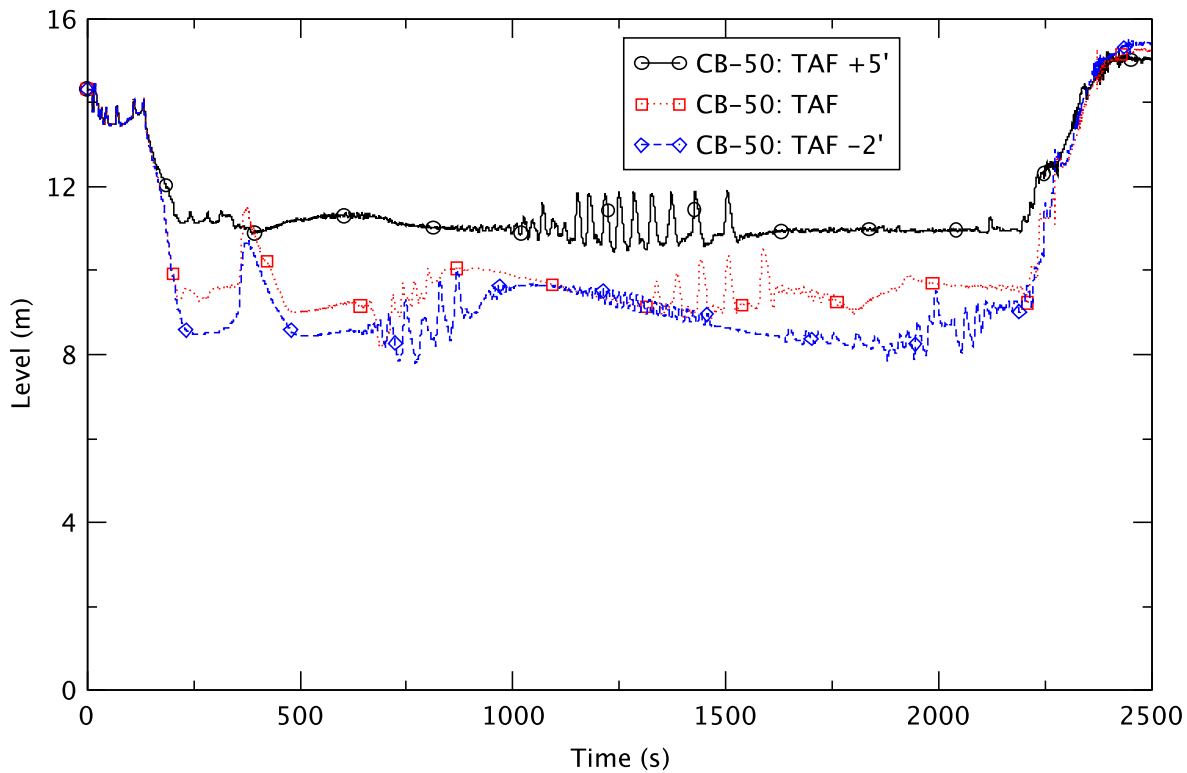


Figure 2.45 Downcomer Water Level - EOFPL, 85% Flow Cases

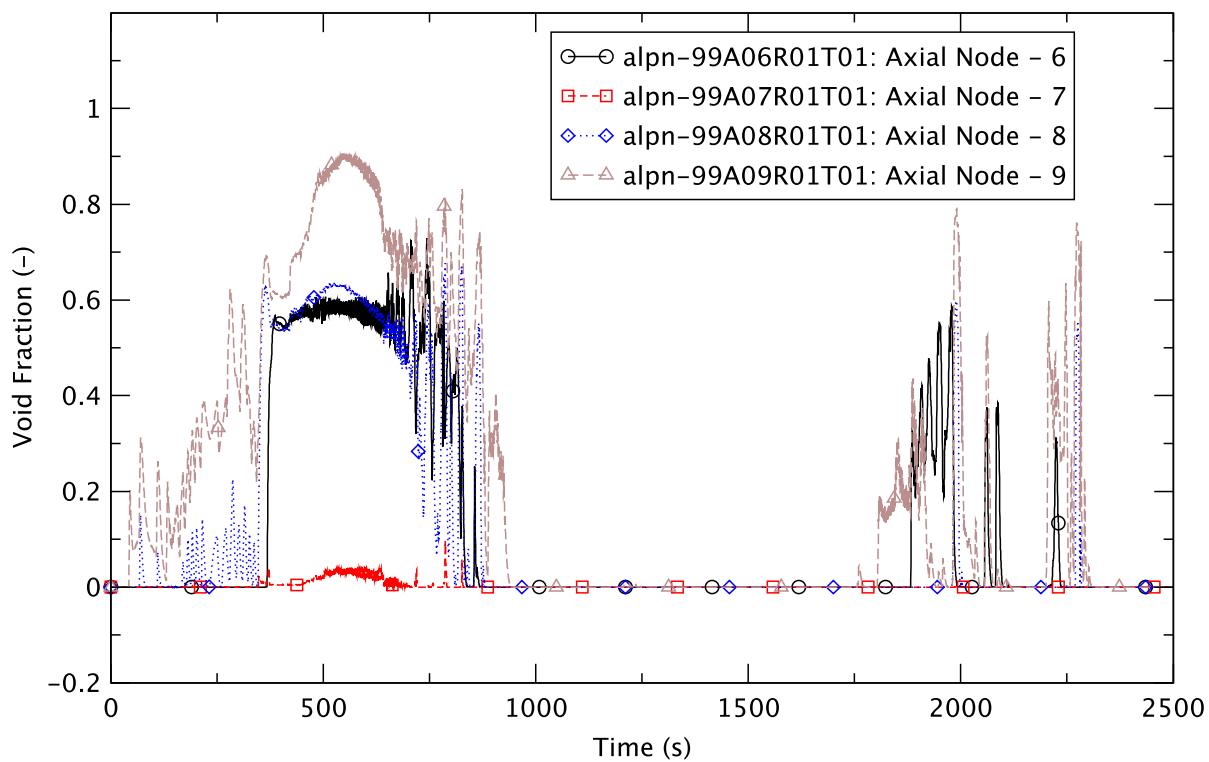


Figure 2.46 Void Fraction in Core Bypass (Ring-1) - EOFPL, TAF-2, 85% Flow

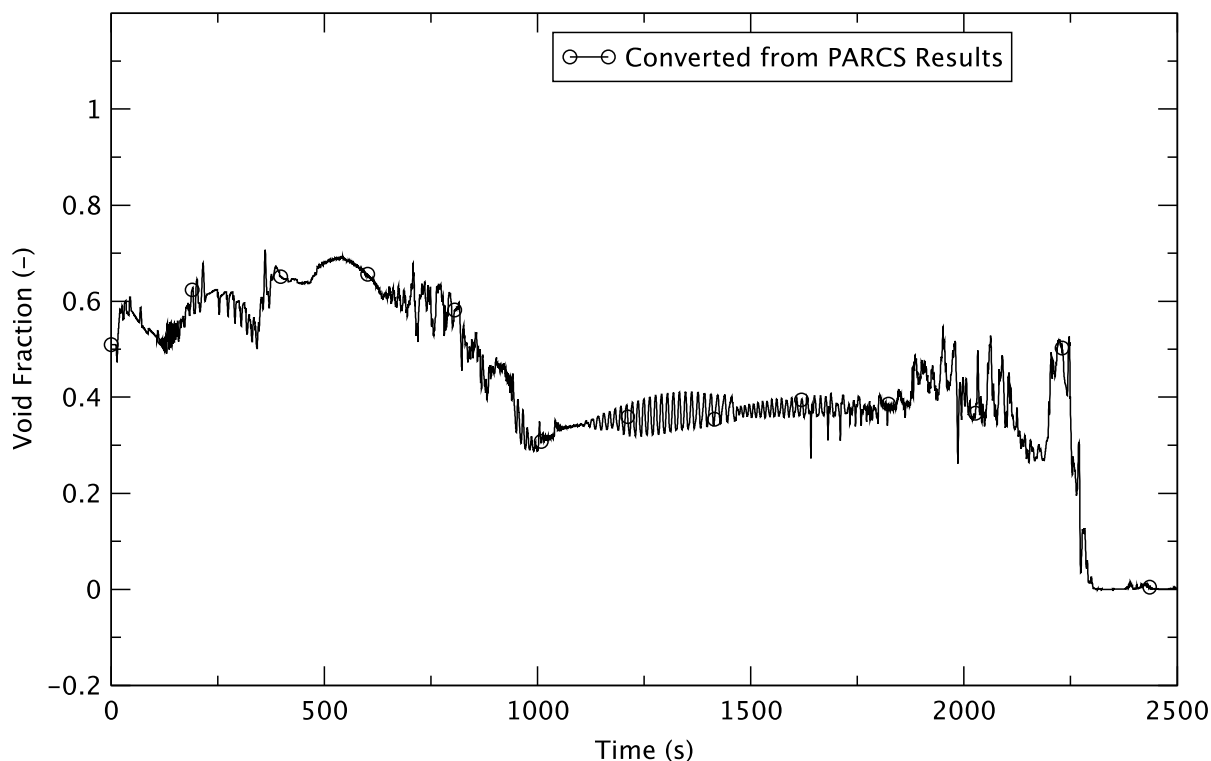


Figure 2.47 Core Average Void Fraction - EOFPL, TAF-2, 85% Flow

For the TAF+5 case, the continuation of natural circulation after ED translates to a slower decay in reactor power. A slower depressurization rate then follows after the reactor pressure has dropped to about 2.5 MPa (Figure 2.43). The substantial core flow in the TAF+5 case also promotes boron mixing in the core, as is evidenced in the monotonic increase in the core boron inventory (Figure 2.48). This buildup ultimately adds enough negative reactivity to shut down the reactor. Figure 2.41 shows that the reactor power begins its exponential decay at about 500 s.

For the cases of TAF and TAF-2 at about 750 s, coincident with the refilling of the lower plenum, there is a marked increase in the core's boron inventory. The subsequent increase in boron at 1500 s and 2000 s, respectively, for the TAF case and the TAF-2 case, is associated with re-mixing of stratified boron in the bottom of the lower plenum. The re-mixing is treated with an increase in the concentration of the injected boron, as calculated by the boron-transport control scheme (see discussion in Section 2.3.7 and Appendix A in [4]). The enhanced boron concentration reflects the increased core flow due to feedwater flow and a higher level. For all three cases, the boron inventory rises after level recovery, beginning at 2180 s. The effective injection boron concentration for the three sensitivity cases is shown in Figure 2.49 to Figure 2.51. The increases in boron concentration above nominal are attributed to the re-mixing of settled boron in the lower plenum of the reactor vessel; we note that re-mixing is assumed to be a function of coolant flow in the lower plenum.

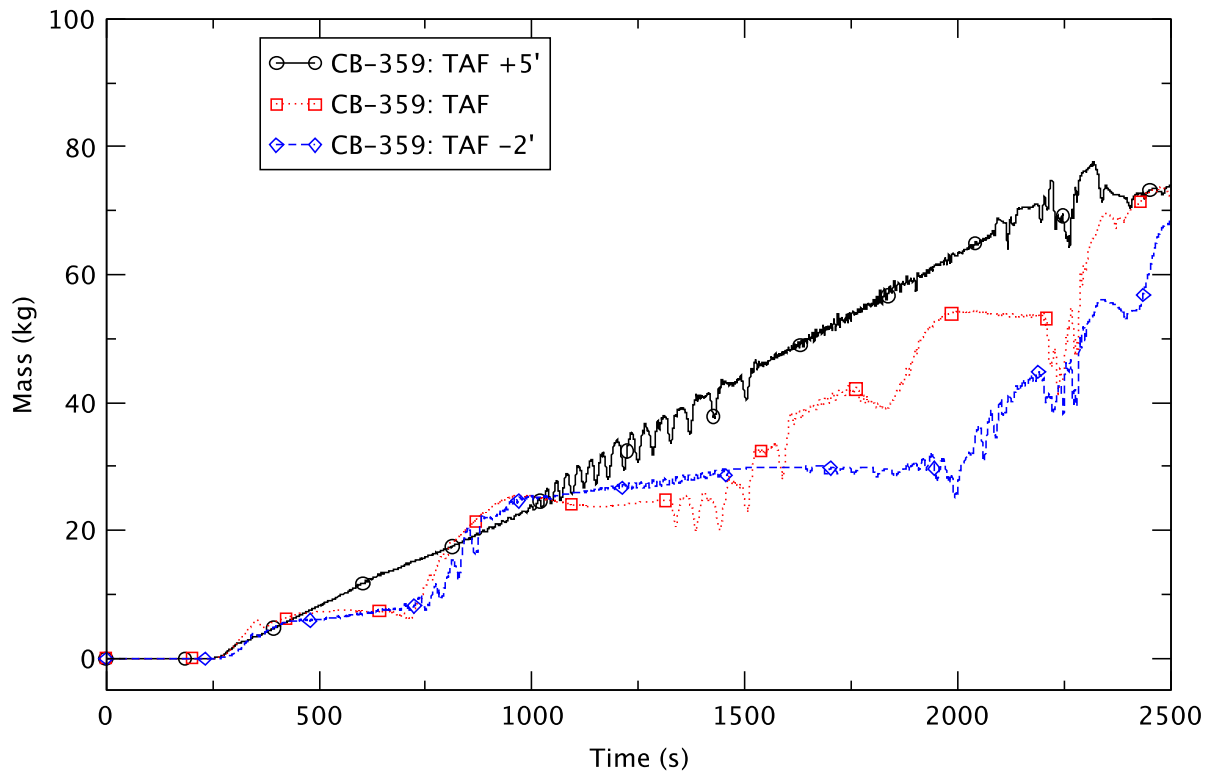


Figure 2.48 Boron Inventory in the Core - EOFPL, 85% Flow Cases

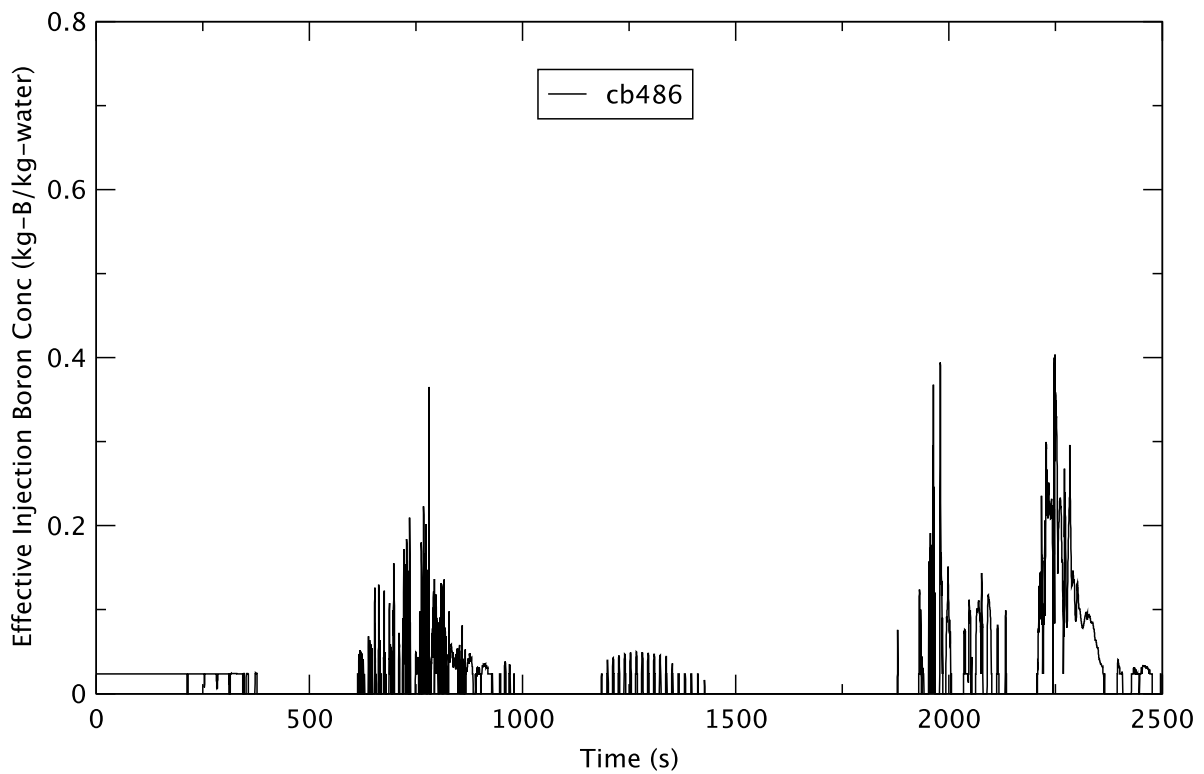


Figure 2.49 Effective Injection Boron Concentration - EOFPL, TAF-2, 85% Flow

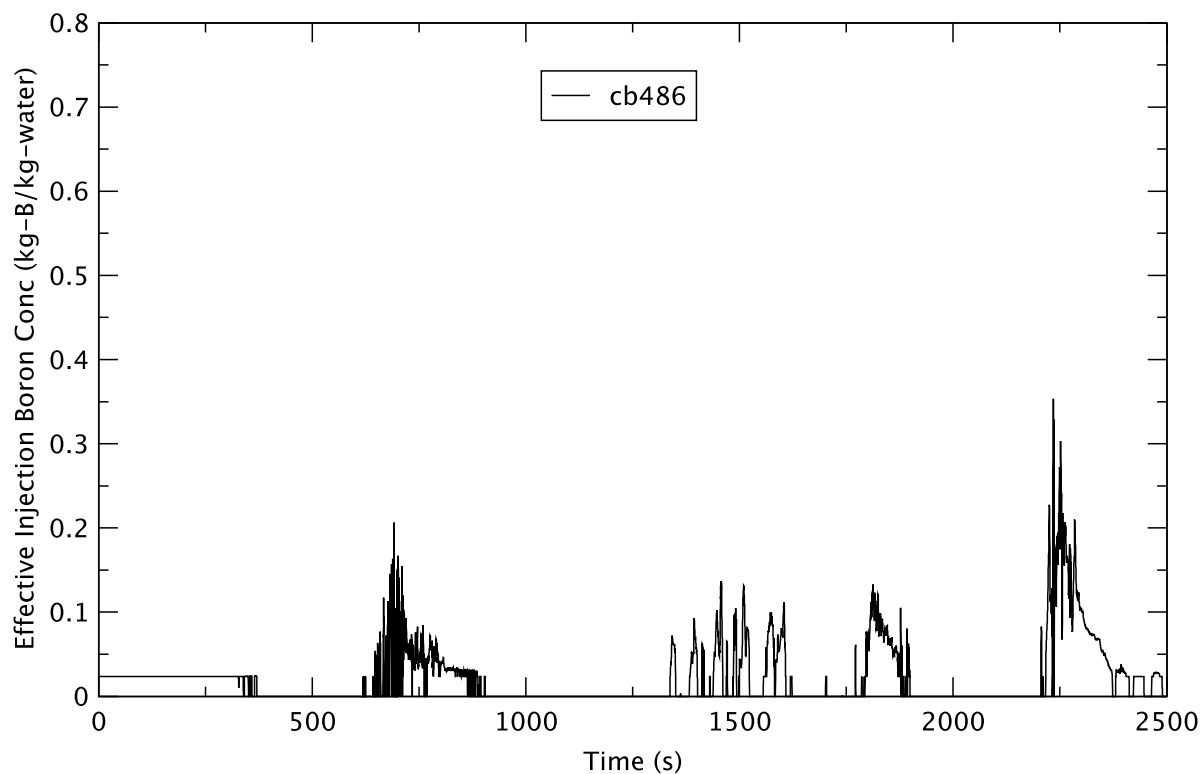


Figure 2.50 Effective Injection Boron Concentration - EOFPL, TAF, 85% Flow

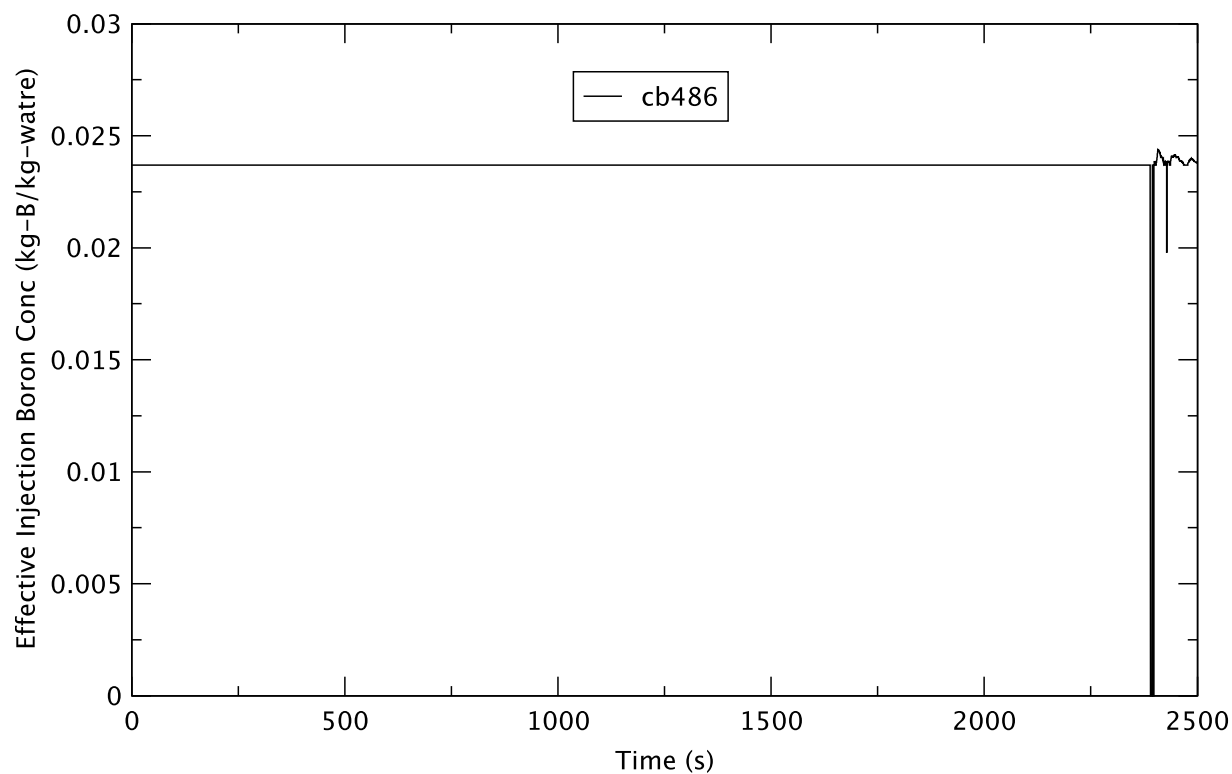


Figure 2.51 Effective Injection Boron Concentration - EOFPL, TAF+5, 85% Flow

For the TAF+5 case, the boron transport model predicts 100% mixing for almost the entire time of the simulated transient (Figure 2.51). The exception is a momentary drop in the mixing coefficient after the initiation of level recovery, caused by a drop in core flow subsequent to the displacement of voids in the core by coolant flow from the downcomer after the recovery of the water level.

The reactivity components calculated by PARCS are shown in Figure 2.52 and Figure 2.53, respectively, for TAF+5 and TAF (Figure 2.37 is the corresponding plot for TAF-2). For TAF and TAF-2, there is a decrease in core reactivity after depressurization due to voiding in the core and a recovery of reactivity after refilling it. For TAF+5, the total core reactivity remains relatively unchanged until about 1000 s. As the transient progresses, only the injected boron contributes negative reactivity to the core. Both the fuel (Doppler) and coolant (moderator density) reactivities are positive. The figures show that restoration of water level at 2180 s causes a positive increase in the moderator density reactivity, but that is more than compensated for by a corresponding increase in the negative contribution from boron reactivity. Therefore, the core remains subcritical during the level recovery.

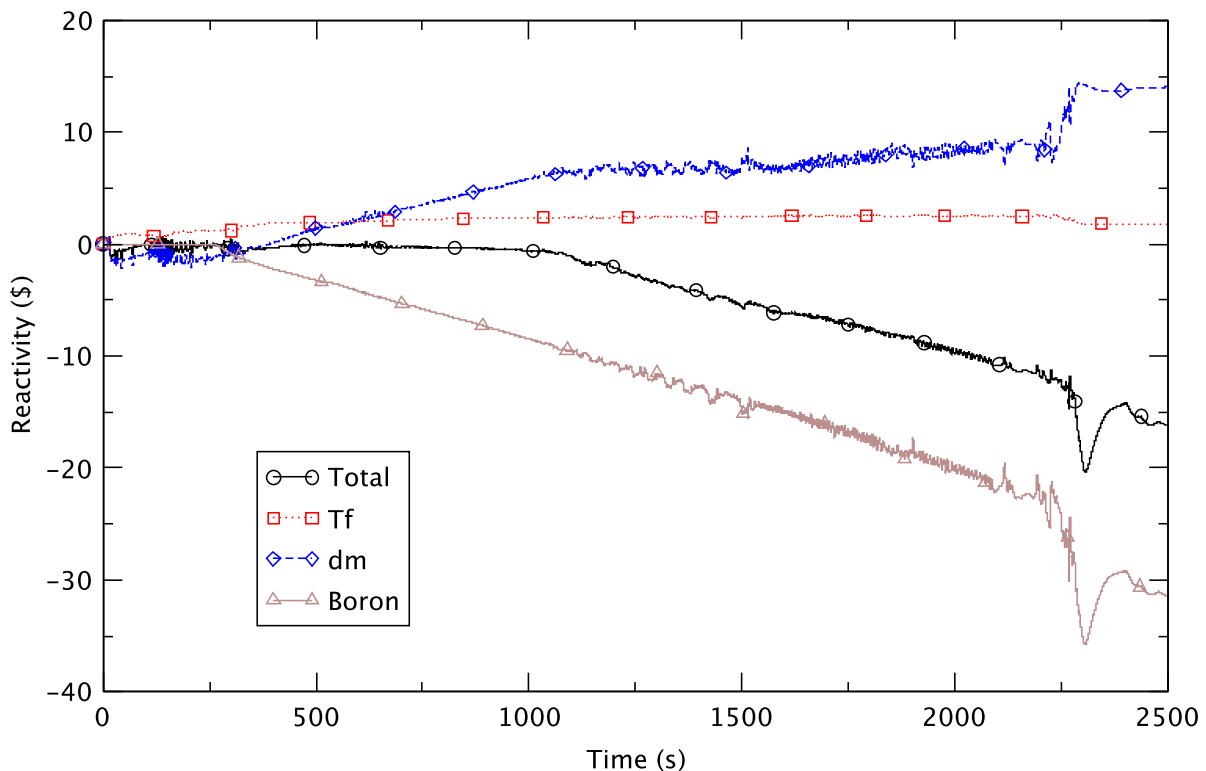


Figure 2.52 Core Reactivity - EOFPL, TAF+5, 85% Flow

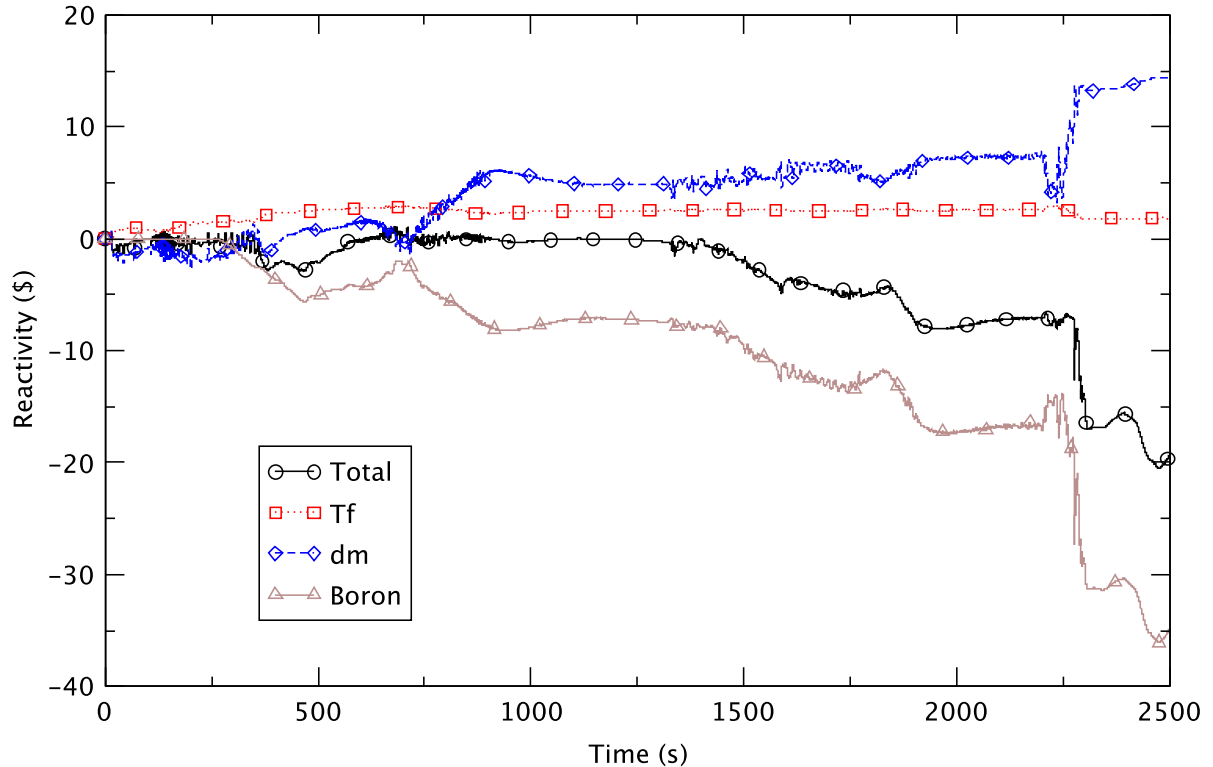


Figure 2.53 Core Reactivity - EOFPL, TAF, 85% Flow

The PCT for the three sensitivity cases is shown in Figure 2.54. In all, the maximum PCT occurs shortly after water level control starts at 130 s and before the emergency depressurization. Apparently, the unstable DWO causes the PCT that occurs when the ratio of power-to-flow is high. In the TAF-2 case, the fuel is predicted to dryout, fail to rewet, and experience heatup. The flow is lowest for this case, which contributes to its higher PCT. For the TAF-2 sensitivity case, there is a second, lower, peak for the PCT after the ED when the lower plenum and the core are refilled, a time when the peak PCT occurs in the corresponding base case (105% flow). For the TAF and TAF+5 base cases (at 105% flow), the maximum PCT occurs much earlier (shortly after MSIV closure; see Table 2.6) than in the corresponding sensitivity cases.

The suppression pool water temperature (Figure 2.55) indicates that the TAF+5 case has the highest energy input to the water in the suppression pool, followed by the TAF and the TAF-2 cases. We attribute these differences to the fact that the power trends downward more slowly for a higher RPV level (see discussion on reactor power earlier in this section). In all three instances, the pool temperature stays below the limit (i.e., saturation temperature at one atmosphere of pressure).

The pressure in the drywell (Figure 2.56) exhibits a similar trend to the temperature of the water in the suppression pool. In all three cases the maximum drywell pressure is low enough so as not to be of concern for containment integrity.

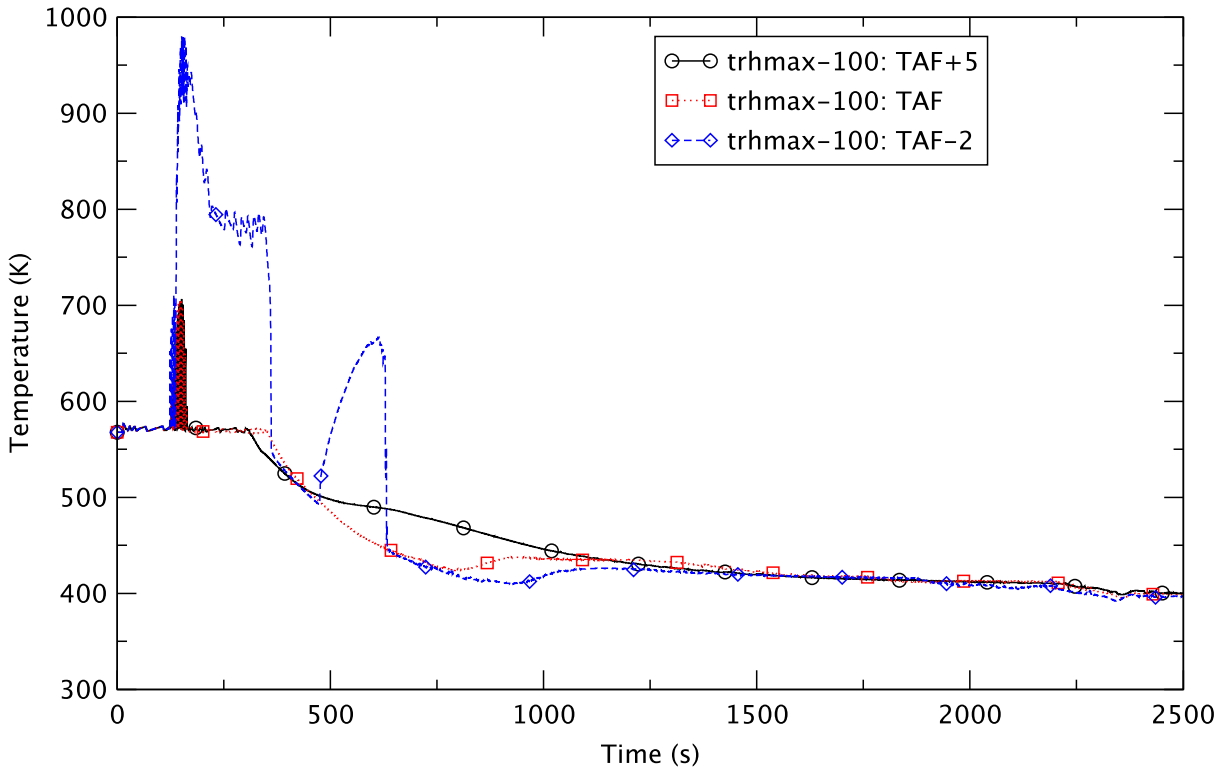


Figure 2.54 Peak Clad Temperature - EOFPL, 85% Flow Cases

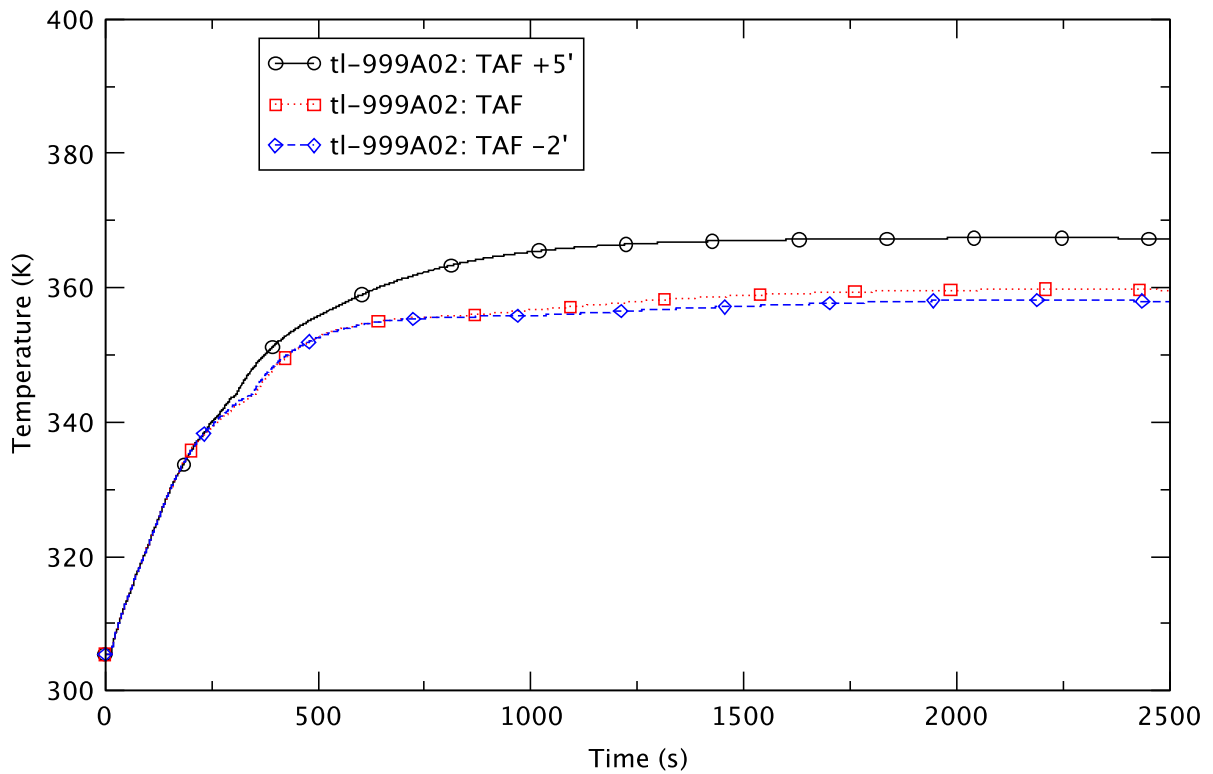


Figure 2.55 Suppression Pool Temperature - EOFPL, 85% Flow Cases

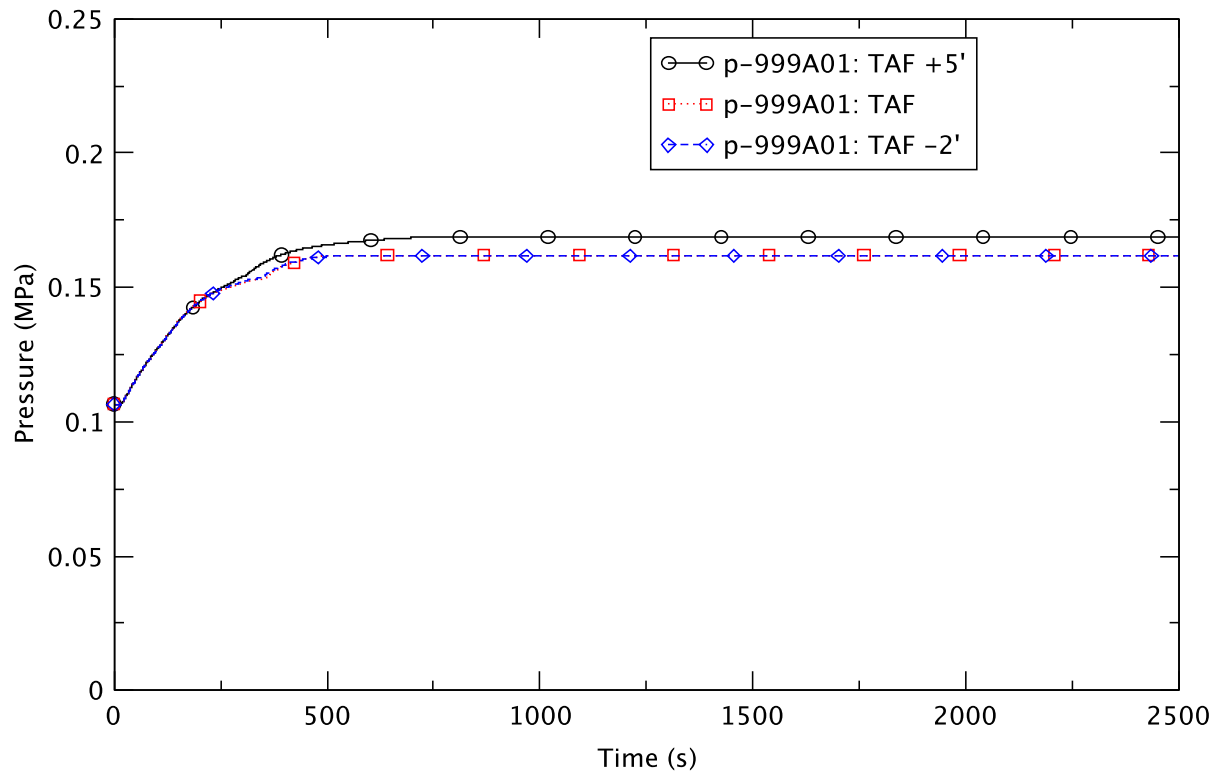


Figure 2.56 Drywell Pressure - EOFPL, 85% Flow Cases

3 SUMMARY AND CONCLUSIONS

This chapter summarizes the results and conclusions for this sensitivity study, which is a continuation of a previous one [4] of ATWS-ED events (i.e., those initiated by closing the main steam isolation valves (MSIVs) and leading to emergency depressurization (ED) once the heat-capacity temperature limit (HCTL) of the suppression pool is exceeded. In the present study, the objective is to understand the sensitivity of ATWS-ED events to operating core flow and spectrally corrected moderator density history (void history) in a typical BWR/5² operating in an expanded operating domain under MELLLA+ conditions.

In this report, we compare the results of the sensitivity cases listed in Table 1.1 with those of the corresponding reference cases in our previous report [4]. This chapter is divided into two sections, a section on what was learned about the sensitivity cases, and a section related to the calculation tool we used, namely TRACE/PARCS.

3.1 ATWS Events Initiated by MSIV Closure – Sensitivity Cases

The sensitivity study was conducted by using the same methodology and ATWS-ED scenario as reported in [4]. The six ATWS-ED cases listed in Table 1.1 investigate the sensitivity of ATWS-ED events to operating core flow and the spectrally corrected moderator density history (void history) in a typical BWR/5 operating in an expanded operating domain under MELLLA+ conditions. For the typical BWR/5^b under consideration, the nominal core flows at beginning-of-cycle (BOC) and end-of-full-power-life (EOFPL) conditions respectively are 85% and 105% of rated flow. The sensitivity studies on core flow, assumed operating flows of 75% (for BOC and EOFPL) and 85% (for EOFPL) of rated flow. The correction to the moderator history is to account for the impact of factors, such as leakage or control state, on the neutron energy spectrum. For the EOFPL 85% flow condition the sensitivity study also considered different water level control strategies: top-of-active-fuel (TAF), TAF+5' and TAF-2', respectively.

The results show the following:

- The ATWS-ED transient (EOFPL, TAF+5) is insensitive to the void history model. The results of the sensitivity case using the spectrally corrected void history (UHSPH) essentially are the same as the base case (the UH case).
- Reducing the initial operating core flow shifts the boiling boundary and power generation towards the core inlet.
- Transient reactor power is higher in the reduced (initial) flow cases than in the corresponding reference cases. The fractional decrease in core flow as a result of the recirculation pump trip (2RPT) is lower for the reduced flow cases leading to a relatively lower reduction in reactivity than the reference cases.
- Higher core power in the reduced flow cases results in
 - A higher PCT
 - more energy relieved to the suppression pool via the SRVs

² For simulating ATWS-ED events we modified the TRACE BWR/5 model into a BWR/4-like model with lower-plenum SLCS injection.

- earlier depressurization time
 - higher drywell pressure
 - higher temperature in the suppression pool .
- In all cases of reduced flow, the reactor remains shutdown by the injected boron.
 - There is no recriticality observed due to either repressurization of the reactor vessel or dilution of boron.
 - The maximum PCT is below 1478 K (2200°F), the limit chosen for this study.
 - Both the drywell pressure and the temperature of the suppression pool stay low enough as not to be of safety concern.
- The progression of the BOC, TAF+5 case at 75% flow generally follows the same trend as the reference case at 85% flow. As noted above, the sensitivity case at reduced core flow has higher reactor power and PCT than does the reference case.
- Reactor power density wave oscillations (DWO) with increasing amplitude at a frequency of ~0.4 Hz is observed in the EOFPL 75% and 85% flow cases after the 2RPT and before the reduction in level has suppressed the reactor power. Evaluation of reactor instability is outside the scope of this sensitivity study.
- Under the EOFPL reduced flow, the magnitude of the power oscillation after the 2RPT is higher for a lower operating flow.
- For the EOFPL reduced flow cases (75% and 85% rated flow) the maximum PCT occurs shortly after the initiation of level control at 130 s when the core flow still is relatively high. For the TAF-2 sensitivity cases, there is a second peak in the PCT after the depressurization at a time when the reactor is at or close to the decay heat level. Though the second peak in the PCT is much lower than the first one, we calculated that it is higher than the maximum PCT for the corresponding reference case (EOFPL, 105% flow, TAF-2). For the two cases of reduced flow, the unstable DWO apparently causes the maximum PCT that occurs when the reactor power-to-flow ratio is high.
- For the EOFPL reference cases (105% initial flow; see Section 4.4 in [4]), the timing of the maximum PCT depends on the level-control strategy. For level control to TAF and TAF+5, the maximum PCT occurs at 14.3 s when the reactor still is undergoing pressurization, i.e., before the MSIVs are fully closed. For level control to TAF-2, the maximum PCT occurs at 700 s when core flow is very low and the core is voided, so generating a higher maximum PCT than in the other two cases.
- The effects of level control with reduced core flow for the EOFPL condition are generally similar to the trends exhibited by the corresponding reference cases at 105% flow. There are two exceptions here. They are in the timing of the maximum PCT (see earlier discussion), and the condition of core flow after the emergency depression (ED) for the TAF+5 case.
- For the EOFPL sensitivity case (85% flow) at TAF+5, natural circulation flow persists throughout the ED. For the reference case (105% flow, TAF+5), natural circulation flow is broken after the ED and is not re-established until after the lower plenum is refilled, at about 750 s.

Similar to the analyses described in [4], the findings from the sensitivity cases demonstrate the effectiveness of the operator's actions in mitigating reactor power in an ATWS-ED transient. These actions include controlling the water level, emergency depressurization, and the injection of boron. In all cases analyzed, the peak clad temperature (PCT) stayed below the chosen limit of 1478 K (2200°F), no recriticality was predicted, as was no over-heating of the suppression pool or over-pressurization of the drywell. In summary, the sensitivity study shows that the PCT is the parameter most affected by reduced initial operating flow, but also, the magnitude of power oscillation is increased and the frequency of oscillation coincides with that characterized by density wave oscillations in BWRs.

3.2 Applying TRACE/PARCS to ATWS-ED Events

As an advanced tool for analyzing system transients, the TRACE/PARCS package has numerous modeling parameters that the analyst can select to overcome some numerical difficulties encountered in simulating a transient scenario. This also is the case in this sensitivity study. TRACE/PARCS input options specific to the simulation of ATWS-ED events were discussed in [4]. However, we had to update the code to enable us to complete all six sensitivity cases. We employed the three TRACE executables, summarized in Table 2.2, for the current work. Appendix A gives more background information on using different versions of TRACE. These results in the appendix demonstrate that the updated version of the code can duplicate the major features predicted by the old version for the same ATWS-ED transient.

The sensitivity of the results of ATWS-ED to the size of the time-step and the choice of numerical method [stability enhanced two step (SETS) versus semi-implicit (S-I)] is examined in Appendix B. In using the SETS method, the results were shown to be insensitive to a reduction of the maximum time-step size from 0.05 s to 0.025 s. Calculations discussed in the appendix also demonstrate that by judiciously choosing the size of the maximum time-step, SETS and S-I produce essentially identical results. A scoping calculation described in Appendix B suggests that there is bifurcation in results when the computation is started from slightly different initial conditions. The parameter(s) that drive the solution to a certain path is unclear; however, the results seem to be sensitive to differences in modeling and in numerical methods.

4 REFERENCES

1. J. Harrison, GE Hitachi, letter to U.S. Nuclear Regulatory Commission, "Accepted Version of GE Licensing Topical Report NEDC-33006P-A, Revision 3 (TAC No. MD0277)," MFN 09-362, June 19, 2009 (ADAMS Accession No. ML091800512)
2. L-Y. Cheng et al., "BWR Anticipated Transients Without Scram in the MELLLA+ Expanded Operating Domain – Part 1: Model Development and Events Leading to Instability," NUREG/CR-7179, BNL-NUREG-105323-2014, Brookhaven National Laboratory, March 3, 2014.
3. L-Y. Cheng et al., "BWR Anticipated Transients Without Scram in the MELLLA+ Expanded Operating Domain – Part 2: Sensitivity Studies for Events Leading to Instability," NUREG/CR-7180, BNL-NUREG-105327-2014, Brookhaven National Laboratory, March 20, 2014.
4. L-Y. Cheng et al., "BWR Anticipated Transients Without Scram in the MELLLA+ Expanded Operating Domain – Part 3: Events Leading to Emergency Depressurization," NUREG/CR-7181, BNL-105328-2014, Brookhaven National Laboratory, April 22, 2014.
5. P. Yarsky, "Applicability of TRACE/PARCS to MELLLA+ BWR ATWS Analyses, Revision 1," U.S. Nuclear Regulatory Commission, Office of Nuclear Regulatory Research, November 18, 2011, ADAMS Accession No. ML113350073.
6. NRC, "Standard Review Plan," Section 15.8, NUREG 0800, U.S. Nuclear Regulatory Commission, March 2007.

APPENDIX A

Comparison of TRACE Executables

LIST OF FIGURES

| | | |
|-------------|---|------|
| Figure A.1 | Reactor Power - EOFPL, TAF-2..... | A-4 |
| Figure A.2 | Reactor Pressure - EOFPL, TAF-2 | A-5 |
| Figure A.3 | Core Flow - EOFPL, TAF-2..... | A-5 |
| Figure A.4 | Downcomer Water Level - EOFPL, TAF-2 | A-6 |
| Figure A.5 | Steamline Flow - EOFPL, TAF-2..... | A-6 |
| Figure A.6 | Feedwater Flowrate - EOFPL, TAF-2..... | A-7 |
| Figure A.7 | Lower Plenum Temperature - EOFPL, TAF-2 | A-7 |
| Figure A.8 | Core Average Void Fraction - EOFPL, TAF-2 | A-8 |
| Figure A.9 | Boron Inventory in the Core - EOFPL, TAF-2..... | A-8 |
| Figure A.10 | Suppression Pool Temperature - EOFPL, TAF-2 | A-9 |
| Figure A.11 | Drywell Pressure - EOFPL, TAF-2 | A-9 |
| Figure A.12 | Reactor Power - EOPFL, TAF-2, 75% Flow | A-10 |
| Figure A.13 | Downcomer Water Level - EOFPL, TAF-2, 75% Flow..... | A-11 |
| Figure A.14 | Core Flow - EOFPL, TAF-2, 75% Flow | A-11 |
| Figure A.15 | Feedwater Flowrate - EOFPL, TAF-2, 75% Flow | A-12 |
| Figure A.16 | Total Core Reactivity - EOFPL, TAF-2, 75% Flow..... | A-12 |
| Figure A.17 | Doppler Reactivity - EOFPL, TAF-2, 75% Flow..... | A-13 |
| Figure A.18 | Moderator Density Reactivity - EOFPL, TAF-2, 75% Flow | A-13 |
| Figure A.19 | Boron Reactivity - EOFPL, TAF-2, 75% Flow..... | A-14 |

LIST OF TABLES

| | | |
|-----------|--|-----|
| Table A.1 | Version of TRACE Executable Used | A-3 |
|-----------|--|-----|

This appendix provides additional background information on the use of three versions of the TRACE/PARCS executable in analyzing the six ATWS-ED sensitivity cases. The objective is to confirm that the three versions of the executable are able to generate similar results for a particular ATWS-ED case. Table A.1 gives the version of the executable used for each sensitivity case.

Table A.1 Version of TRACE Executable Used

| Case ID | Exposure | Core Flowrate, % | Reactor Water Level Strategy | TRACE Executable |
|----------------|-----------------|-------------------------|-------------------------------------|-------------------------|
| 4B | BOC | 75 | TAF+5 | V5.540_fxValveChoke.x |
| 10D | EOFPL | 75 | TAF-2 | V5.0p3P32m07co_x64.exe |
| 10A | EOFPL | 85 | TAF+5 | V5.540_fxValveChoke.x |
| 11A | EOFPL | 85 | TAF | V5.540_fxValveChoke.x |
| 12A | EOFPL | 85 | TAF-2 | V5.0p3P32m07co.x |
| 10C | EOFPL UHSPH | 105 | TAF+5 | V5.540_fxValveChoke.x |

The Linux and Windows executables are identified by filename extensions “.x” and “.exe” respectively. All eleven of the base reference cases were analyzed using V5.540_fxValveChoke.x, a version very similar to the latest released version of TRACE (V5.541 is V5 Patch 3). However, this version of the executable failed to complete two of the EOFPL cases at reduced flow (75% and 85%) with the water level reduction to TAF-2. The difficulty appears to be related to failure of PARCS to converge when the reactor power is at decay-heat levels. A revised version of TRACE, V5.0p3P32m07co, subsequently was used to complete these two TAF-2 sensitivity cases.

The following are two of the relevant changes made in the PARCS module of TRACE that enable the completion of the TAF-2 simulations:

1. A limiter was added to the ADF adjustment factor, on the left and right faces of the considered node.
2. For the NEM kernel, a limit was also placed on the lowest value for the surface flux.

An EOFPL base case was rerun with this new version of the executable to confirm the equivalency of the two versions of the executable. Results from them are compared in the first part of this appendix.

The new version of the TRACE executable successfully completed the EOFPL TAF-2 85% flow case. However, using the Linux executable V5.0p3P32m07co.x to run the same case but starting with 75% core flow, we noted an anomalous power spike about 700 s. The Windows version of the new executable, V5.0p3P32m07co_x64.exe, completed the case without the power spike. We compare the findings from the Linux and Windows version of the executable in the second part of this appendix. They gave identical results until the occurrence of the power spike.

The following figures (Figure A.1 to Figure A.11) are from the execution of the EOFPL TAF-2 base case (105% flow) by the two versions of the TRACE executable, namely, V5.540_fxValveChoke.x (the old version), and V5.0p3P32m07co.x (the new one). Both runs

were done with the semi-implicit numerical scheme and a maximum time-step size of 0.02 s. A comparison of their results demonstrates that the new version of TRACE can duplicate the following major features predicted by the old version for an ATWS-ED transient:

- power spike after MSIV closure
- power and flow decrease after 2RPT
- level control
- timing of ED
- reactor pressure
- level swell after ED
- boron inventory in the core

Any minor differences in the results they produced will not lead to different conclusions of the sensitivity study.

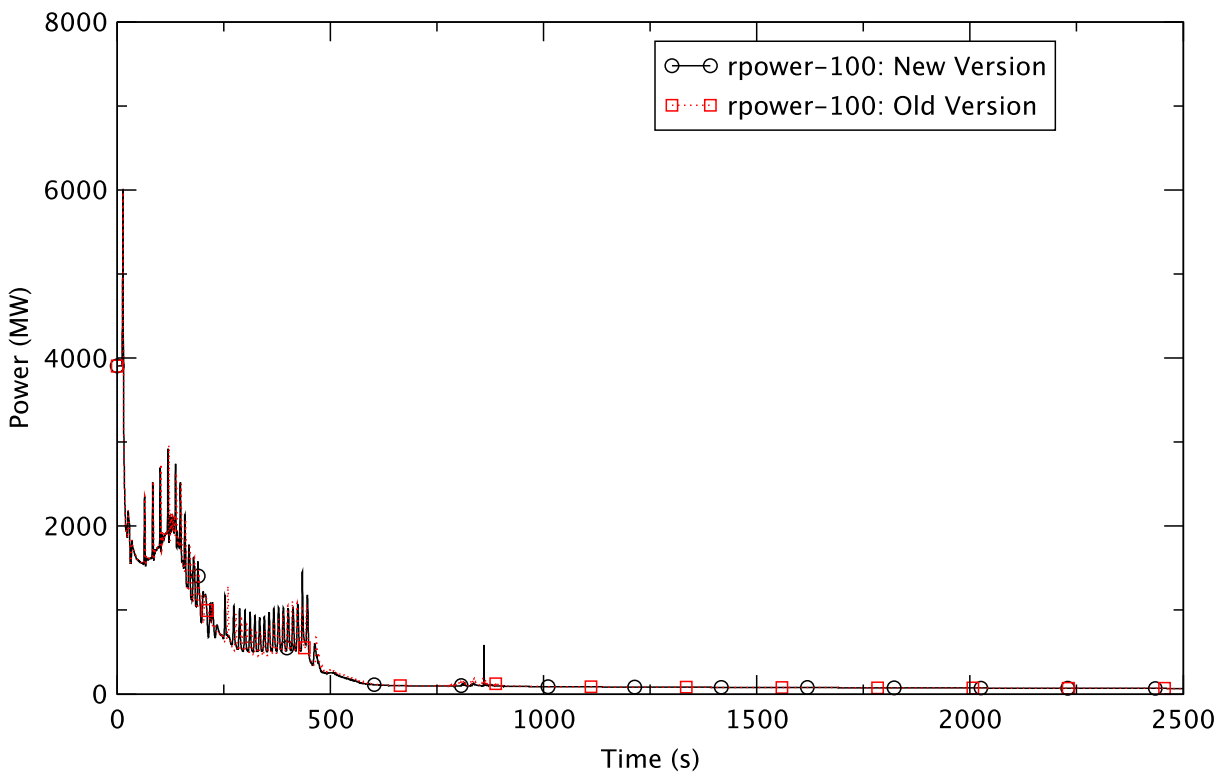


Figure A.1 Reactor Power - EOFPL, TAF-2

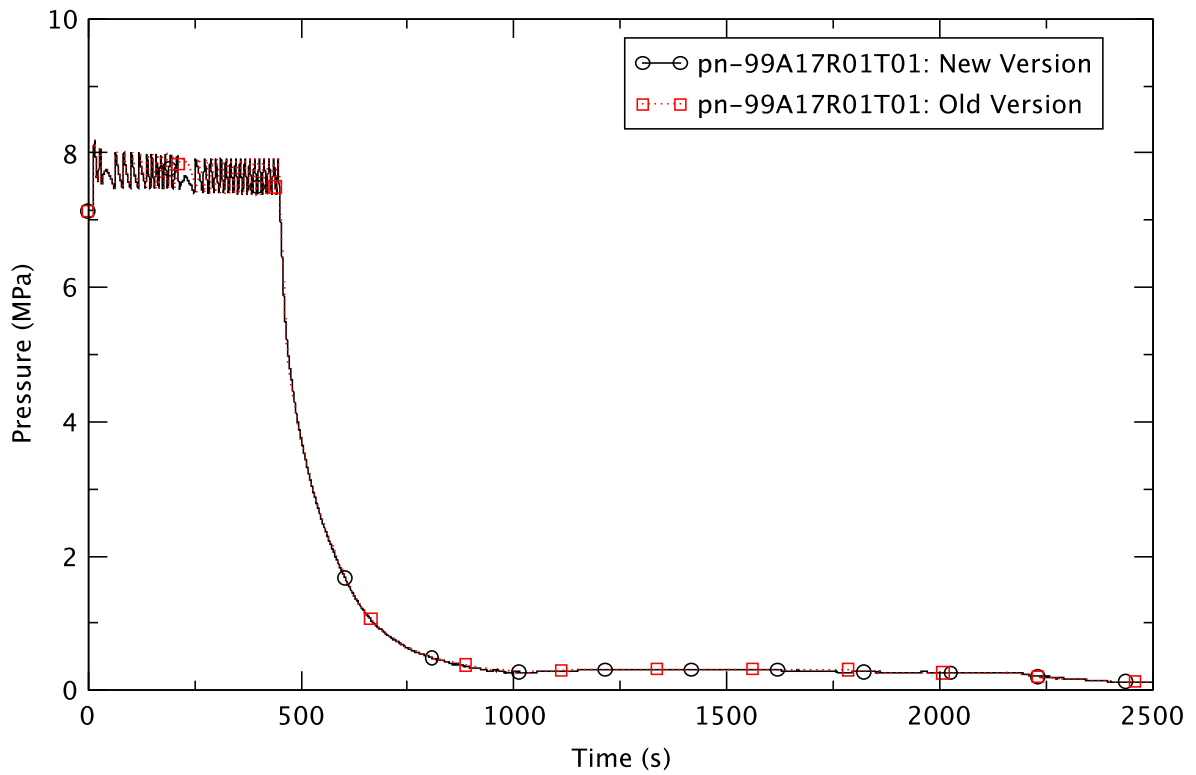


Figure A.2 Reactor Pressure - EOFPL, TAF-2

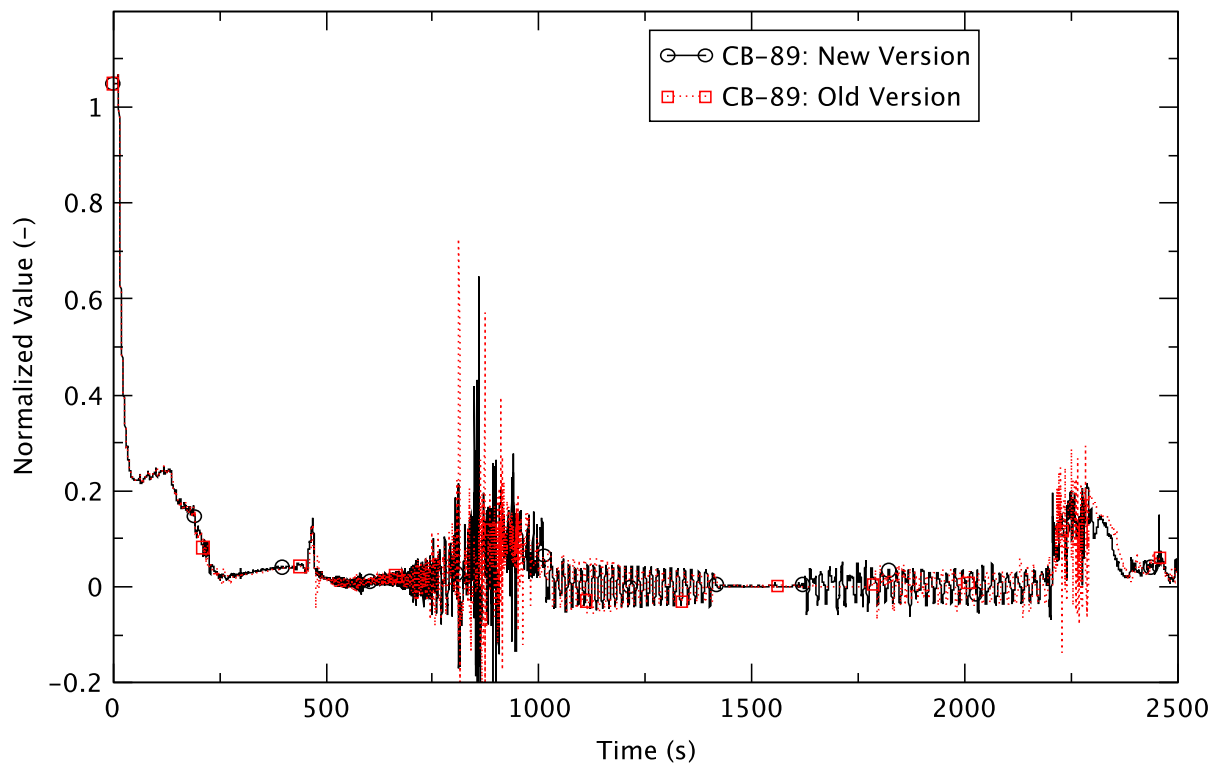


Figure A.3 Core Flow - EOFPL, TAF-2

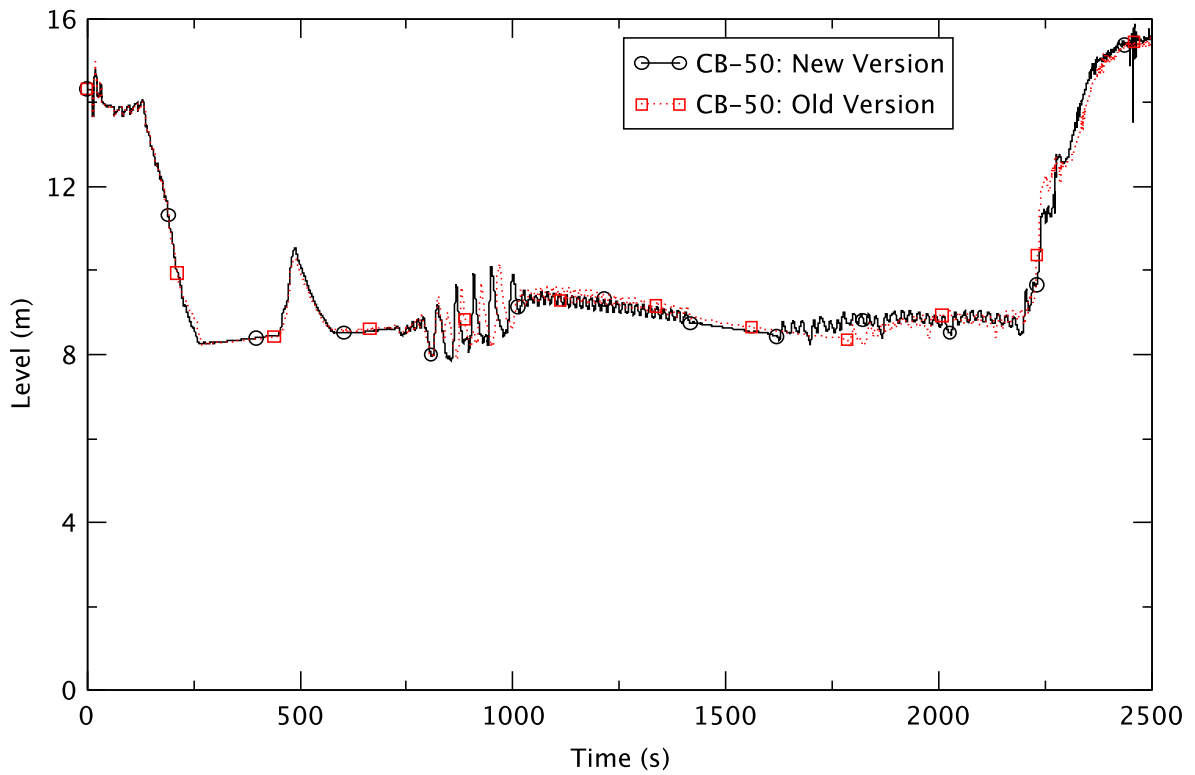


Figure A.4 Downcomer Water Level - EOFPL, TAF-2

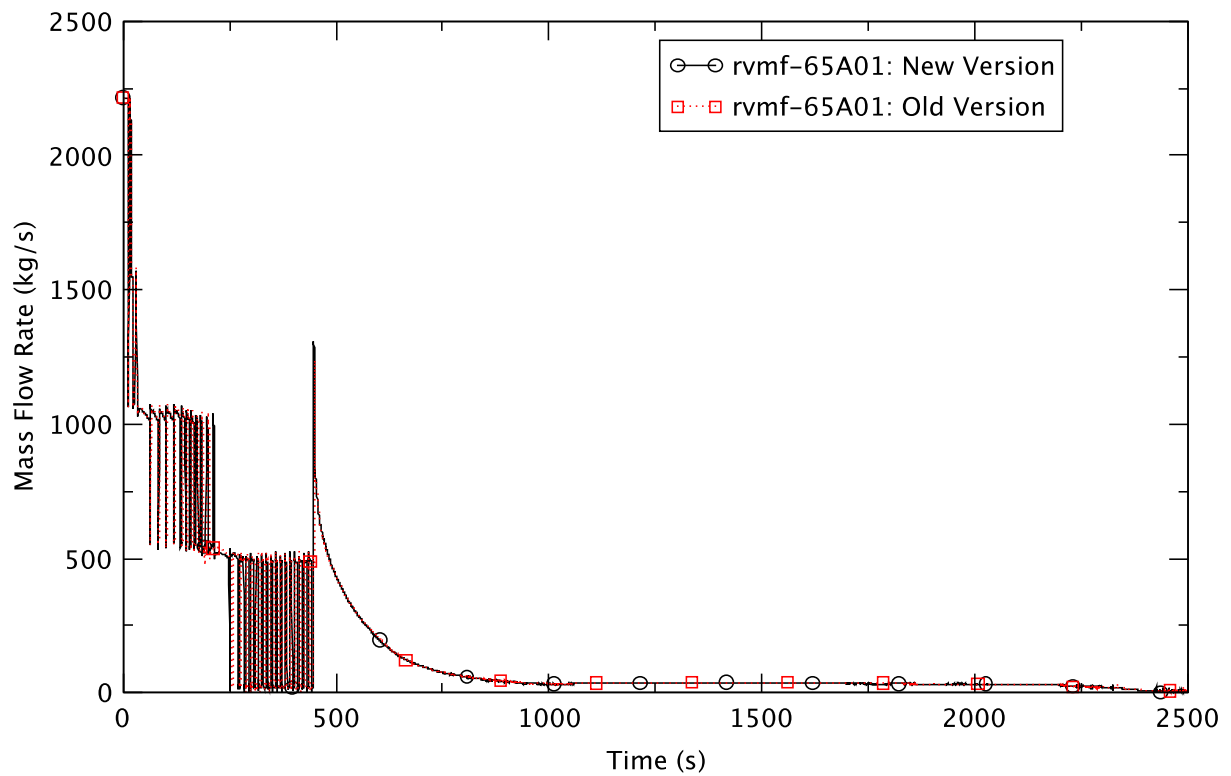


Figure A.5 Steamline Flow - EOFPL, TAF-2

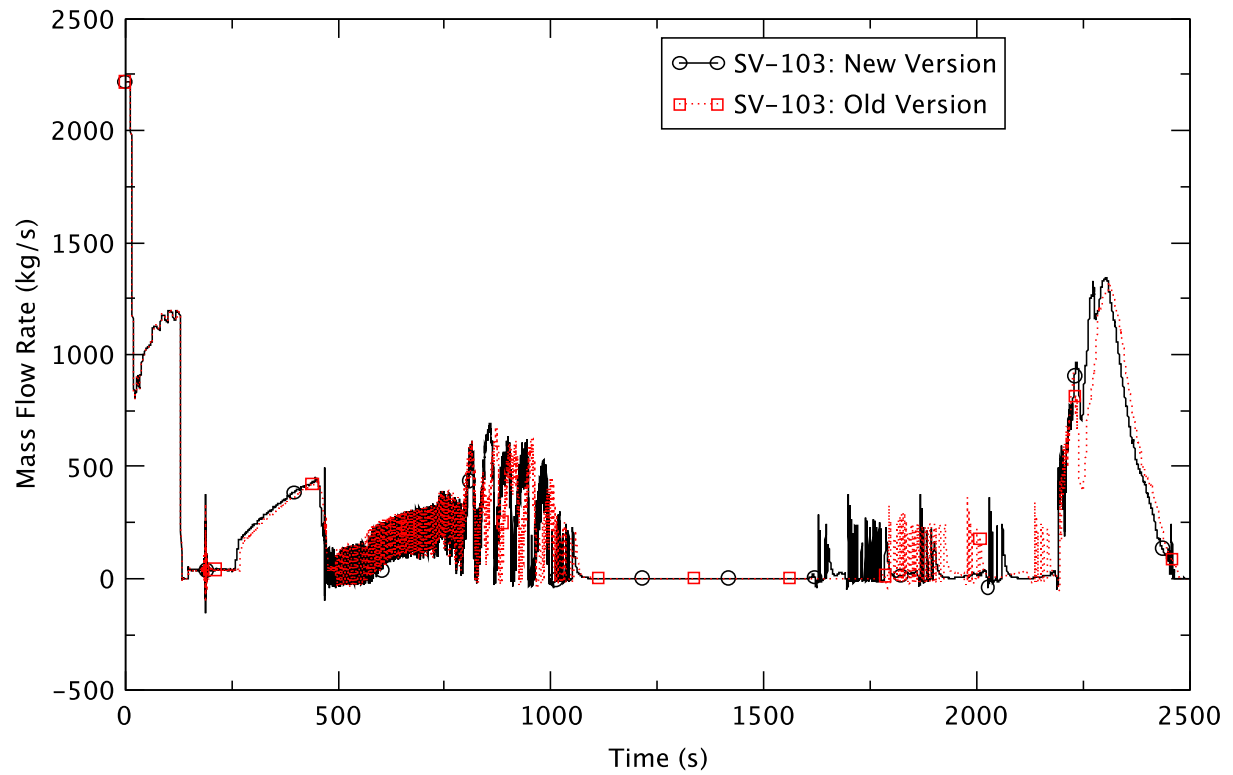


Figure A.6 Feedwater Flowrate - EOFPL, TAF-2

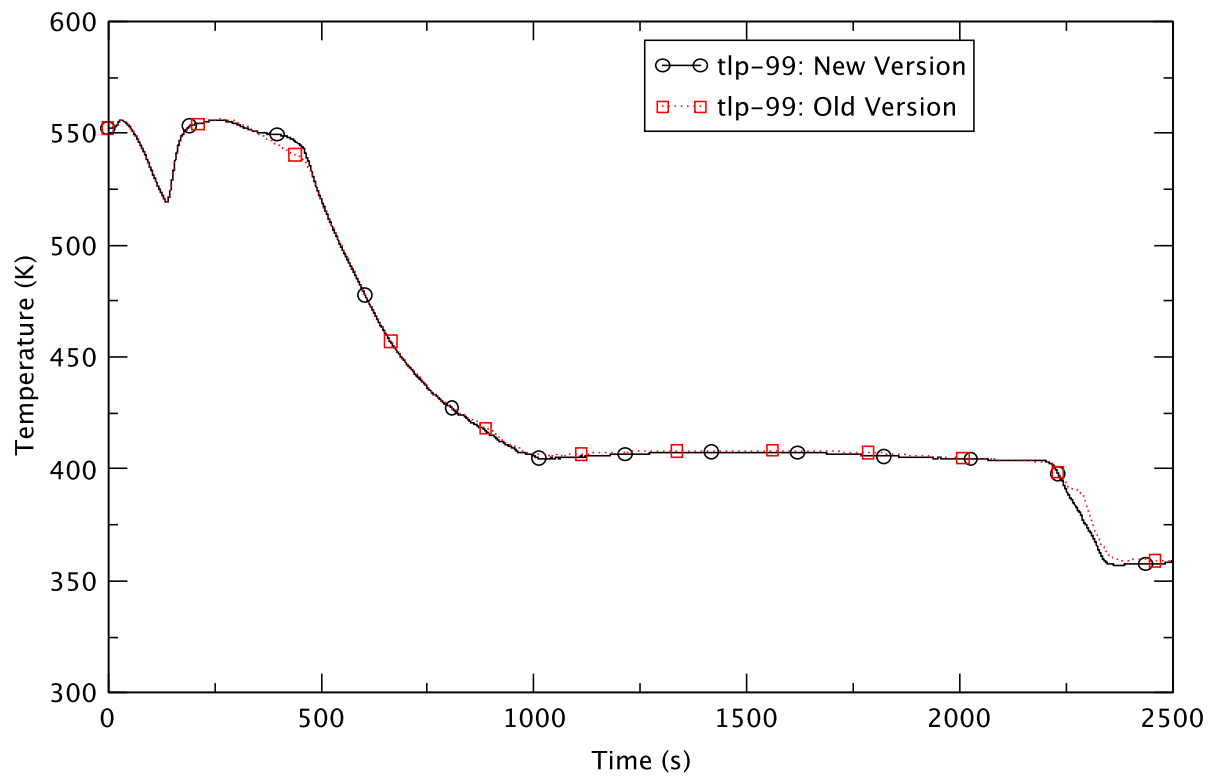


Figure A.7 Lower Plenum Temperature - EOFPL, TAF-2

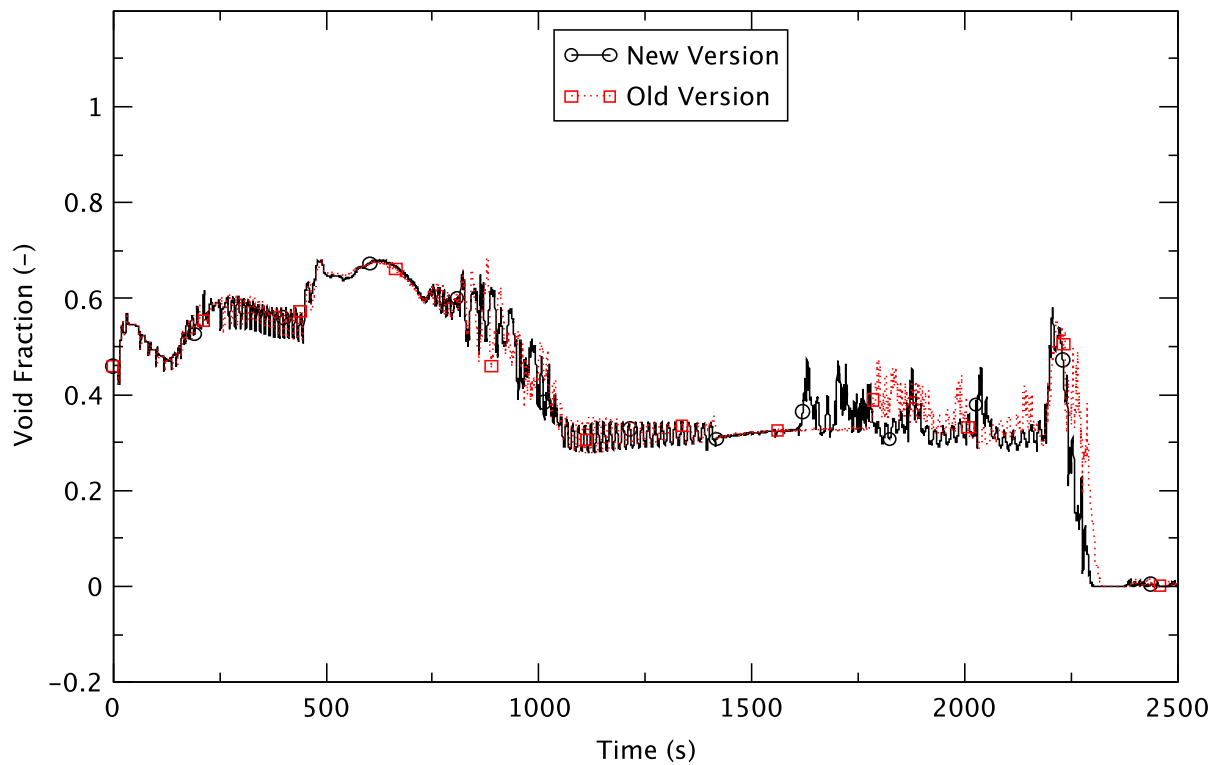


Figure A.8 Core Average Void Fraction - EOFPL, TAF-2

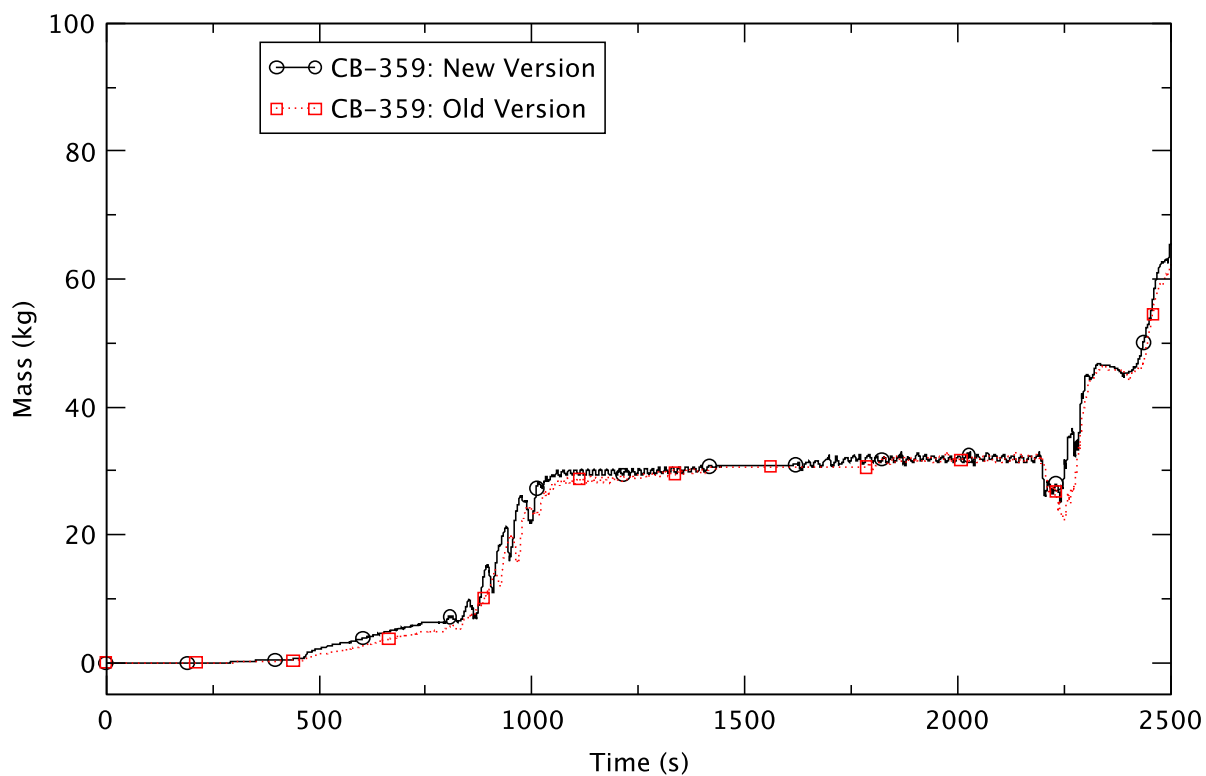


Figure A.9 Boron Inventory in the Core - EOFPL, TAF-2

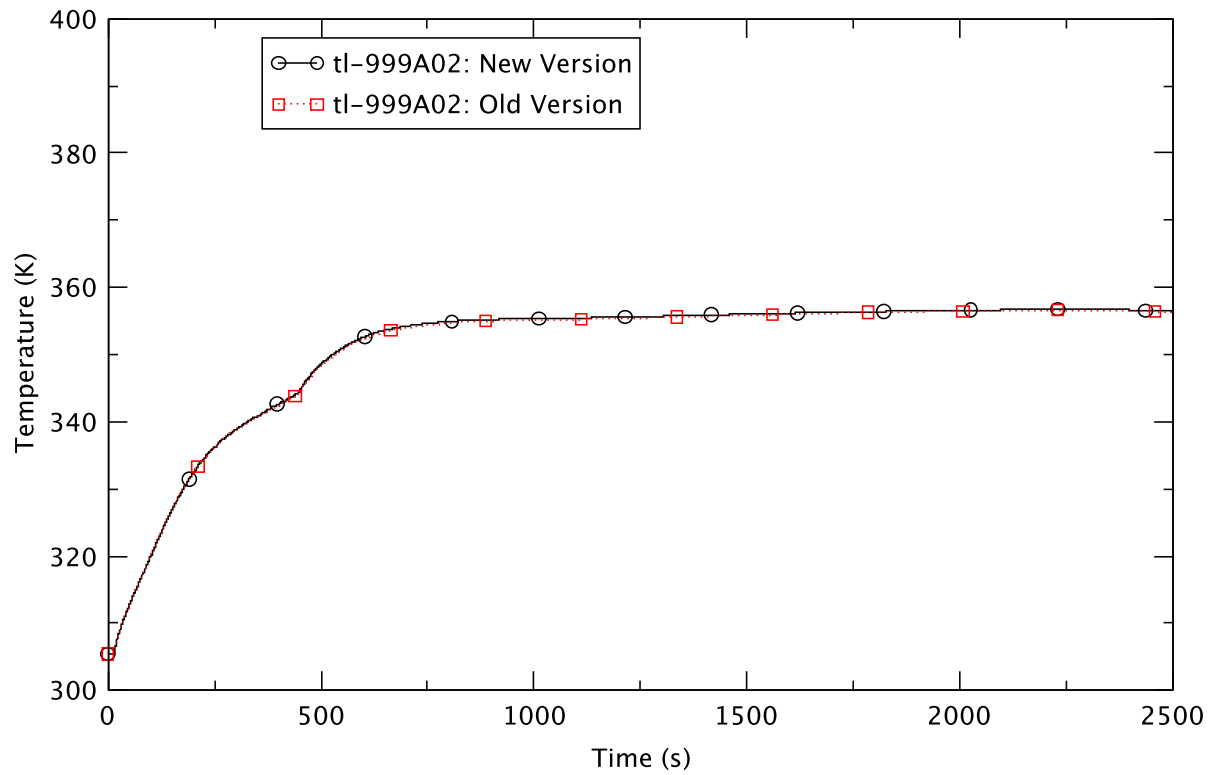


Figure A.10 Suppression Pool Temperature - EOFPL, TAF-2

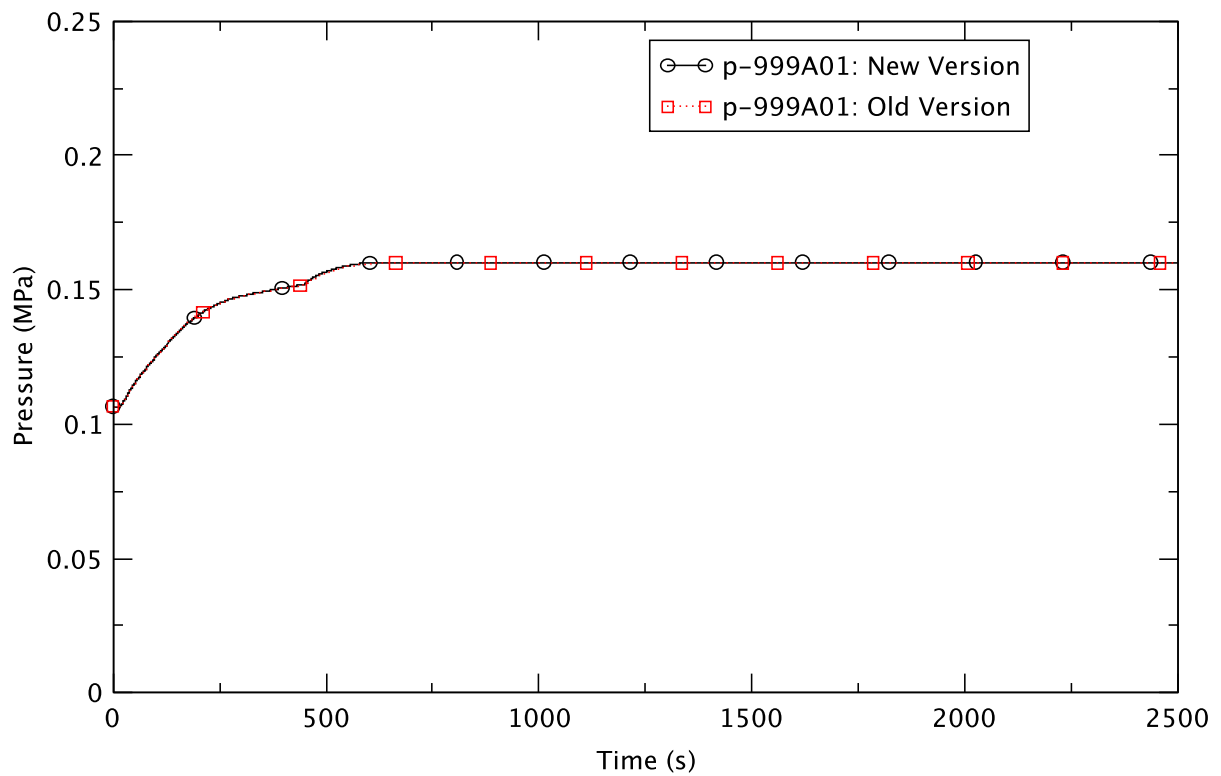


Figure A.11 Drywell Pressure - EOFPL, TAF-2

The following figures (Figure A.12 to Figure A.19) are from the execution of the EOFPL TAF-2 75% flow case using two TRACE executables. They are from the same code modification cycle (V5.0p3P32m07co), but are for two different computer platforms, Linux and Windows. Both runs were done with the semi-implicit numerical scheme and a maximum time-step size of 0.02 s. Preceding the power spike, there are some differences between the two executables at around 650 s, e.g., in the downcomer water level (Figure A.13). Comparing the overall results from the two executables demonstrates that both versions of TRACE produce essentially identical results until shortly before the power spike appears at ~700 s. Thus, it was reasonable to apply the equivalent executable for the Windows platform, namely, V5.0p3P32m07co_x64.exe to simulate the EOFPL TAF-2 75% flow case while the cause of the anomaly in the Linux version is being investigated.

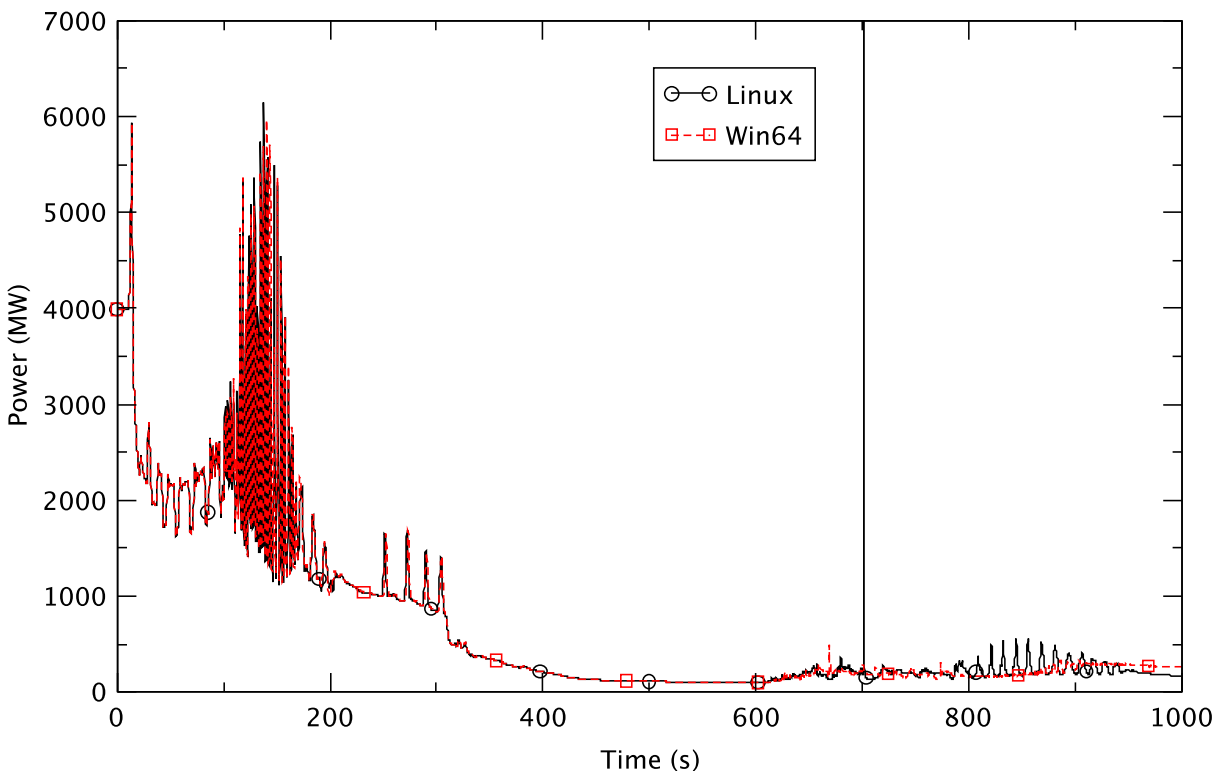


Figure A.12 Reactor Power - EOPFL, TAF-2, 75% Flow

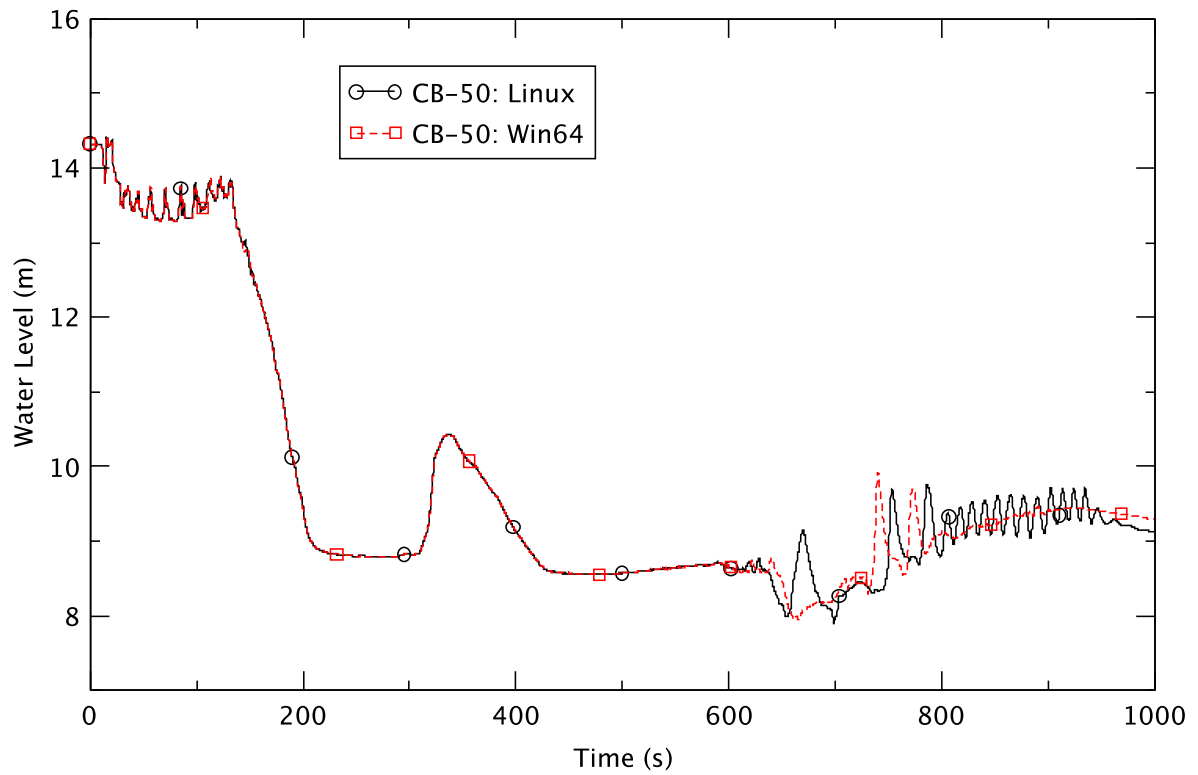


Figure A.13 Downcomer Water Level - EOFPL, TAF-2, 75% Flow

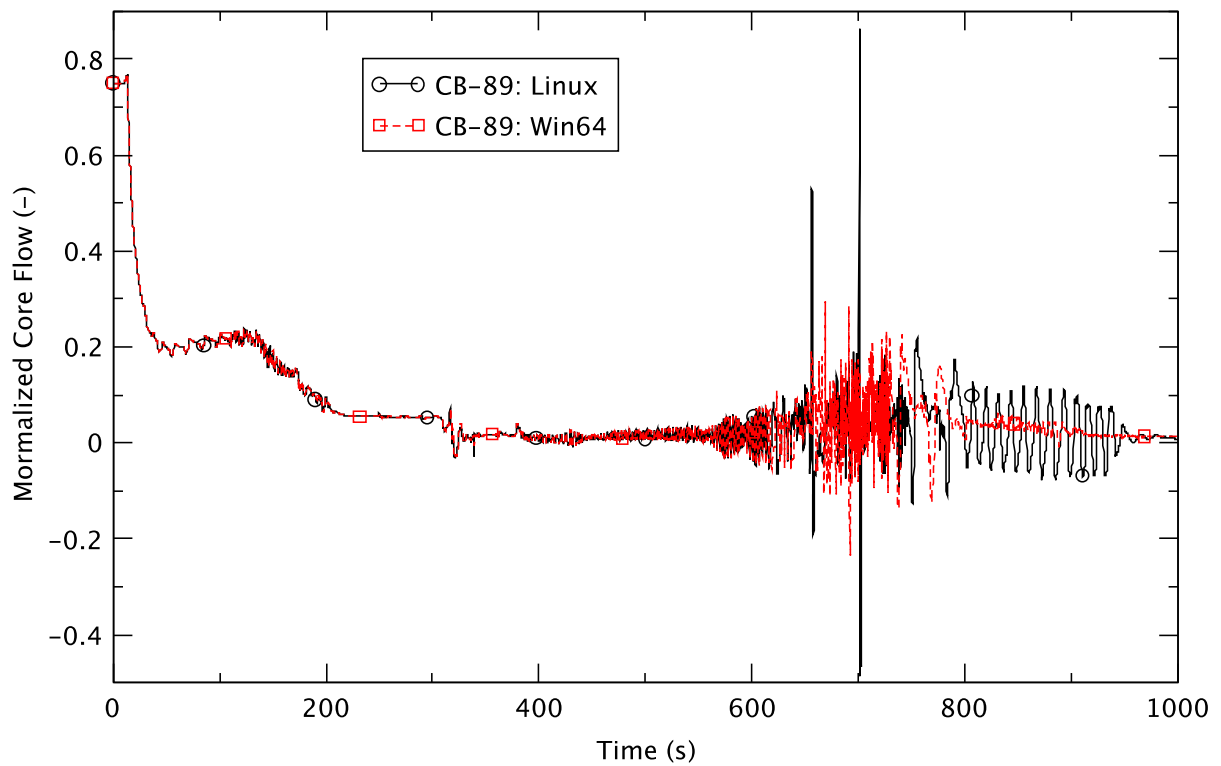


Figure A.14 Core Flow - EOFPL, TAF-2, 75% Flow

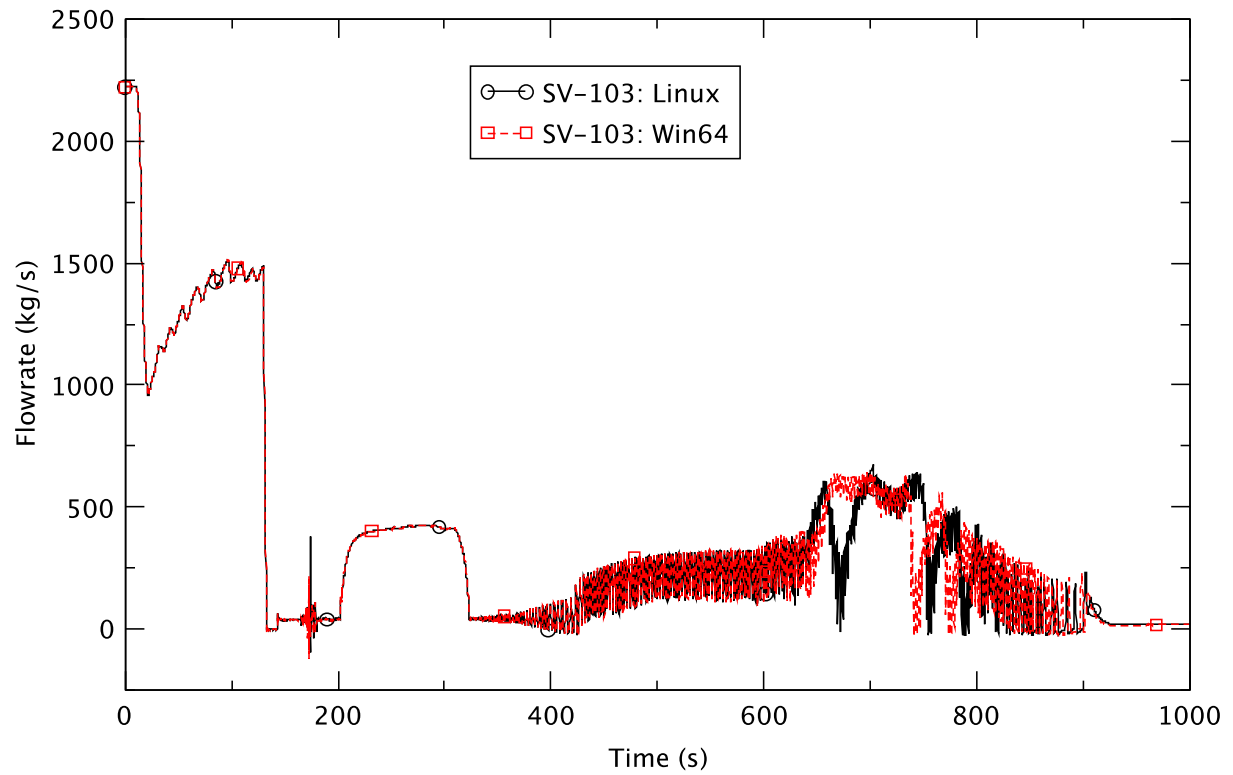


Figure A.15 Feedwater Flowrate - EOFPL, TAF-2, 75% Flow

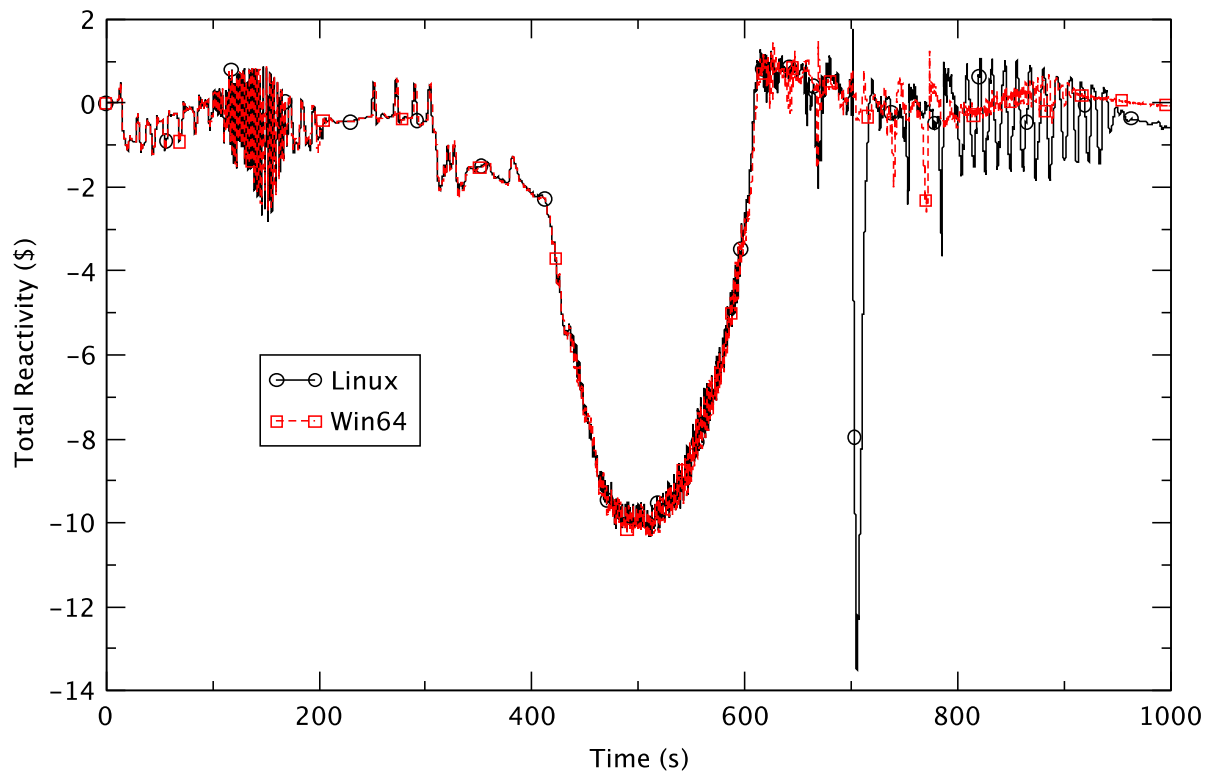


Figure A.16 Total Core Reactivity - EOFPL, TAF-2, 75% Flow

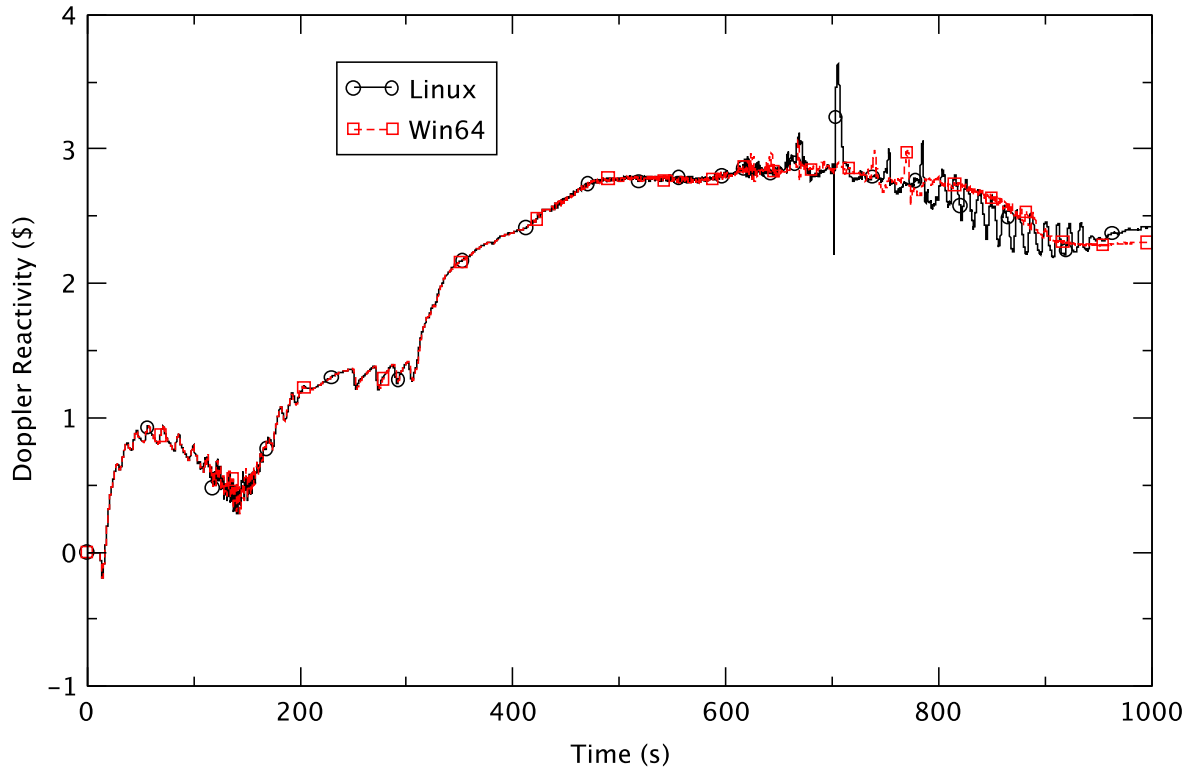


Figure A.17 Doppler Reactivity - EOFPL, TAF-2, 75% Flow

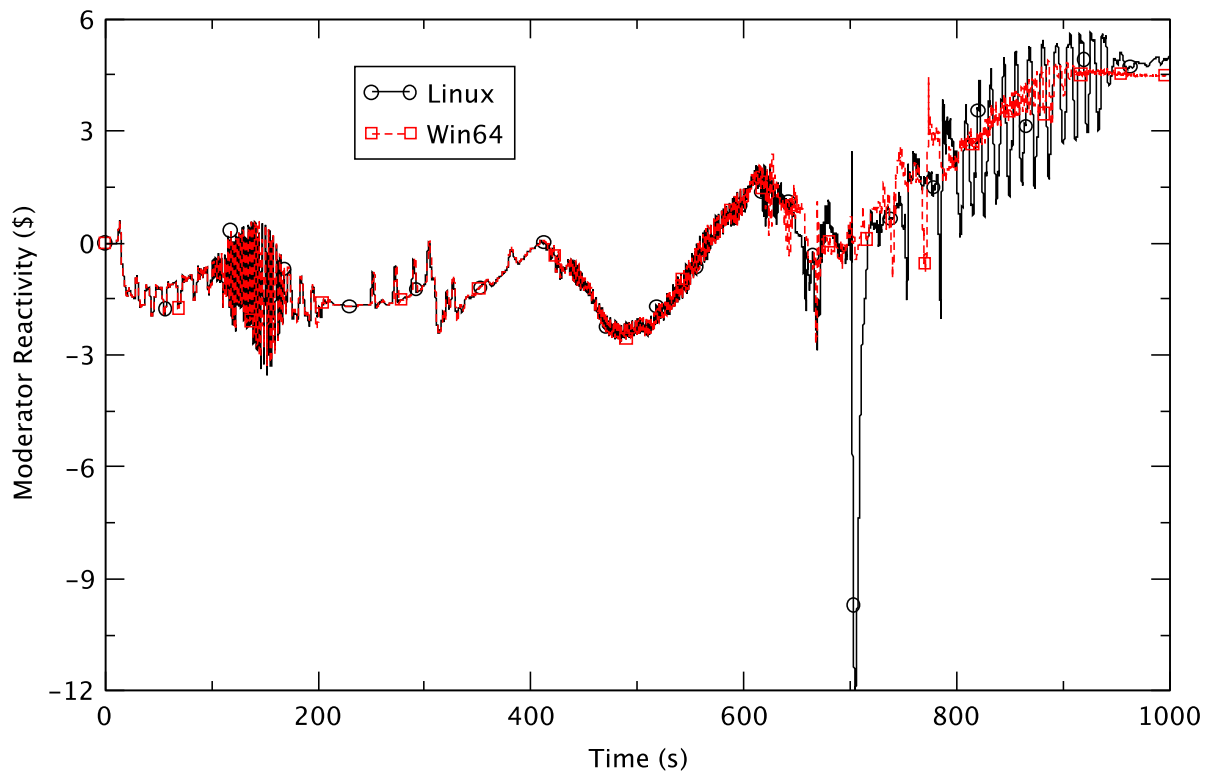


Figure A.18 Moderator Density Reactivity - EOFPL, TAF-2, 75% Flow

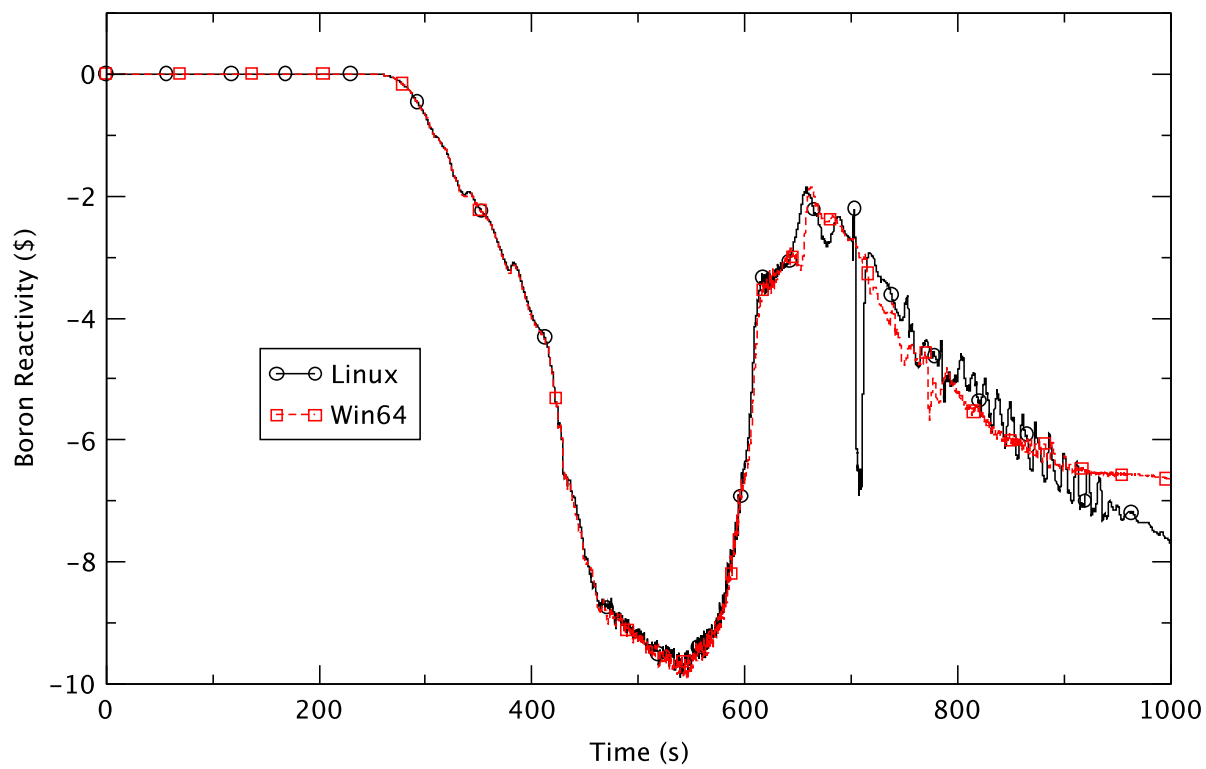


Figure A.19 Boron Reactivity - EOFPL, TAF-2, 75% Flow

APPENDIX B

Selection of Time-Step Size and Numerical Method

LIST OF FIGURES

| | | |
|-------------|---|------|
| Figure B.1 | Case 11 - Reactor Power..... | B-5 |
| Figure B.2 | Case 11 - Reactor Pressure..... | B-6 |
| Figure B.3 | Case 11 - Core Flow..... | B-6 |
| Figure B.4 | Case 11 - Downcomer Water Level | B-7 |
| Figure B.5 | Case 11 - Feedwater Flowrate..... | B-7 |
| Figure B.6 | Case 11 - Boron Inventory in the Core..... | B-8 |
| Figure B.7 | Case 11 - Core Reactivity..... | B-8 |
| Figure B.8 | Case 11 - Peak Clad Temperature..... | B-9 |
| Figure B.9 | Case 5 - Reactor Power..... | B-10 |
| Figure B.10 | Case 5 - Core Flowrate..... | B-10 |
| Figure B.11 | Case 5 - Downcomer Water Level | B-11 |
| Figure B.12 | Core Power - Different Initial Steady-State..... | B-12 |
| Figure B.13 | Downcomer Water Level - Different Initial Steady-State..... | B-12 |

LIST OF TABLES

| | | |
|-----------|---|-----|
| Table B.1 | Summary of Time-Step Size and Numerical Method for ATWS-ED..... | B-4 |
|-----------|---|-----|

This appendix provides additional background information on selecting the numerical method and the size of the time-step for analyzing the ATWS-ED cases by TRACE.

TRACE offers the option of selecting one of two related numerical methods for solving fluid-dynamics equations in the spatial one-dimensional (1D), and three-dimensional (3D) components. The default Stability Enhancing Two-Step (SETS) method advantageously avoids Courant stability limits on time-step size, but has the disadvantage of relatively high numerical diffusion. A namelist input option permits selecting a semi-implicit (S-I) method that has substantially less numerical diffusion but time-step sizes are restricted to a material Courant limit; this method should be the choice for analyzing BWR stability. For the current work of analyzing ATWS-ED cases, the primary objective is to assess the response of key components to the operator actions, rather than the reactor's stability. Since the SETS method allows violation of the Courant limit to the time-step size, long transients, such as ATWS can be modeled with larger time-steps. The larger time-steps support calculations for such transients, and generally, can be completed in a reasonable time. Therefore, we selected it as the default method for analyzing ATWS-ED cases. However, SETS loses efficiency when the problem requires reducing the size of the time-step to very small values. Then, it is appropriate to use the more robust S-I method to resolve the problem.

The following are the general guidelines used in the current work for selecting time-step size and deciding to apply the S-I method.

- 1) Apply SETS with a maximum time-step size of 0.05 s.
- 2) If problem failed, reduce time-step size to 0.025 s.
- 3) If problem still failed, reduce size of time-step to 0.01 s sometime before the last failure.
- 4) If again there was failure, apply S-I with a maximum time-step size of 0.02 s.

We found that it took about the same amount of CPU time to complete a 2500 s ATWS-ED transient using either the S-I method or the SETS method with a maximum time-step size of 0.01 s.

Table B.1 summarizes the maximum time-step size and the numerical method applied in the 17 ATWS-ED cases.

Table B.1 Summary of Time-Step Size and Numerical Method for ATWS-ED

| Case ID | Exposure | Flow rate % | RWL Strategy | SLCS Injection | Comment |
|----------------|-----------------|--------------------|---------------------|-----------------------|---|
| 6 | BOC | 85 | TAF-2 | Lower Plenum | Terminated at 1816 s (SETS 0.025 s) Re-ran successfully with 0.01 s max time-step after 1500 s |
| 7 | PHE | 85 | TAF+5 | Lower Plenum | Completed (SETS 0.05 s) |
| 4 | BOC | 85 | TAF+5 | Lower Plenum | Completed (SETS 0.05 s) |
| 7C | PHE | 85 | TAF+5 | Upper Plenum | Completed (SETS 0.05 s) |
| 5 | BOC | 85 | TAF | Lower Plenum | Terminated at 1291 s (SETS 0.05 s) Completed (SETS 0.025 s) |
| 10 | EOFPL | 105 | TAF+5 | Lower Plenum | Completed (SETS 0.05 s) |
| 12 | EOFPL | 105 | TAF-2 | Lower Plenum | Terminated at 768 s (SETS 0.025 s) Re-run with 0.01 s max time-step after 500 s; failed at 800.937 s Completed (S-I 0.02 s) |
| EDSI | BOC | 85 | TAF | Lower Plenum | Completed (S-I 0.02 s) |
| 9 | PHE | 85 | TAF-2 | Lower Plenum | Terminated at 1760 s (SETS 0.025 s) Re-ran successfully with 0.01 s max time-step after 1500 s |
| 8 | PHE | 85 | TAF | Lower Plenum | Completed (SETS 0.05 s) |
| 11 | EOFPL | 105 | TAF | Lower Plenum | Terminated at 2058 s (SETS 0.05 s) Re-run with 0.025 s max time-step; failed at 817.775 s Re-ran successfully with 0.05 s (SETS) max time-step to 1500 s; 0.025 s max time-step to 2000s and 0.01 s max time-step to 2500 s |
| 4B | BOC | 75 | TAF+5 | Lower Plenum | Completed (SETS 0.05 s) |
| 10D | EOFPL | 75 | TAF-2 | Lower Plenum | Terminated at 618 s (SETS 0.025 s) Re-run with 0.01 s max time-step after 500 s; failed at 615.447 s Re-run with S-I and 0.02 s max time-step; terminated at 628 s. Completed (S-I 0.02 s) ¹ |
| 10A | EOFPL | 85 | TAF+5 | Lower Plenum | Completed (SETS 0.05 s) |
| 11A | EOFPL | 85 | TAF | Lower Plenum | Completed (SETS 0.025 s) |

| | | | | | |
|-----|----------------|-----|-------|--------------|--|
| 12A | EOFPL | 85 | TAF-2 | Lower Plenum | Terminated at 669 s (SETS 0.025 s) Re-run with 0.01 s max time-step after 500 s; failed at 693.926 s Re-run with S-I and 0.02 s max time-step; terminated at 707 s. Completed (S-I 0.02 s) ² |
| 10C | EOFPL UHSPH | 105 | TAF+5 | Lower Plenum | Terminated at 1757 s (SETS 0.05 s) Completed re-run with max time-step reduced to 0.025 s after 1500 s |

¹ Completed using Windows executable V5.0p3P32m07co_x64.exe. See Appendix A for more discussion.

² Completed using Linux executable V5.0p3P32m07co.x. The CSTEP input for the CONTAN component was changed from 1.0 to 0.5 to avoid failure in the thermal-hydraulic calculation.

In completing the 17 ATWS-ED cases, we undertook a series of assessment runs. User experience in selecting time-step size and numerical method is discussed next.

Effect of Time-Step Size

An EOFPL base case with level control to TAF is used to illustrate the effect of time-step size on simulating an ATWS-ED transient. The completion of the case required some adjustments to the time-step size during the course of the work. As summarized in Table B.1 a run with a 0.05 s maximum time-step size failed at 2058 s while a 0.025 s case failed earlier at 817 s. The following plots compare the results from these two runs.

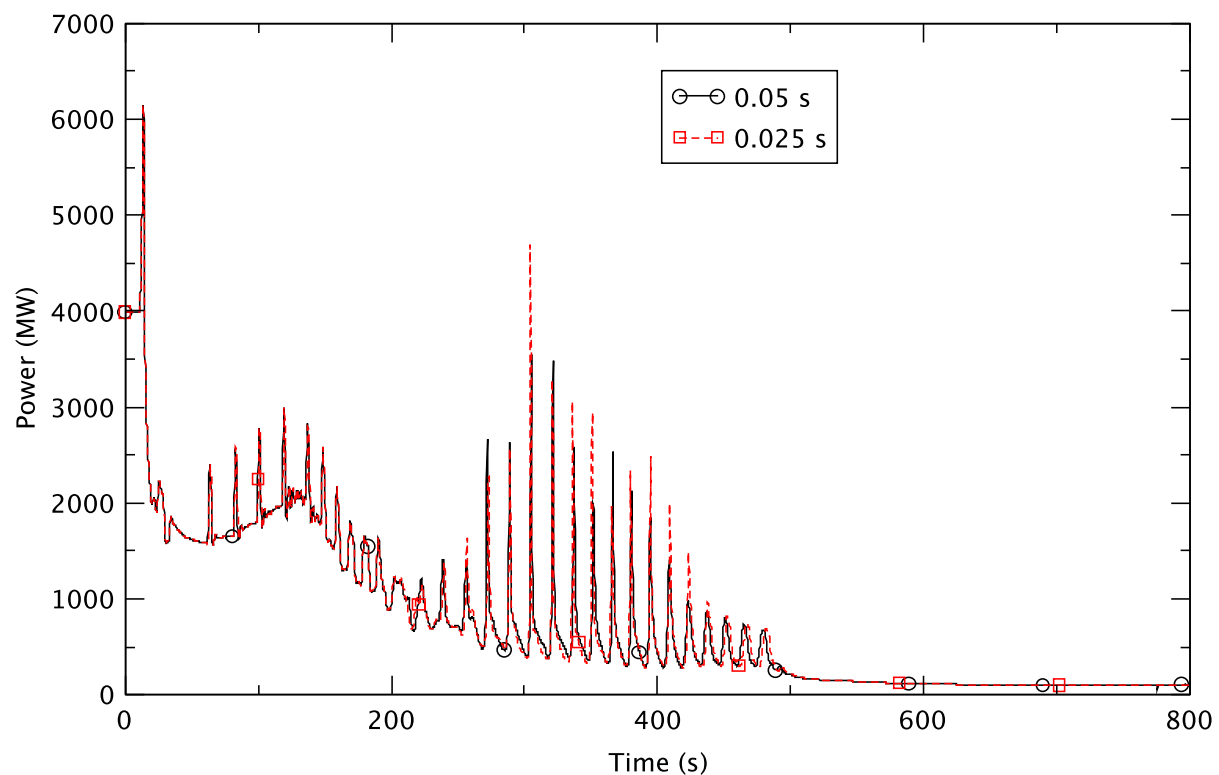


Figure B.1 Case 11 - Reactor Power

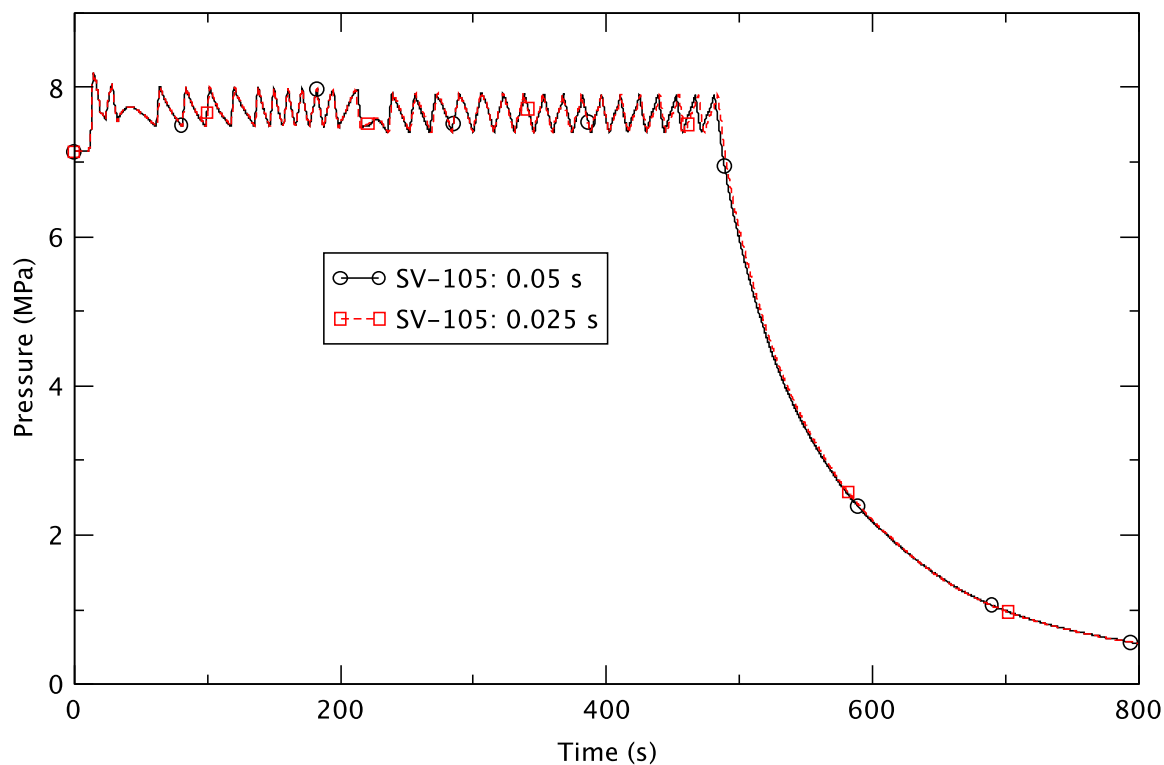


Figure B. 2 Case 11 - Reactor Pressure

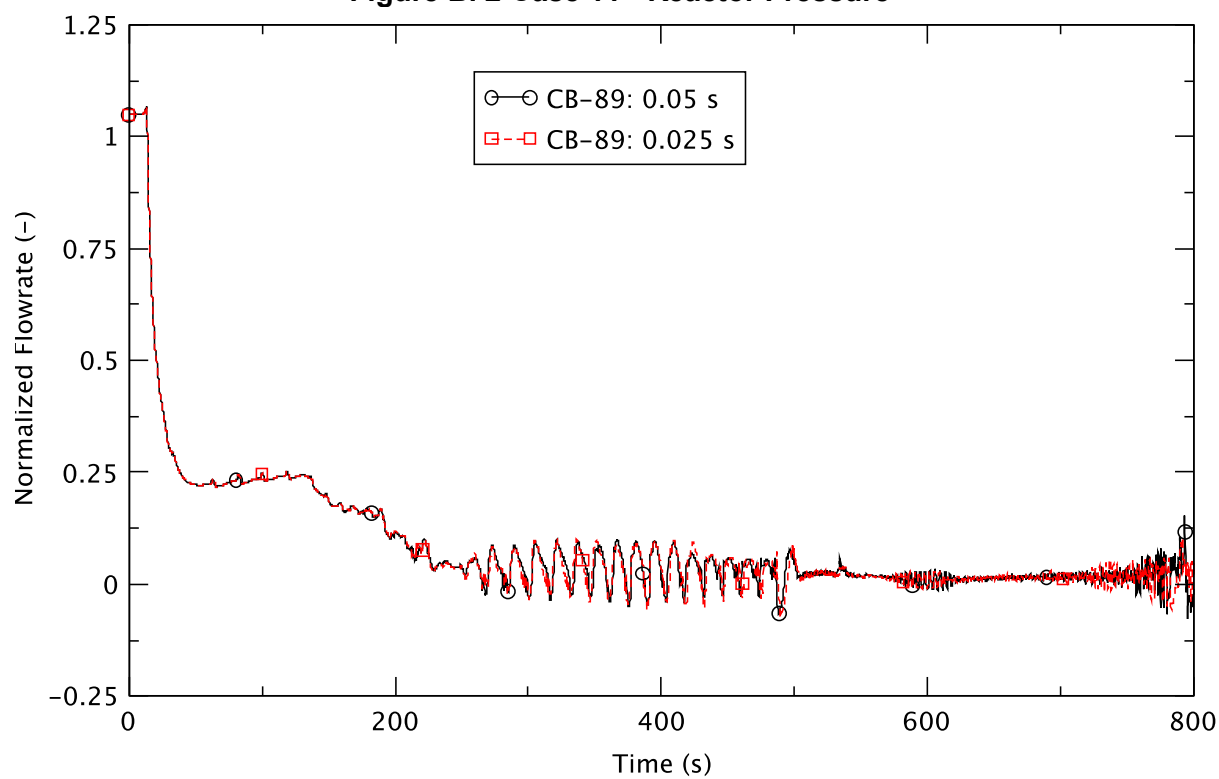


Figure B.3 Case 11 - Core Flow

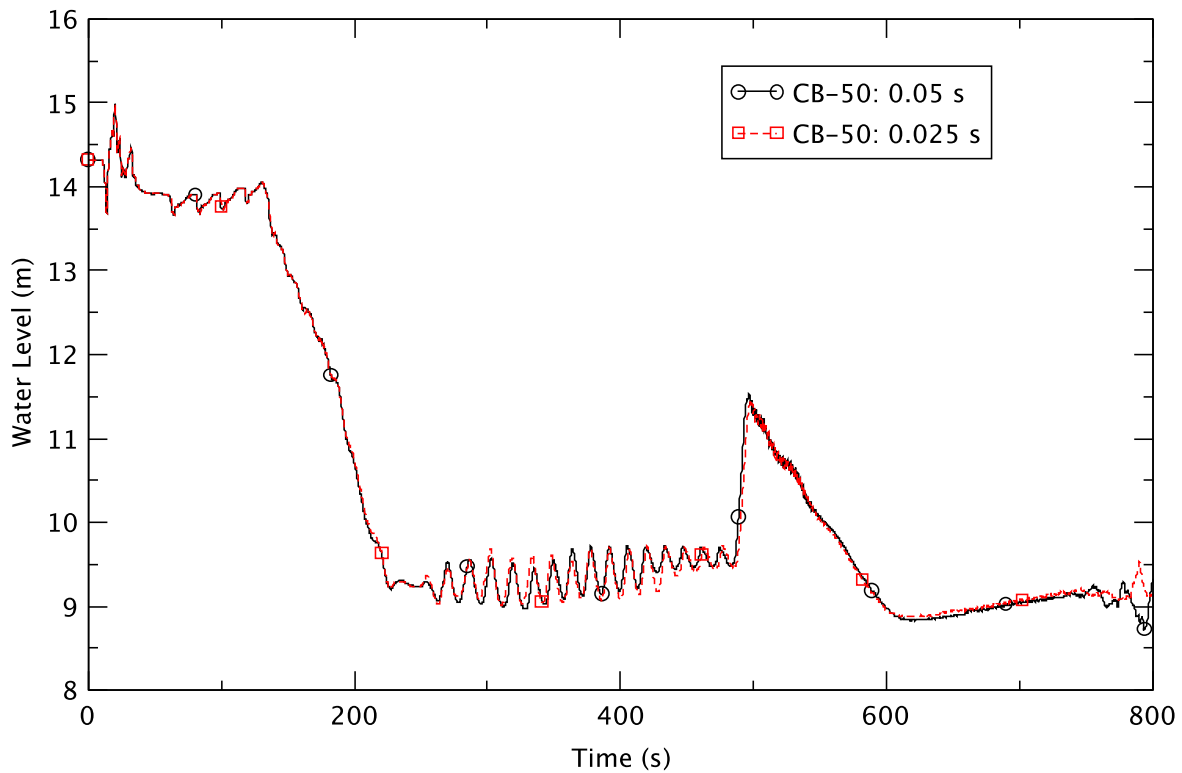


Figure B.4 Case 11 - Downcomer Water Level

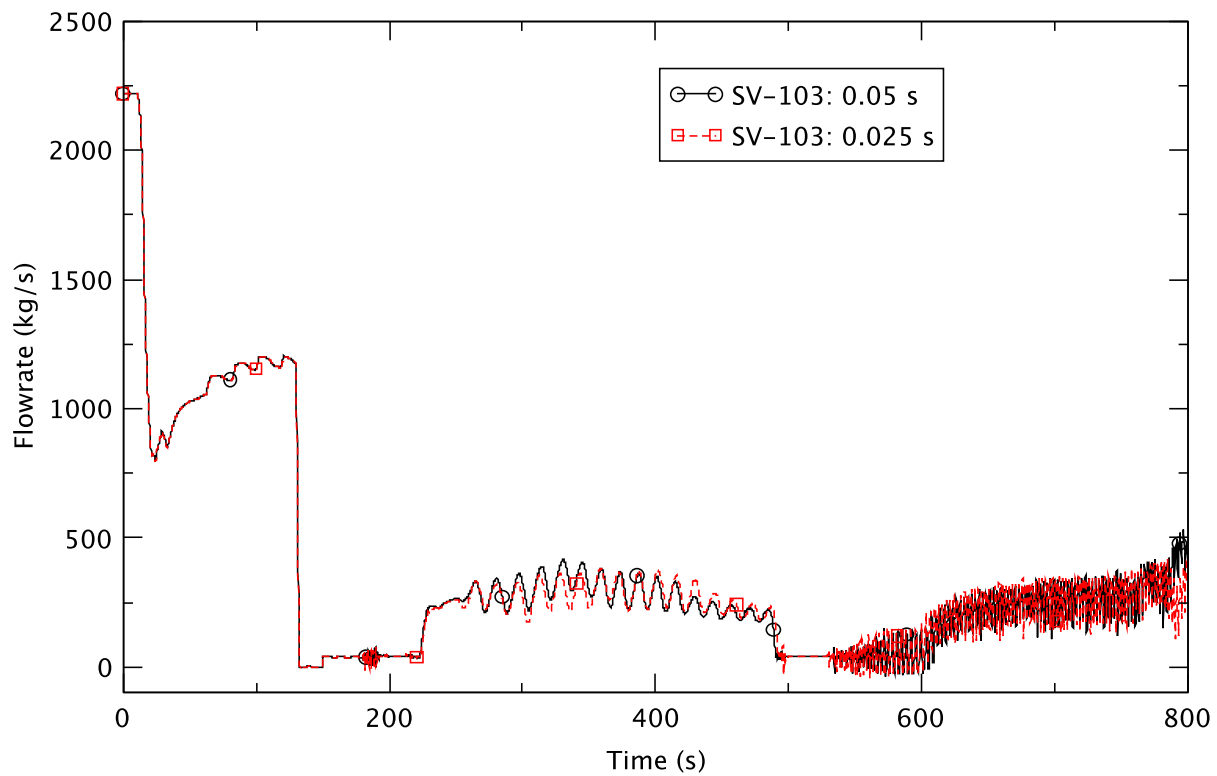


Figure B.5 Case 11 - Feedwater Flowrate

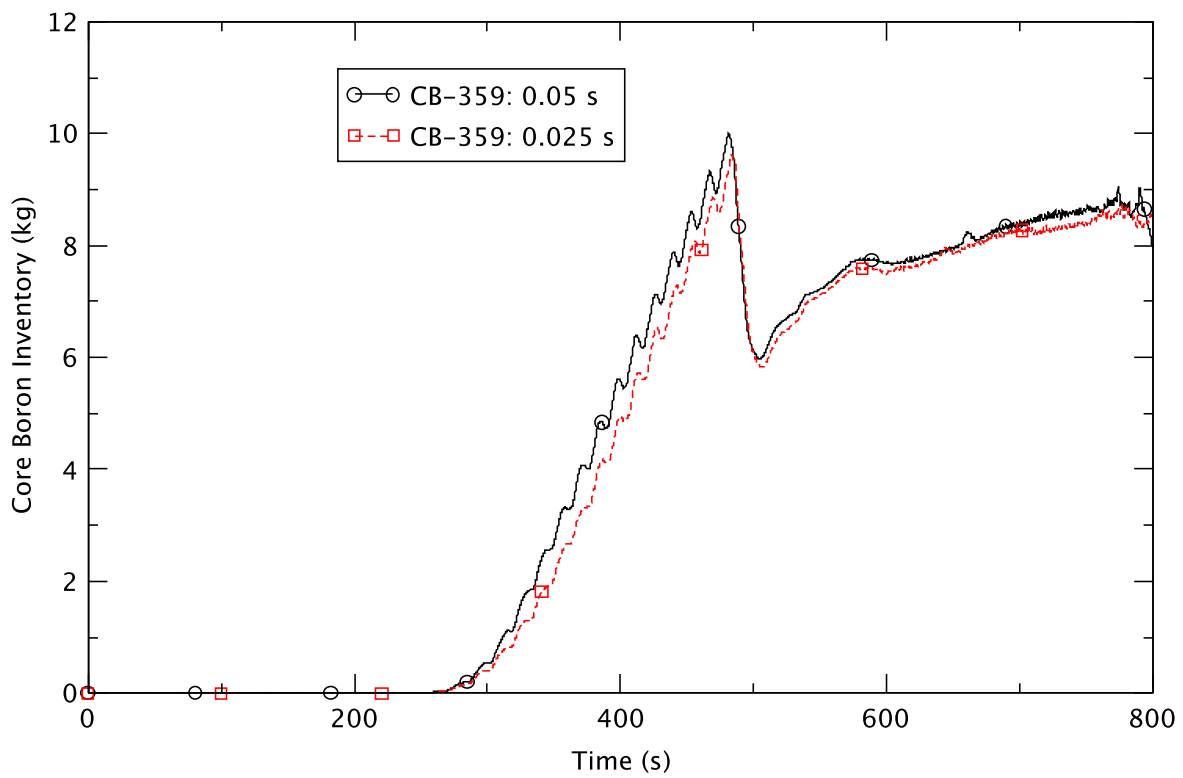


Figure B.6 Case 11 - Boron Inventory in the Core

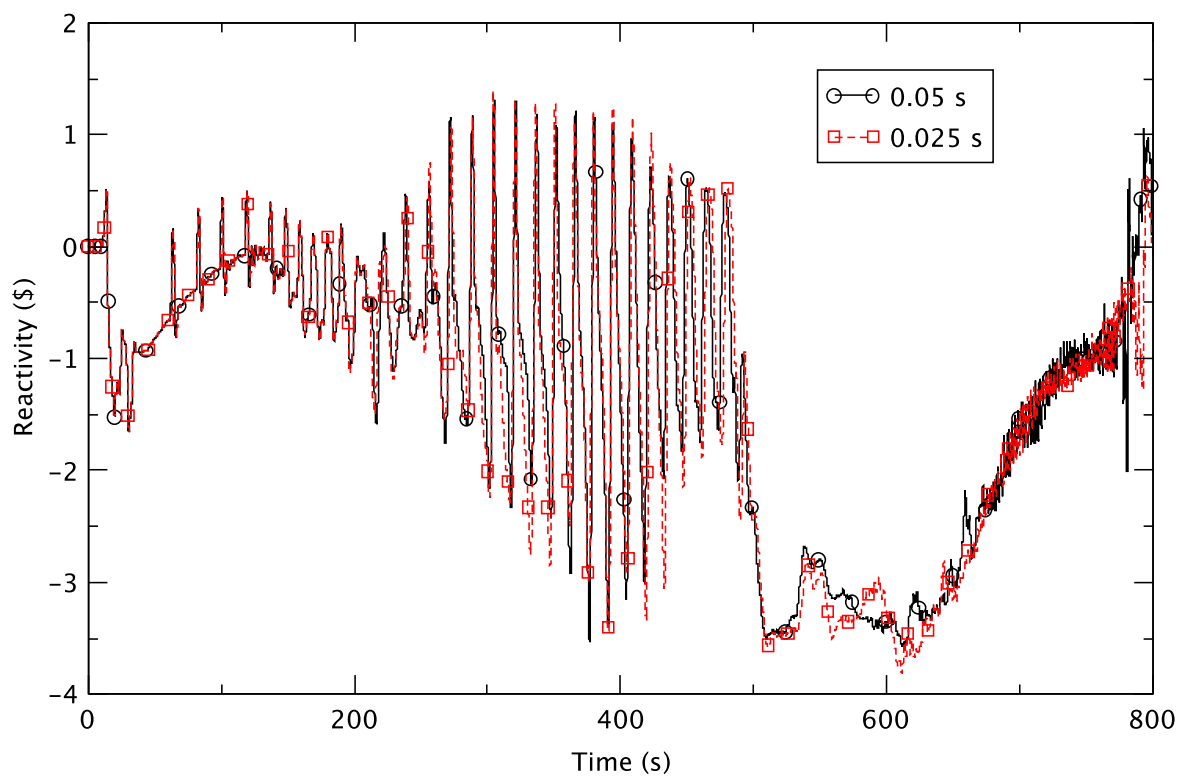


Figure B.7 Case 11 - Core Reactivity

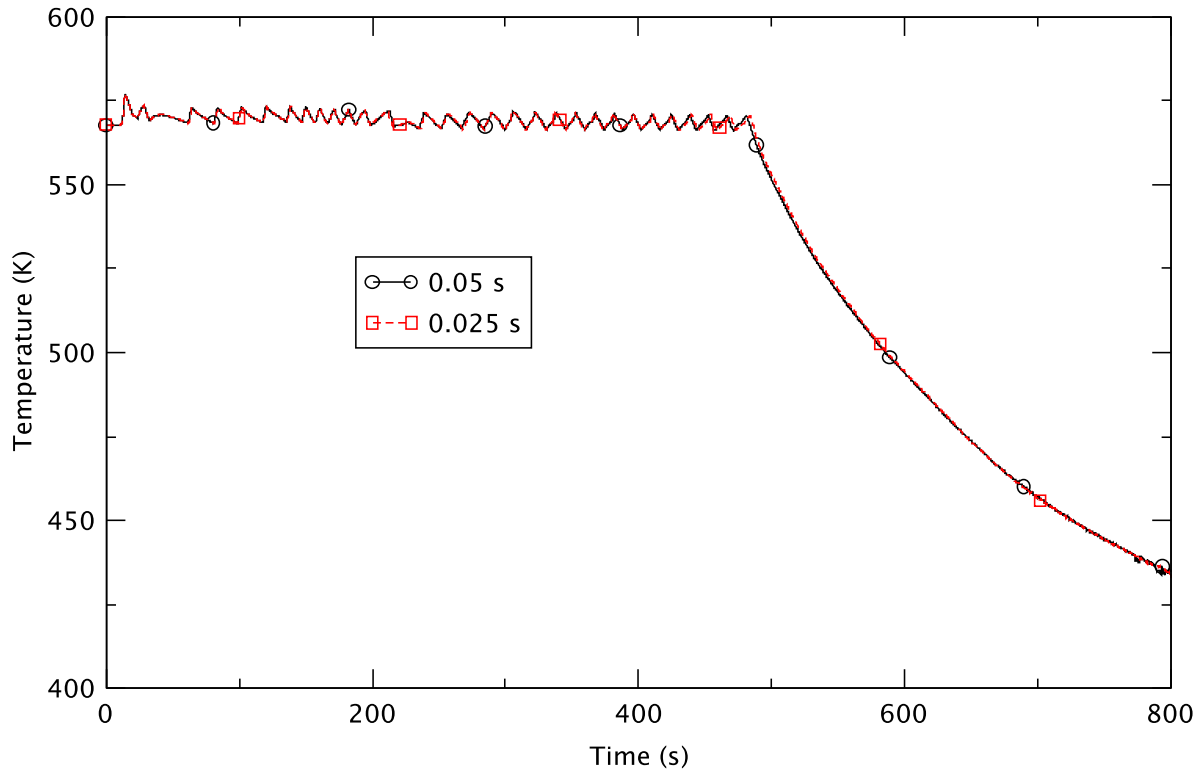


Figure B.8 Case 11 - Peak Clad Temperature

Up to the failure point, the two cases compare favorably. However, the immediate cause of their failure appears to differ. The 0.025 s case terminated when the PARCS outer iteration failed to converge after the set number of iterations (750) and passed bad power (“NaN”) information to TRACE. The 0.05 s case terminated upon failure of the TRACE outer iteration when the reduction in the time-step reached the limit of 1E-8. In all the ATWS-ED transients analyzed, the power transient was dominated by events occurring in the first few hundred seconds; the later part of the transient is not too important. The plots show that the results in the first few hundred seconds are not sensitive to the time-step size. By judiciously selecting the time-step sizes during the course of the transient (Table B.1), the TAF case completed the 2500 s simulation successfully.

Effect of Numerical Method

We used a BOC base case with level control to TAF (Case 5) to demonstrate the effect of the numerical method, viz., SETS versus semi-implicit (S-I), on the ATWS-ED results. The case was run using the Windows executable, and the result from the first 500 s is shown in the following figures. We note that the SETS case had a maximum time-step size of 0.05 s while the S-I case’s corresponding limit was to 0.02 s.

The two numerical methods provide almost identical results, as shown in Figure B.9 to Figure B.11.

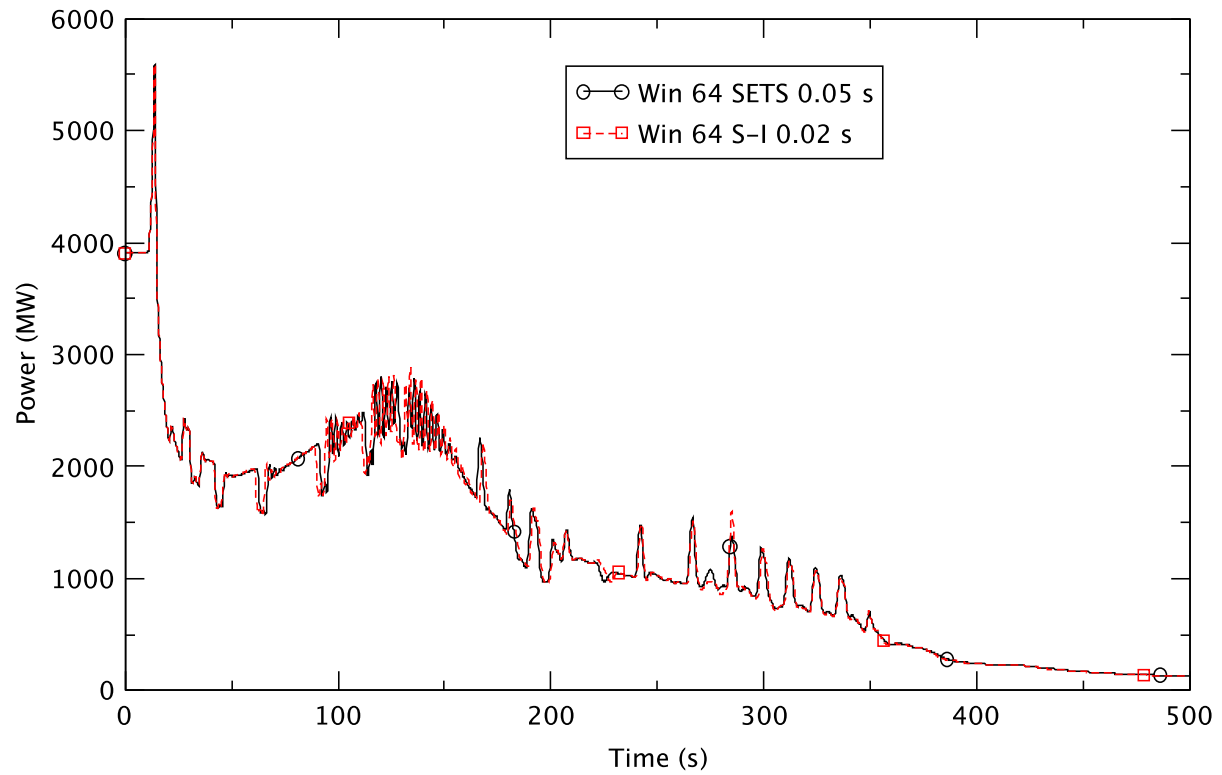


Figure B.9 Case 5 - Reactor Power

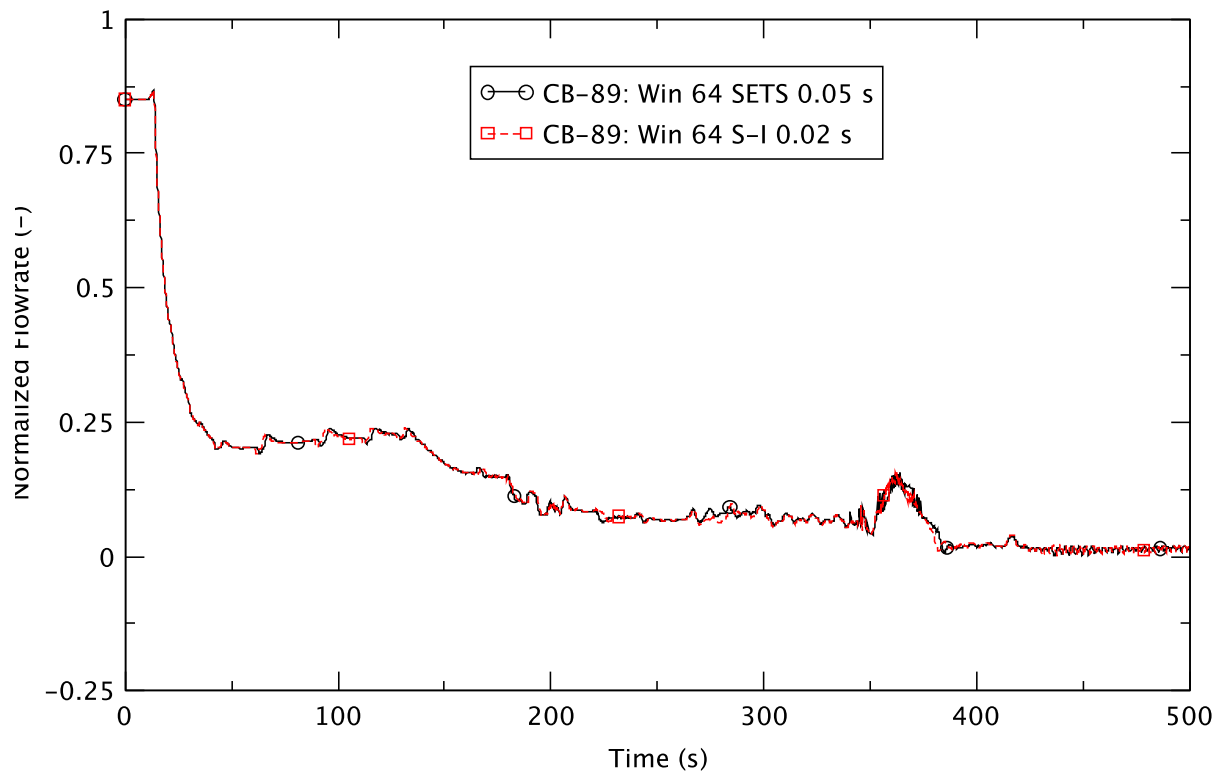


Figure B.10 Case 5 - Core Flowrate

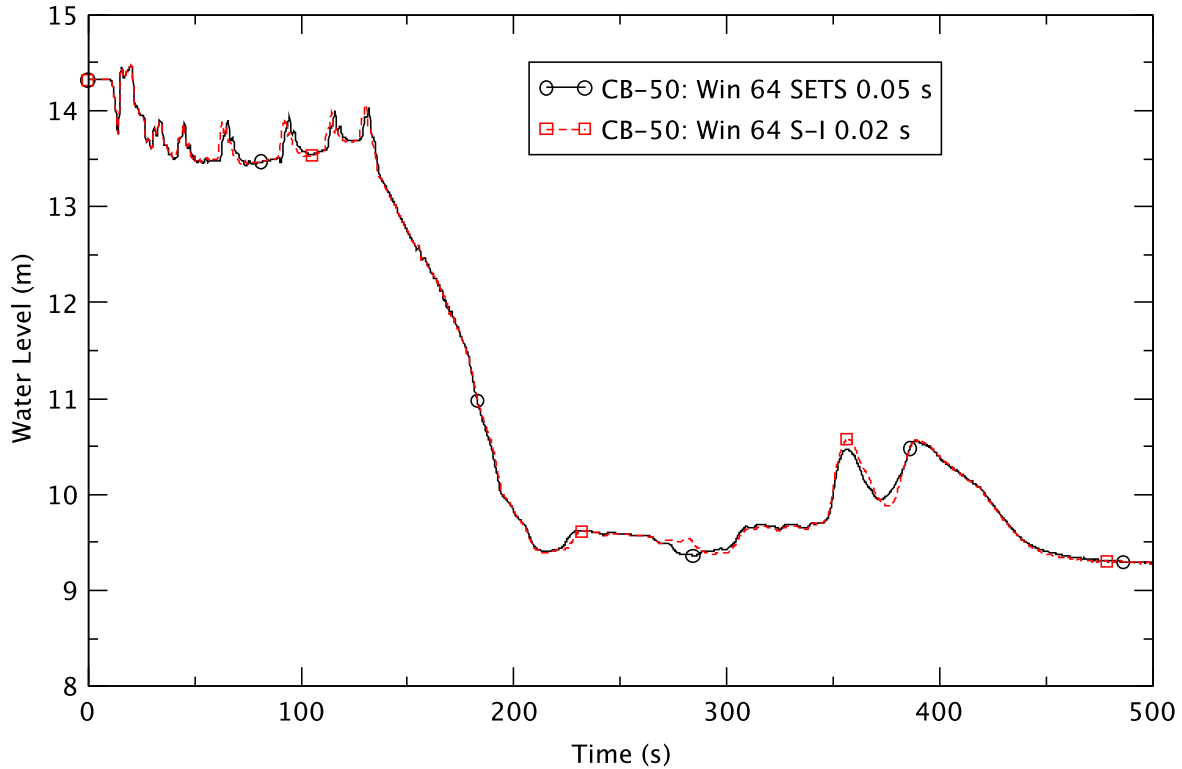


Figure B.11 Case 5 - Downcomer Water Level

Effect of Initial Steady-State

All ATWS-ED transient cases were run as a restart from a coupled steady-state (see Section 2.1 in [4] for a discussion of the work flow for executing a TRACE analysis). It is observed that there is bifurcation in results when the computation is started from slightly different initial conditions. Two BOC base cases with level control to TAF were run using the S-I numerical method. Each case was started from a slightly different initial steady-state. Two coupled steady-states were generated, one using the S-I method and a maximum time-step size of 0.01 s (initial condition SS1) and the other using the SETS method and a maximum time-step size of 0.02 s (initial condition SS2). Results of the two cases are shown in Figure B.12 and Figure B.13. At ~350 s, the two cases diverge on slightly different paths. Both paths seem to be possible in the calculations and which one is taken seems to be sensitive to modeling and differences in numerical methods. For the case with the SS1 steady-state, the natural circulation flow was maintained after the emergency depressurization whereas for the SS2 steady-state, the natural circulation was broken. In both cases, the reactor power was decaying and the difference does not appear to significantly impact the outcome of the transient.

We note that a similar pattern of an ATWS-ED transient diverging into two different solutions was observed in comparing the SETS and the S-I method for a BOC TAF case [4]. A preliminary explanation for the source of the diverging results, i.e., using different PARCS options [the exponential extrapolation option (Expo_opt) and the implicitness option (THETA)], was shown not to be the case. The controlling factor in the diverging result is the initial steady-state.

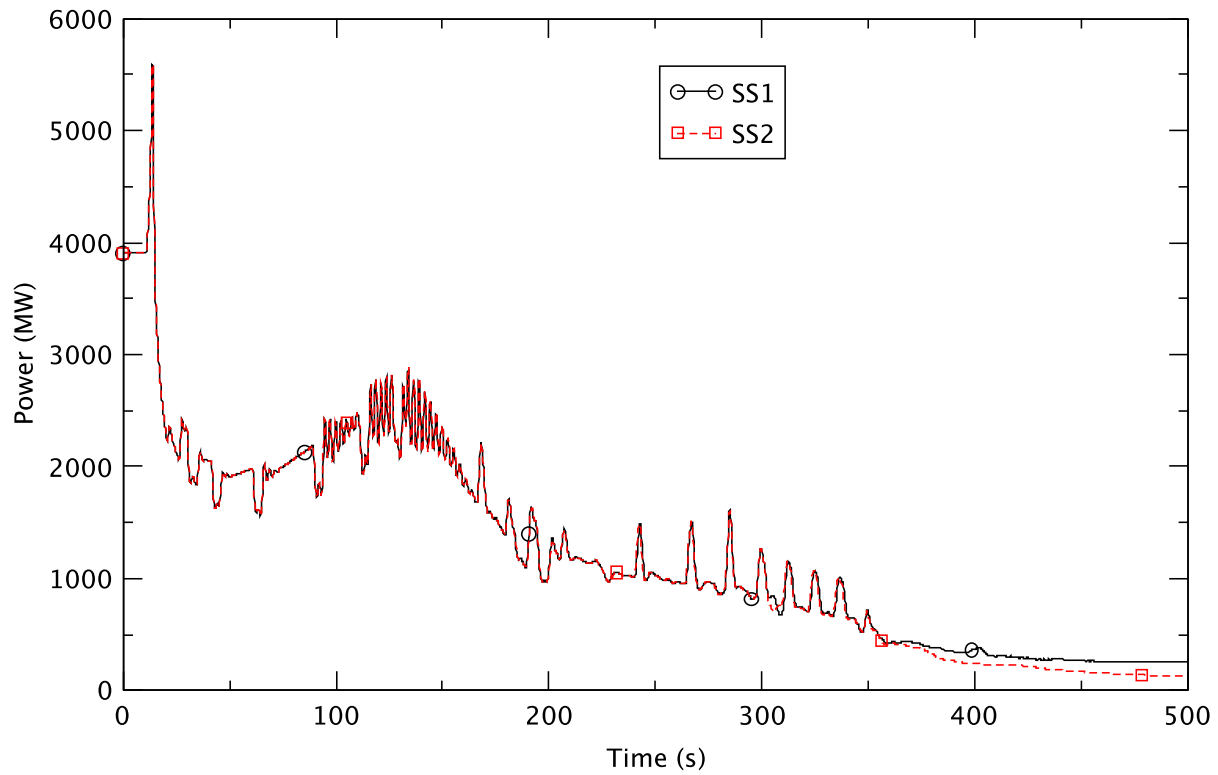


Figure B.12 Core Power - Different Initial Steady-State

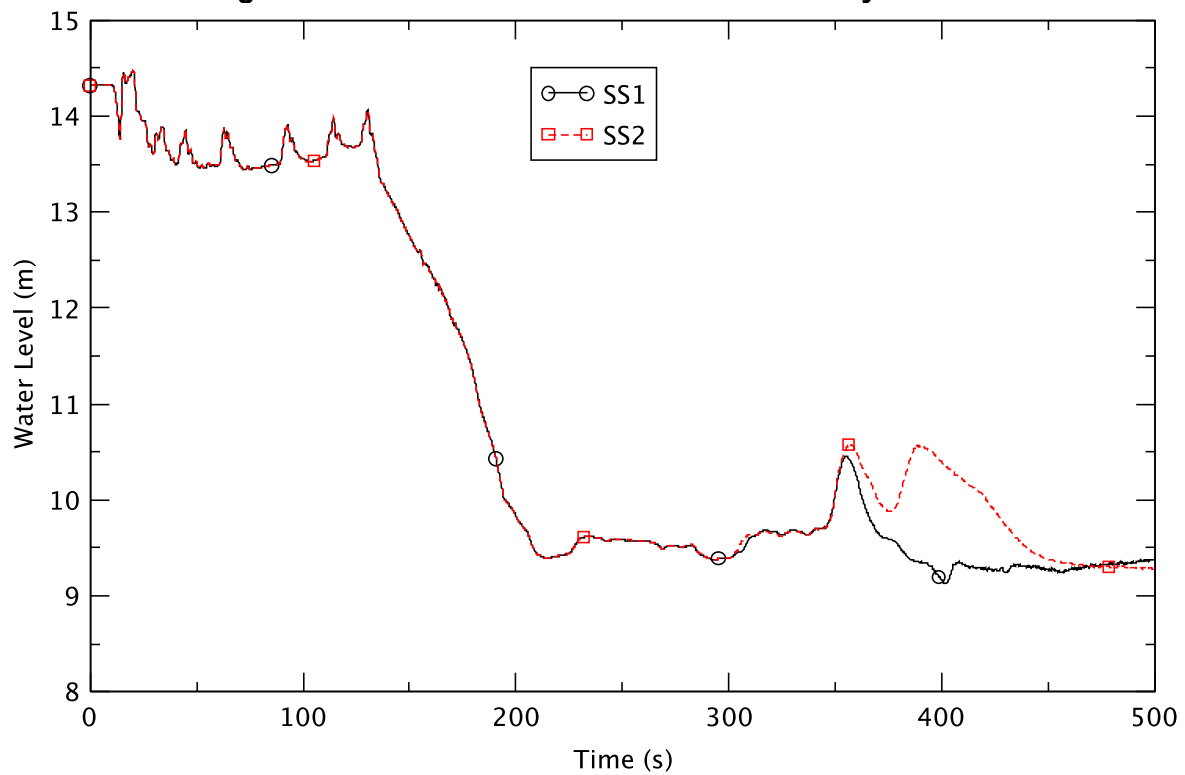


Figure B.13 Downcomer Water Level - Different Initial Steady-State

| | | | | | |
|---|--|---|--|--|--------------|
| NRC FORM 335 (12-2010) NRCMD 3.7 | | U.S. NUCLEAR REGULATORY COMMISSION | | 1. REPORT NUMBER (Assigned by NRC, Add Vol., Supp., Rev., and Addendum Numbers, if any.) NUREG/CR-7182 BNL-NUREG-105330-2014 | |
| BIBLIOGRAPHIC DATA SHEET (See instructions on the reverse) | | | | | |
| 2. TITLE AND SUBTITLE BWR Anticipated Transients Without Scram in the MELLLA+ Expanded Operating Domain Part 4: Sensitivity Studies for Events Leading to Emergency Depressurization | | | | 3. DATE REPORT PUBLISHED | |
| | | | | MONTH June | YEAR 2015 |
| | | | | 4. FIN OR GRANT NUMBER V6150 / F6018 | |
| 5. AUTHOR(S) Lap-Yan Cheng, Joo Seok Baek, Arantxa Cuadra, Arnold Aronson, David Diamond, Peter Yarsky | | | | 6. TYPE OF REPORT Technical | |
| | | | | 7. PERIOD COVERED (Inclusive Dates) 6/1/10 – 6/30/15 | |
| 8. PERFORMING ORGANIZATION - NAME AND ADDRESS (If NRC, provide Division, Office or Region, U. S. Nuclear Regulatory Commission, and mailing address; if contractor, provide name and mailing address.) Nuclear Science & Technology Department Brookhaven National Laboratory Upton, NY 11973-5000 | | | | | |
| 9. SPONSORING ORGANIZATION - NAME AND ADDRESS (If NRC, type "Same as above", if contractor, provide NRC Division, Office or Region, U. S. Nuclear Regulatory Commission, and mailing address.) Division of Systems Analysis Office of Nuclear Regulatory Research U.S. Nuclear Regulatory Commission Washington DC 20555-0001 | | | | | |
| 10. SUPPLEMENTARY NOTES Tarek Zaki, NRC Project Manager | | | | | |
| 11. ABSTRACT (200 words or less) This is the fourth in a series of reports on the response of a boiling water reactor (BWR) to anticipated transients without reactor scram (ATWS) when operating in the expanded operating domain MELLLA+ (maximum extended load line limit analysis plus). In this report, we analyze the ATWS events initiated by the closure of main steam isolation valves and requiring emergency depressurization (ED). The analysis is done at the beginning-of-cycle and end-of-full-power-life. Our objective is to understand the sensitivity of ATWS-ED events to the initial operating core flow and to the spectrally corrected moderator density history (void history). We also consider different strategies for controlling the water level. We simulate the ATWS events for 2500 seconds, a sufficiently long time for us to identify and understand the response of key components and the potential for damaging the fuel or causing the containment to fail. These events lead to the automatic trip of recirculation pumps, and to the operator actions to manually activate the automatic depressurization system when the wetwell (suppression pool) has reached the heat capacity temperature limit, and to regulate power by controlling the water level and injecting soluble boron. The simulations were carried out using the TRACE/PARCS code system and the models we developed for a previous study with all relevant BWR systems. | | | | | |
| 12. KEY WORDS/DESCRIPTORS (List words or phrases that will assist researchers in locating the report.) TRACE/PARCS; Anticipated Transients Without Scram (ATWS); Boiling Water Reactor (BWR); emergency depressurization; operator action; safety analysis; containment function; Maximum Extended Load Line Limit Analysis Plus (MELLLA+) | | | | 13. AVAILABILITY STATEMENT unlimited | |
| | | | | 14. SECURITY CLASSIFICATION (This Page) unclassified | |
| | | | | (This Report) unclassified | |
| | | | | 15. NUMBER OF PAGES | |
| | | | | 16. PRICE | |



Federal Recycling Program



**UNITED STATES
NUCLEAR REGULATORY COMMISSION**
WASHINGTON, DC 20555-0001

OFFICIAL BUSINESS



NUREG/CR-7182

**BWR Anticipated Transients Without Scram in the MELLLA+ Expanded
Operating Domain, Part 4**

June 2015